For Referen

NOT TO BE TAKEN FROM THIS

For Reference

NOT TO BE TAKEN FROM THIS ROOM

Ex libris
universitatis
albertaensis

University of Alberta
Printing Department

Digitized by the Internet Archive
in 2018 with funding from
University of Alberta Libraries

https://archive.org/details/laboratoryinvest00adam

DEPARTMENT OF CHEMICAL AND
PETROLEUM ENGINEERING

I

Thesis
1962(F)
#1

THE UNIVERSITY OF ALBERTA

"A LABORATORY INVESTIGATION OF MISCIBLE FLUID DISPLACEMENT"

by

James A. Adamson

A THESIS
SUBMITTED TO THE FACULTY OF GRADUATE STUDIES
IN PARTIAL FULFILMENT OF THE REQUIREMENTS FOR THE DEGREE
OF MASTER OF SCIENCE IN PETROLEUM ENGINEERING

FACULTY OF ENGINEERING
DEPARTMENT OF CHEMICAL AND PETROLEUM ENGINEERING

EDMONTON, ALBERTA

June, 1962

UNIVERSITY OF ALBERTA

FACULTY OF GRADUATE STUDIES

The undersigned hereby certify that they have read, and recommend to the Faculty of Graduate Studies for acceptance, a thesis entitled "A Laboratory Investigation of Miscible Fluid Displacement", submitted by J.A. Adamson, B.Sc., in partial fulfilment of the requirements for the degree of Master of Science in Petroleum Engineering.

June, 1962

ABSTRACT

Recent studies of the mechanism involved when a reservoir fluid is displaced miscibly by a light hydrocarbon mixture have resulted in the development of theoretical methods to predict the approximate conditions necessary in order that miscibility may occur. One of these methods employs the use of a pseudo-ternary phase diagram and requires the calculation of the critical temperature and pressure of a mixture of both the displacing and displaced phases. A brief theoretical analysis of the procedure was undertaken and comparisons were made between the method used to calculate criticals by the prediction correlation and newer methods of critical calculation.

The second part of the study is devoted to examining the mechanism of miscible fluid displacement in liquid systems and how it is influenced by viscous fingering. A unique method of recording pressure profiles as a function of time during an actual miscible displacement has been devised. Production data and pressure profiles along the core for various time increments were obtained and are plotted and discussed. Experimental results indicate that ideal miscible displacements take place only at low viscosity ratios and that laboratory verification of theoretical miscible predictions requires strict control of all causes of poor core sweep efficiency.

ACKNOWLEDGEMENTS

The writer wishes to express grateful appreciation to Dr. D.L. Flock who contributed his advice, guidance and encouragement throughout this project.

Acknowledgement is extended to Mr. Ray Kirby, Mr. Frank Butz and the staff of the department workshop for their help in building the equipment. Mr. Ken Balcombe is also thanked for his assistance in procuring materials. The writer would like to extend particularly grateful acknowledgement to his friends and colleagues who provided valuable advice and criticism and to typists Miss Georgina Thomas and Mrs. Isobel Slator who prepared the final text.

The financial assistance of the Alberta Research Council and the University of Alberta is also gratefully acknowledged.

TABLE OF CONTENTS

Page

List of Tables i

List of Figures iii

INTRODUCTION 1

PREDICTION OF MISCIBILITY 3

- Theory of Benham, Dowden and Kunzman 3
- Discussion of Benham, Dowden and Kunzman Correlation 8
- Alternate Theoretical Considerations 11
  - Method of Organick 13
  - Method of Kurata and Katz 14
  - Method of Eilerts 16
- Experimental Apparatus 19
- Experimental Procedure 24

RESULTS AND DISCUSSION 26

- Theoretical Results and Discussion of Critical Calculations 26
- Discussion of Experimental Results 33
- Discussion of Experimental Apparatus 46

SUMMARY AND CONCLUSIONS 50

RECOMMENDATIONS 54

NOMENCLATURE 55

Page

BIBLIOGRAPHY 57

APPENDIX A 60

APPENDIX B A-8

LIST OF TABLES

		Page
Table 1	Comparison of Critical Calculations	27
Table 2	Standard Deviations of Critical Calculations	28
Table 3	Recoveries of Reservoir Liquid	41
Table 4	Growth of Mixing Zones	44
Table 1-A	Compositions of Sample Hydrocarbon Mixtures	A-1
Table 2-A	Calculation of Criticals by Organick's Method for C-1	A-2
Table 3-A	Calculation of Criticals by Organick's Method for CH-P-843	A-3
Table 4-A	Calculation of Criticals by Modified Kurata-Katz Method for C-1	A-4
Table 5-A	Calculation of Criticals by Modified Kurata-Katz Method for CH-P-843	A-5
Table 6-A	Calculation of Criticals by Eilert's Method for C-1	A-6
Table 7-A	Calculation of Criticals by Eilert's Method for CH-P-843	A-7
Table 1-B	Description of Berea Sandstone Core	B-1
Table 2-B	Fluid Properties	B-2
Table 3-B	Air Permeability Data	B-3
Table 4-B	Liquid (Varsol) Permeability Data	B-4
Table 5-B	Pressure Profile Data Flowing Varsol	B-5
Table 6-B	Pressure Profile Data Flowing Varsol	B-6
Table 7-B	Pressure Profile Data Flowing Propane	B-7
Table 8-B	Pressure Profile Data Flowing Pentane	B-8
Table 9-B	Production Data: Displacement No. D	B-9
Table 10-B	Production Data: Displacement No. E	B-12

		Page
Table 11-B	Production Data: Displacement No. F	B-14
Table 12-B	Production Data: Displacement No. G	B-16
Table 13-B	Production Data: Displacement No. H	B-18
Table 14-B	Pressure Profile Data: Displacement No. D	B-20
Table 15-B	Pressure Profile Data: Displacement No. E	B-22
Table 16-B	Pressure Profile Data: Displacement No. F	B-23
Table 17-B	Pressure Profile Data: Displacement No. H	B-24
Table 18-B	Voltage Calibration of Transducers	B-25

LIST OF FIGURES

		Page
Figure 1	Miscible Displacement of Reservoir Fluid by Rich Gas (after Benham, Dowden and Kunzman)	4
Figure 2	Critical Points for Mixtures of Reservoir Fluid E, Propane and Methane (after Benham, Dowden and Kunzman)	6
Figure 3	Predicted Phase Conditions at 2500 psia for a Miscible Displacement (after Benham, Dowden and Kunzman)	7
Figure 4	Schematic Diagram of Displacement Apparatus	20
Figure 5	Differential Pressure versus Time from Recording Oscillograph	22
Figure 6	The Ratio of the Viscosity of the Reservoir Oil to the Viscosity of the Solvent (μ_o/μ_s) versus The Recovery of Oil (% OIP) at Solvent Breakthrough	42
Figure 1-B	The Pressure Differential Across Each Section of Core versus the Flow Rate of Varsol	B-26
Figure 2-B	The Pressure Defferential Across Each Section of Core versus the Flow Rate of Varsol	B-27
Figure 3-B	The Pressure Differential Across Each Section of Core versus the Flow Rate of Propane	B-28
Figure 4-B	The Pressure Differential Across Each Section of Core versus the Flow Rate of Pentane	B-29
Figure 5-B	The Recovery of Original Oil in Place versus the Cumulative Fluid Injected for Displacement No. D	B-30
Figure 6-B	The Oil Production Rate and GOR versus the Cumulative Fluid Injected for Displacement No. D	B-31
Figure 7-B	The Ratio of the Pressure Drop per Inch at (any time to) The Original Pressure Drop per Inch versus the Pore Volumes of Fluid Injected for Displacement No. D	B-32
Figure 8-B	The Recovery of Original Oil in Place versus the Cumulative Fluid Injected for Displacement No. E	B-33
Figure 9-B	The Oil Production Rate and GOR versus the Cumulative Fluid Injected for Displacement No. E	B-34

Page

Figure 10-B The Ratio of the Pressure Drop per Inch (at any time) to the Original Pressure Drop per Inch versus the Pore Volumes of Fluid Injected for Displacement No. E B-35

Figure 11-B The Recovery of Original Oil in Place versus the Cumulative Fluid Injected for Displacement No. F. B-36

Figure 12-B The Oil Production Rate and GOR versus the Cumulative Fluid Injected for Displacement No. F B-37

Figure 13-B The Ratio of the Pressure Drop per Inch (at any time) to the Original Pressure Drop per Inch versus the Pore Volumes of Fluid Injected for Displacement No. F B-38

Figure 14-B The Recovery of Original Oil in Place versus the Cumulative Fluid Injected for Displacement No. G B-39

Figure 15-B The Oil Production Rate and GOR versus the Cumulative Fluid Injected for Displacement No. G B-40

Figure 16-B The Recovery of Original Oil in Place versus the Cumulative Fluid Injected for Displacement No. H. B-41

Figure 17-B The Oil Production Rate and GOR versus the Cumulative Fluid Injected for Displacement No. H B-42

Figure 18-B The Ratio of the Pressure Drop per Inch (at any time) to the Original Pressure Drop per Inch versus the Pore Volumes of Fluid Injected for Displacement No. H B-43

INTRODUCTION

The ideal miscible displacement of reservoir oil depends upon the formation of a graded staturation bank between the original oil in place and the injected displacing fluid. This bank is all in a single phase with no interfaces present and therefore there are no capillary forces to cause the oil to be retained in pore channels as residual oil. This situation can be achieved by employing one or more different methods; namely LPG slug process, solvent flooding, high pressure gas drive or condensing gas drive. These processes are briefly outlined below:-

1) Miscible LPG Slug: A predetermined quantity of liquified petroleum gas, usually propane, is injected into the reservoir initially and is driven toward the producing wells by a secondary phase of water or dry gas.

2) Solvent Flooding: The entire reservoir is flooded with a solvent such as alcohol or LPG and some provision is made for recovering the solvent at the end of the flood.

3) High Pressure Gas Drive: Lean gas is injected into the reservoir at very high pressures and this injected gas absorbs intermediate hydrocarbons (C_2 - C_6) from the reservoir oil. This enrichment continues until a graded saturation bank is built up at the flood front thereafter miscibly displacing the reservoir oil ahead of it.

4) Enriched or Condensing Gas Drive: In this process gas rich in intermediate hydrocarbons (C_2 - C_6) is injected into the reservoir under conditions that will allow a large portion of these intermediate components to condense upon contact with the reservoir oil. Thus a low viscosity, graded saturation bank is formed which is driven toward the producing wells by the subsequently injected uncondensed gas.

Three of the factors which influence the efficiency of miscible drives are the reservoir temperature and pressure and the composition of the injected fluid. A certain pressure for a given temperature must prevail to maintain miscible conditions between oil and injected fluid. Proper requirements for pressure control of the reservoir must therefore be known in advance of commencement of a project for properly controlled miscible drive operations. The intermediate composition of the injected gas must also be controlled such that the composition will be a critical one and miscible drive can be achieved.

The mechanisms of high pressure gas drive and condensing gas drive have been described for the simple case of three pure components. Certain authors(3, 33) have endeavoured to use this description to determine quantitatively the conditions under which miscibility will be obtained for the case of crude oil and natural gas. This requires that the several components of the fluids be divided into three groups, each of which behaves like a pure substance.

The primary objectives of this research project were to carry out preliminary theoretical investigations of prediction of miscibility and to experimentally study the mechanism of a miscible displacement. It should be pointed out that the test results reported are for a liquid-liquid miscible drive, where it is known miscibility exists. This system was selected so that quantitative relationships between viscous fingering and viscosity ratio could be obtained.

PREDICTION OF MISCIBILITY

Theory of Benham, Dowden and Kunzman.

A recent analysis of the mechanism of miscible displacement by Benham, Dowden and Kunzman, has led to the development of a simplified method for predicting conditions of miscibility for an enriched gas drive. Their work makes use of a pseudo-ternary diagram, Figure 1, in which the mixture of reservoir oil and enriched injected gas is divided into three components, namely C_1 and C_2 - C_4 from the injected gas and C_{5+} from the reservoir oil. A vertical limiting tie line or limiting tie line of infinite slope is then imposed upon the diagram to indicate the phase conditions which can prevail during miscible displacement.

Justification of the use of this type of ternary representation is reported as follows: "if one considers a position some distance from the injection point, the character of the C_{5+} fraction in the liquid phase probably will not change by an appreciable amount during its approach to miscibility. Also if considerations are limited to the region close to the critical point and the associated limiting tie line, the character of the intermediate fraction will be close to that of the injection mixture. Therefore, a pseudo-ternary phase diagram (drawn using intermediates of character equal to that of the injection mixture and C_{5+} fractions having a character equal to that of the reservoir fluid) will have quantitative significance in the region of the critical point".

The use of the vertical limiting tie-line concept is explained by the fact that most hydrocarbon systems which were studied exhibited limiting tie lines of negative slope. Applying the afore stated assumption it is then concluded that: "the limiting, miscible, injection fluid

FIG. NO. I

MISCIBLE DISPLACEMENT OF RESERVOIR FLUID BY RICH GAS (AFTER BENHAM, DOWDEN AND KUNZMAN)

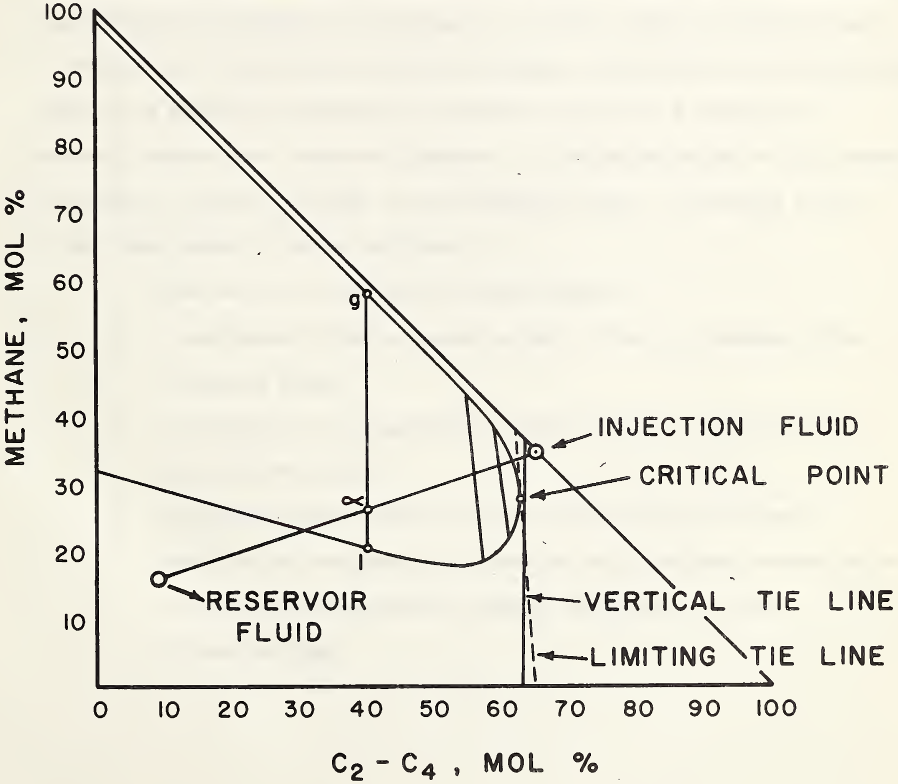

composition may be calculated by combining reservoir fluid with various mixtures of potential displacing fluid LPG and methane in various proportions and calculating the critical temperature and pressure for those mixtures".

A number of such calculations were carried out and the results for one particular reservoir fluid and a number of different displacing fluid mixtures are shown on Figure 2. By extending these calculations to cover a number of different reservoir fluids and displacing fluid compositions, a generalized correlation was developed. The final result of this work was a correlation of the maximum permissible methane concentration in the displacing fluid for a miscible displacement of reservoir fluids as a function of reservoir temperature, reservoir pressure, C_{5+} molecular weight of the reservoir fluid and C_{2+} molecular weight of the displacing fluid. An example of one of the final charts is shown on Figure 3.

The use of a chart such as this entails:-

1) Calculation of the molecular weight of the C_{5+} fraction of the reservoir fluid.
2) Calculation of the molecular weight of the C_2 - C_4 fraction of the displacing fluid.
3) Entry onto the correct correlation chart for the reservoir pressure and temperature in question and subsequent determination of the maximum permissible methane concentration in the displacing fluid.

FIG. NO. 2

CRITICAL POINTS FOR MIXTURES OF RESERVOIR FLUID E, PROPANE AND METHANE (AFTER BENHAM, DOWDEN AND KUNZMAN)

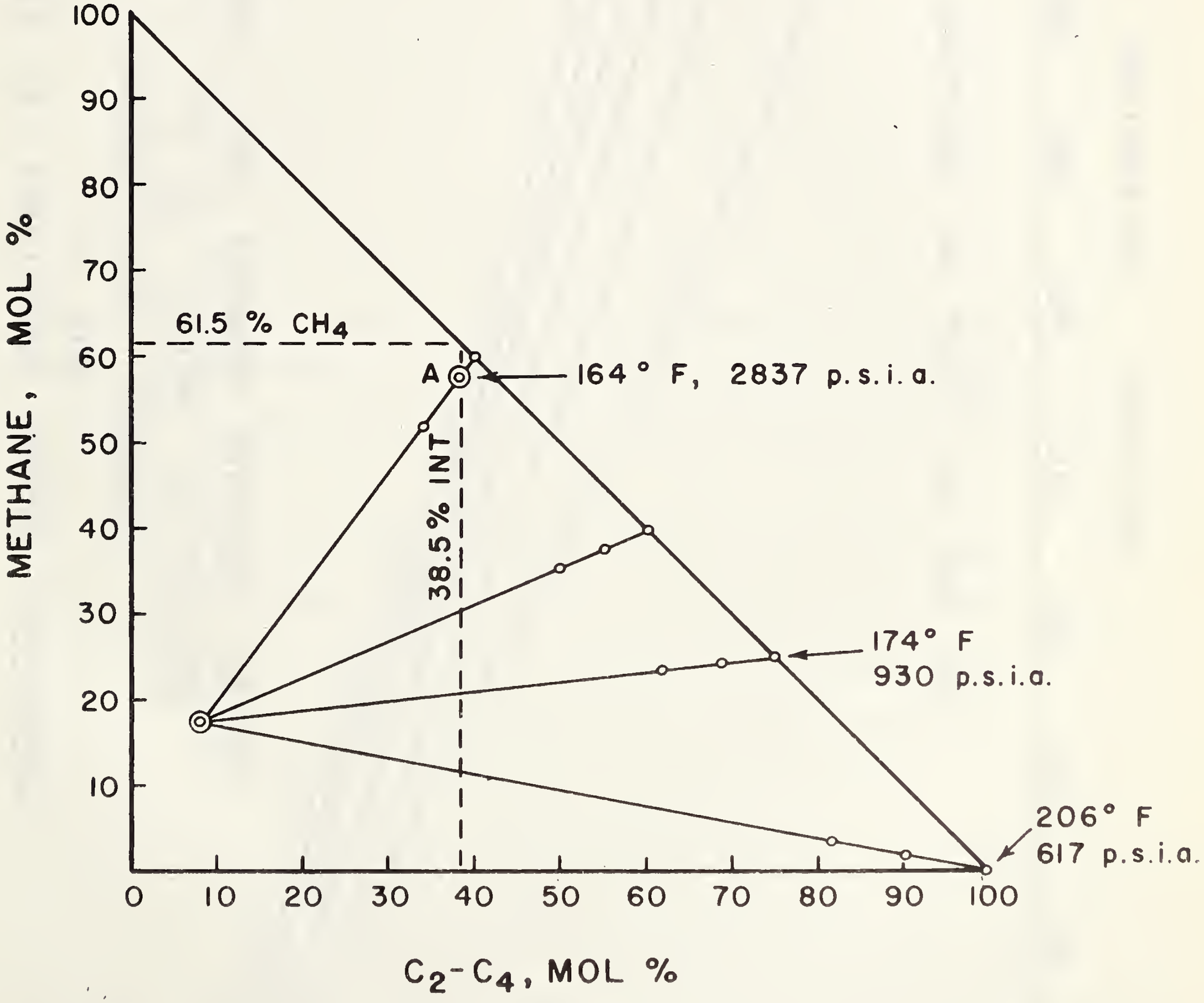

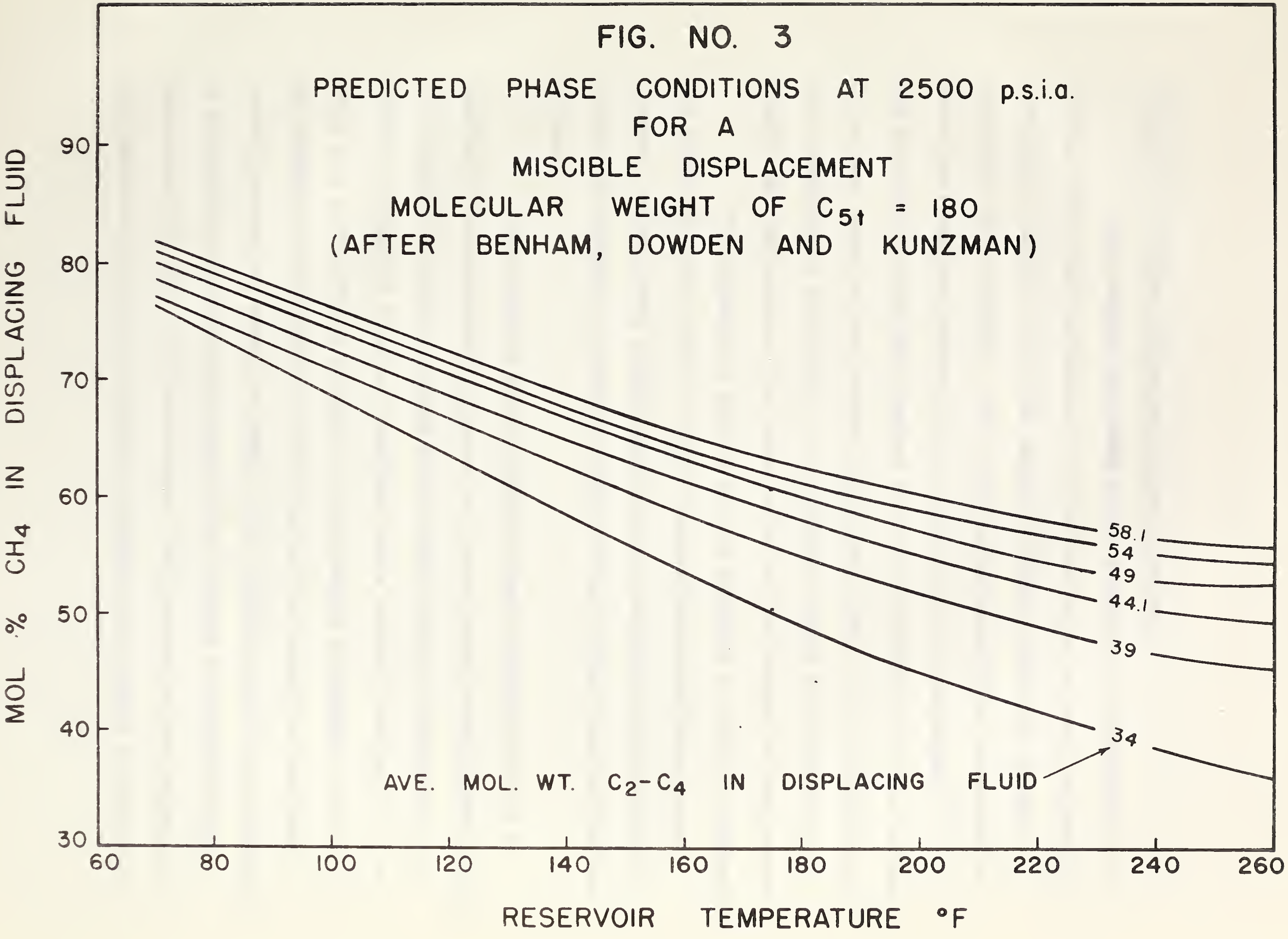

FIG. NO. 3

PREDICTED PHASE CONDITIONS AT 2500 p.s.i.a.
FOR A
MISCIBLE DISPLACEMENT
MOLECULAR WEIGHT OF C_{5+} = 180
(AFTER BENHAM, DOWDEN AND KUNZMAN)

Discussion of Benham, Dowden and Kunzman Correlation.

Work recently undertaken at the University of Alberta has led to some interesting speculation as to the feasibility of predicting miscible conditions, whether it be by the method of Benham, Dowden and Kunzman or by some other procedure. Use of the pseudo-ternary type representation for a multicomponent mixture has been questioned by recent authors(9) on the basis that it does not represent the true composition of various mixtures of gas and liquid in each section of the porous media. It is contended that the composition of any mixture in a particular section of the porous media depends upon the nature of the porous media and the velocity of displacement.

The mechanism by which a wet gas displaces a crude oil (condensing gas drive) is, for a period of time, a non-equilibrium gas displacement process. In the actual displacement process a saturation profile (gas-oil) in terms of distance is initially established and in some cases may continue to grow.

Even supposing that the pseudo-ternary representation can be considered thermodynamically rigorous in a porous media, certain other aspects of it must be considered. Benham et al. assumed that the limiting tie line would be of negative slope and therefore that a vertical limiting tie line would give a conservative estimate as to the amount of methane to be used for injection fluid dilution. This assumption can probably be considered correct provided the amount of ethane in the injection fluid is not excessive. No consideration, however, was taken for the presence of non-hydrocarbon components (H_2S, CO_2, N_2) in the mixture. The presence of such components will undoubtedly affect the critical temperature and pressure of the mixture

as well as the shape of the two-phase region on the diagram. Whether or not the assumption of a vertical limiting tie line will hold in cases of mixtures containing appreciable amounts of non-hydrocarbon components should be determined. Recent studies(33) have indicated that different groupings of components can be used when constructing a ternary diagram. It has been suggested that the best ternary representation can be obtained by dividing a mixture into the components:-

1) C_1, CO_2, and N_2
2) C_2-C_6 and H_2S
3) C_{7+}

Critical conditions for mixtures studied by Benham, Dowden and Kunzman were calculated using the method of Kurata and Katz(19) as modified by Davis, Bertuzzi, Gore and Kurata(8). Various mixtures of displacing fluid and reservoir fluid were used to calculate these criticals. It is therefore evident that the correct proportions of reservoir fluid and displacing fluid along with an accurate method of calculating criticals must be employed in order that the final correlations have some degree of accuracy.

Knowing the temperature and pressure of the reservoir and knowing the composition of the reservoir fluid, one can, by a series of trial and error calculations, determine a mixture which will have as its critical properties the pressure and temperature conditions of the reservoir. Once the composition of this mixture has been obtained it is possible to ascertain the proportions of displacing fluid and reservoir fluid which are in equilibrium at this condition. However, can it be assumed that the

proportions of these fluids will remain the same throughout the critical zone in the porous media? If they do not then loss of miscibility can occur.

Alternate Theoretical Considerations

It was originally thought that the controlling factor in determining the accuracy of the Benham et al. prediction was the calculation of the critical conditions. With this in mind an investigation of alternate methods of calculating criticals was undertaken. It was found that many methods have been developed to predict the critical temperature and pressure of mixtures and they are presented in literature(8, 10,12,19,22,25,29). The earliest of these was in 1937 when Smith and Watson(29) developed a correlation to be used on petroleum fractions. Their method requires a knowledge of the gravity of the stock, of its molecular weight, and of the molal average and weighted average boiling points.

Mayfield(22) in 1942 proposed a method for binary paraffinic systems which makes use of a weighted average critical temperature. A critical pressure is calculated using the differences between the weighted average critical pressure and the experimental literature values.

In 1942, Kurata and Katz(19) presented a method which is an extension of Smith and Watson's technique. Their calculation uses molecular weight, pseudo-critical temperature and a new function, M, designed to represent boiling range.

Organick(25) in 1953 was the first to develop a calculation specifically for a multi-component system containing hydrogen. This method uses a weighted average for calculation of critical temperature. To calculate critical pressure by this method however it is necessary to know the molal average boiling point and the weight average equivalent molecular weight.

In 1953, Davis, Bertuzzi, Gore and Kurata(8) modified the method which had previously been developed by Kurata and Katz. They

corrected the weighted average critical temperature for each binary pair in the system. This was done because deviation is greatest at nearly equal weight fractions. They also modified and substituted an arbitrary variable, M*, for the M function in the Kurata and Katz method. This was done to correct for the presence of nitrogen.

Eilerts(10) in 1957 developed a series of correlations for binary and complex mixtures based upon the boiling points of the pure components, the molal average boiling point, the pseudo-critical pressure, and a weighted combination of the critical temperatures and boiling points of the pure components.

In 1960, Grieves and Thodos(12) presented a new approach for calculating critical temperatures and pressures of mixtures containing aliphatic, napathenic and aromatic hydrocarbons as well as hydrogen. They introduced two dimensionless temperature parameters (γ and θ) which are defined by the molal average boiling point, the boiling point and the dew point of the mixture, all at atmospheric pressure. This method was developed primarily for binary systems and consequently it has not been used to any great extent on complex mixtures.

After a preliminary examination of the various methods of calculating criticals was completed it was decided to examine three of them in detail. The methods which were deemed to be best suitable for calculating critical conditions of a miscible type mixture were Organick's; the Davis, Bertuzzi, Gore and Kurata modification and Eilerts'.

Method of Organick.

Critical Temperature and Pressure.

Organick's method employs the use of two properties:-

1) Molal average boiling point.
2) Weight average equivalent molecular weight.

The molal average boiling point is calculated by the relationship:-

$$\bar{B} = n'_i B_i$$

where $\bar{B}$ = molal average boiling point

n'_i = mole fraction of component "i"

B_i = normal boiling point for component "i".

To obtain the molal average boiling point of the C_{7+} fraction, Organick used a correlation based on the A.S.T.M. distillation curve of the C_{7+} fraction. This correlation relates the slope of the 10% to 90% portion of the curve to the volumetric boiling point and the true boiling point. Using this correlation it is possible to obtain the mole fraction as well as the molal average boiling point of the C_{7+} fraction.

The "weight average equivalent molecular weight" is determined by the relationship:-

$$W = m_i M_{Ei}$$

where W = weight average equivalent molecular weight

m_i = weight fraction of component "i"

M_{Ei} = equivalent molecular weight of component "i".

i) for paraffin hydrocarbons, $M_E = M$

ii) for isomers or olefins, M_E is the molecular weight that a paraffin would have if it had the same boiling point as the isomer or olefin.

iii) for aromatic or napthenic compounds a special characterization factor is used.

Organick then plotted P_c vs T_c for various mixtures and using constant $\overline{B}$'s as a parameter, drew in families of lines. In a like manner he plotted P_c vs T_c again and using constant W's as parameters, drew in another set of lines. He then superimposed one plot upon the other and obtained a plot of P_c vs T_c with a grid of constant $\overline{B}$'s and W's upon it. Organick's investigations were carried out in two specific areas:-

1) Mixtures with $\overline{B}$'s from 700°R to 900°R and W's from 120 to 220.
2) Mixtures with $\overline{B}$'s from 250°R to 360°R and W's from 35 to 120.

In the final correlation Organick joined these two plots together by interpolating between known values. Therefore on his final chart the whole center section has been dotted in.

The use of the Organick method simply entails the calculation of $\overline{B}$ and W for a mixture and then entering the chart to pick off the corresponding P_c and T_c for that particular $\overline{B}$ and W.

Method of Kurata and Katz; - as modified by Davis et.al.

Critical Temperatures.

The critical temperatures of many mixtures are found to be nearly equal to the weight average critical temperatures, mT_c, of these mixtures. Kurata and Katz correlated the critical temperatures of hydrocarbon mixtures using the molal average critical temperature, T_{cn}, and the average molecular weight, with a special treatment for gases containing methane.

The method developed by Davis et al. for volatile mixtures consists of applying a set of corrections to mT_c, the weight average critical temperature. Existing data shows that mT_c approximates the true critical temperature, T_c. The deviation is greatest at nearly-equal weight fractions of any two components and can be approximated by:-

$$T_c - mT_c = A_{1,2}m_1m_2$$

where m_1 and m_2 are the weight fractions of components 1 and 2 respectively. The constant $A_{1,2}$ is characteristic of the particular binary mixture. This relationship was extended to complex mixtures by the equation:-

$$\begin{aligned} T_c - mT_c = {} & A_{1,2}m_1m_2 \quad A_{1,3}m_1m_3 \text{ - - - - - - - -} \\ & A_{2,3}m_2m_3 \quad A_{2,4}m_2m_4 \text{ - - - - - - - -} \end{aligned}$$

where a term is included for every possible binary pair.

Davis et al. derived constants for the above equation from existing data on binary systems. Where existing data were not available, interpolation and extrapolation procedures were used. A number of constants were also obtained from data on complex mixtures but, according to the authors, are subject to considerable error.

Critical Pressure

The critical pressures of the mixtures studied by Davis et al. were correlated by a modification of the method of Kurata and Katz. The original correlation was a plot of T_cP_{cn}/P_c vs T_{cn} with M as a parameter. This correlation was modified in the low temperature region ($T_{cn}\quad 400^{\circ}R$) by substituting an arbitrary variable, M*, for molecular weight, M, in order to account for gases containing nitrogen. When no nitrogen is present, M* is equal to M.

Method of Eilerts:-

Critical Temperature.

Eilerts' method is based upon the fact that the critical temperature of a mixture is higher than the critical temperature of the lightest component and lower than the critical temperature of the heaviest component. Therefore, by averaging the critical temperatures of the components of a multicomponent mixture on the basis of molal concentration and giving additional weight to the heaviest components, he proposed that a critical temperature can be estimated that will approximate the measured critical temperature. The normal absolute boiling point of the respective components was used as a weighting factor in order to emphasize the effect of the critical temperature of the components with high molecular weights on the estimated critical temperature.

Using this principle, Eilerts then obtained a correlation to improve the accuracy in computing the critical temperature of hydrocarbon mixtures. The ratio of the measured critical temperature to estimated critical temperature, Tcm/Tce, was used in preparing a correlation in which the measured critical temperature was related to the function, $(B_H - B_L)/B_F$

where: - B_H = normal boiling point of heavy (liquid) portion of mixture, ^oR

B_L = normal boiling point of light (vapor) portion of mixture, ^oR

B_F = normal boiling point of entire mixture, ^oR.

The correlating function depends for value solely on the composition of the mixture. The final Eilerts' correlation plotted the ratio of the measured critical temperature to estimated critical temperature vs a composition

variable, N_s, with selected values of B_H/B_L as parameters. The composition variable, N_s, was designated as the mole fraction of the mixture which is in the gas phase at 14.7 psia and 75°F. The values for T_{cm} and N_s were obtained from experimental data while T_{ce}, B_H and B_h were calculated.

Critical Pressure.

Eilerts realized that the critical pressure of a natural hydrocarbon mixture is usually higher than that of any component in the mixture and also higher than the molal average of the critical pressures of all components. Although computation of the molal-average critical pressure can be an important step in computing the true critical pressure of a mixture, the molal-average critical pressure alone is not a reliable indication of the true critical pressure. Eilerts developed a correlation plotting the ratio of the measured critical pressure to the molal-average critical pressure vs N_s with B_H/B_L as parameters. Again P_{cm}, the measured critical pressure, and N_s, the mole fraction of the mixture in the vapor phase at 14.7 psia and 75°F, were obtained from experimental data. The molal-average critical pressure, P_{cn}, and the boiling points of the liquid and vapor portions of the mixture, B_H and B_L respectively, were calculated.

Use of the Eilerts' correlations for determining critical temperatures and pressures of mixtures entails calculation of the vapor-liquid equilibrium ratios of each component which would occur at 14.7 psia and 75°F. This, of course, requires an accurate analysis of the components in the C_{7+} portion of the mixture. To obtain this analysis, Eilerts uses the results from a U.S.B.M. distillation on the C_{7+} portion of the mixture.

A comparison of the critical temperatures and pressures obtained using the three different calculation methods on various naturally occurring hydrocarbon mixtures is presented in Table I of the Discussion and Results Section.

Experimental Apparatus:

Figure 4 is a schematic diagram of the experimental apparatus used during this project. The simulated reservoir employed was a consolidated Berea sandstone core, 2 inches in diameter and 36 inches long. The core was mounted in a length of steel casing 4.5 inches in diameter. The annular space between the casing and the core was filled with Shell Epon Resin. A continuous bond between the core and the resin and between the resin and the casing wall was thereby obtained. This insured that there would be no bypassing of fluids past the core. The average porosity of the core was experimentally determined to be 16.3 per cent while the average liquid permeability was 266 millidarcies. The casing and core were mounted between two flanges which were held together with tie-rods.

Pressure taps were drilled at 6 inch intervals along the core and Statham Model PM80TC± 15-350 Differential Pressure Transducers were mounted in series along the core. Originally four of these transducers were used but later this number was changed to three in order that the sections of the core, across which each transducer measured the differential pressure, would be even in length. The transducers had a pressure range of plus or minus 15 pounds per square inch differential and an absolute operating pressure of 5000 p.s.i.a. They were temperature compensated in the interval 0°F to 200°F. The maximum excitation voltage recommended for each transducer was 16 volts and the approximate output resistance of each was 350 ohms. Input voltage to the transducers was supplied by a Kepco Model SC - 18 - 1, voltage regulated D.C. power supply. The D.C. output of this instrument was 0 to 18 volts and 0 to 1 amp. with an A.C. input of 105 to 125 volts at 50 to 65 cps. All voltages within the system were measured with a Non-Linear Systems Model 484A Industrial

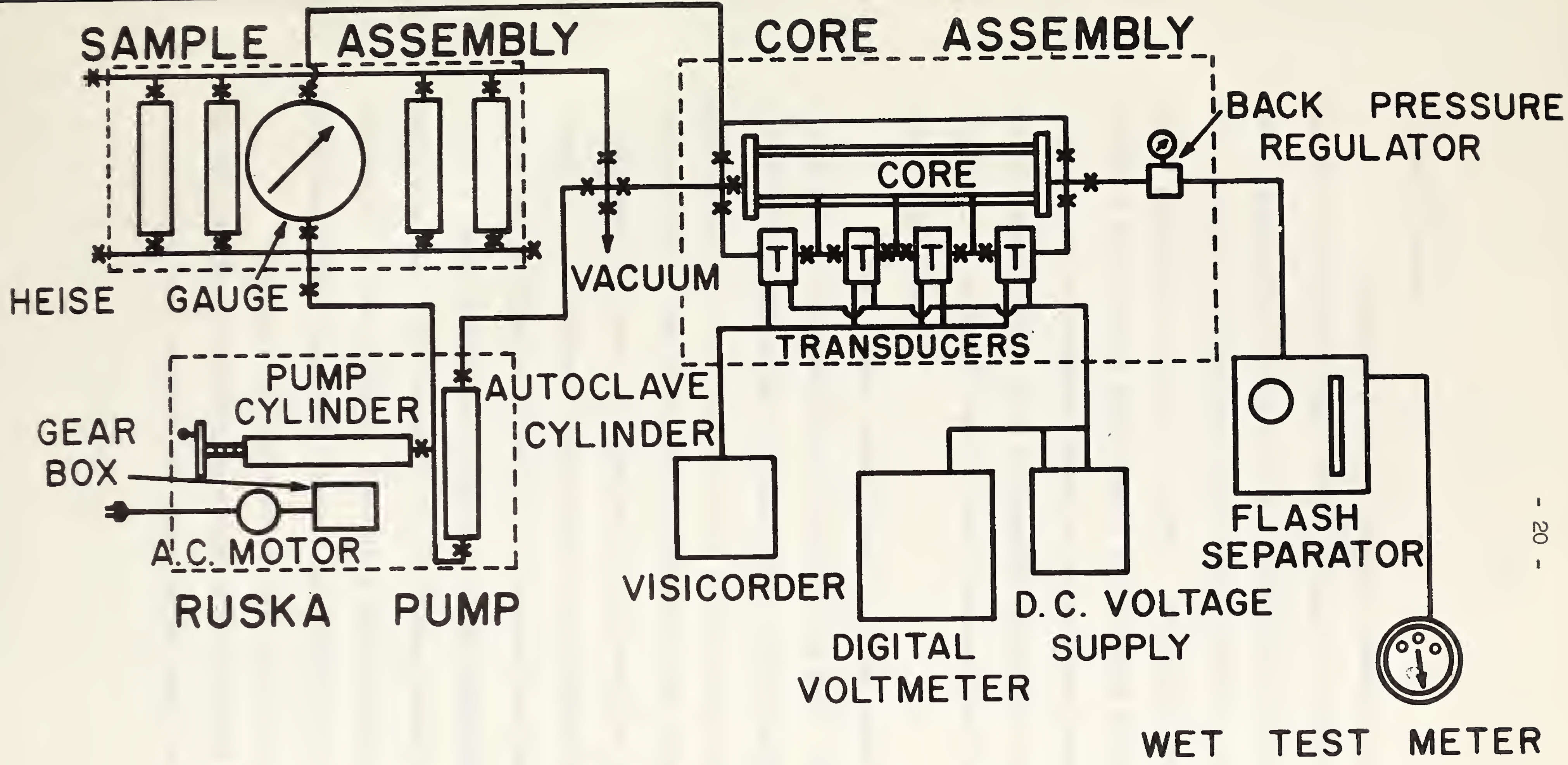

FIG. NO. 4
SCHEMATIC DIAGRAM
OF
DISPLACEMENT APPARATUS

Digital Voltmeter.

The output from the pressure transducers was recorded by a Honeywell Model 906C Visicorder. This instrument is a direct reading type of oscillograph which prints a trace on continuously moving photographic paper. This is done by passing the input current from each transducer to a miniature mirror galvanometer in the Visicorder. The mirror galvanometer then reflects a beam of ultra-violet light onto a moving sheet of photographic paper. Using this equipment a permanent record of differential pressure versus time between any two pressure taps could be obtained throughout a complete displacement. Figure 5 is a reproduction of a chart obtained from the Visicorder during an actual displacement.

The pressure sensing and recording system was calibrated prior to the initial displacement of fluid into the core. This was done by placing a full-scale differential pressure across each transducer and varying the input voltage to the transducer until a full-scale reading was obtained on the Visicorder. The differential pressure on the transducer was then lowered in increments to zero and increased to full-scale to check the Visicorder for linearity. All pressure differentials were measured by a mercury manometer during this calibration procedure. An attempt was made to check the calibration factor of each transducer as reported by the manufacturer but this became impossible due to the insensitivity of voltage measuring devices which were available. It was, however, discovered that full-scale deflection of the diaphragm in the transducer required approximately 0.1 cc of liquid.

The core and transducers were enclosed in a constant temperature air bath while the recording instruments were mounted in an adjacent location. Displacements were carried out using a Ruska Model 2243 - B11l - U Q Positive

DIFFERENTIAL PRESSURE vs. TIME from RECORDING OSCILLOGRAPH

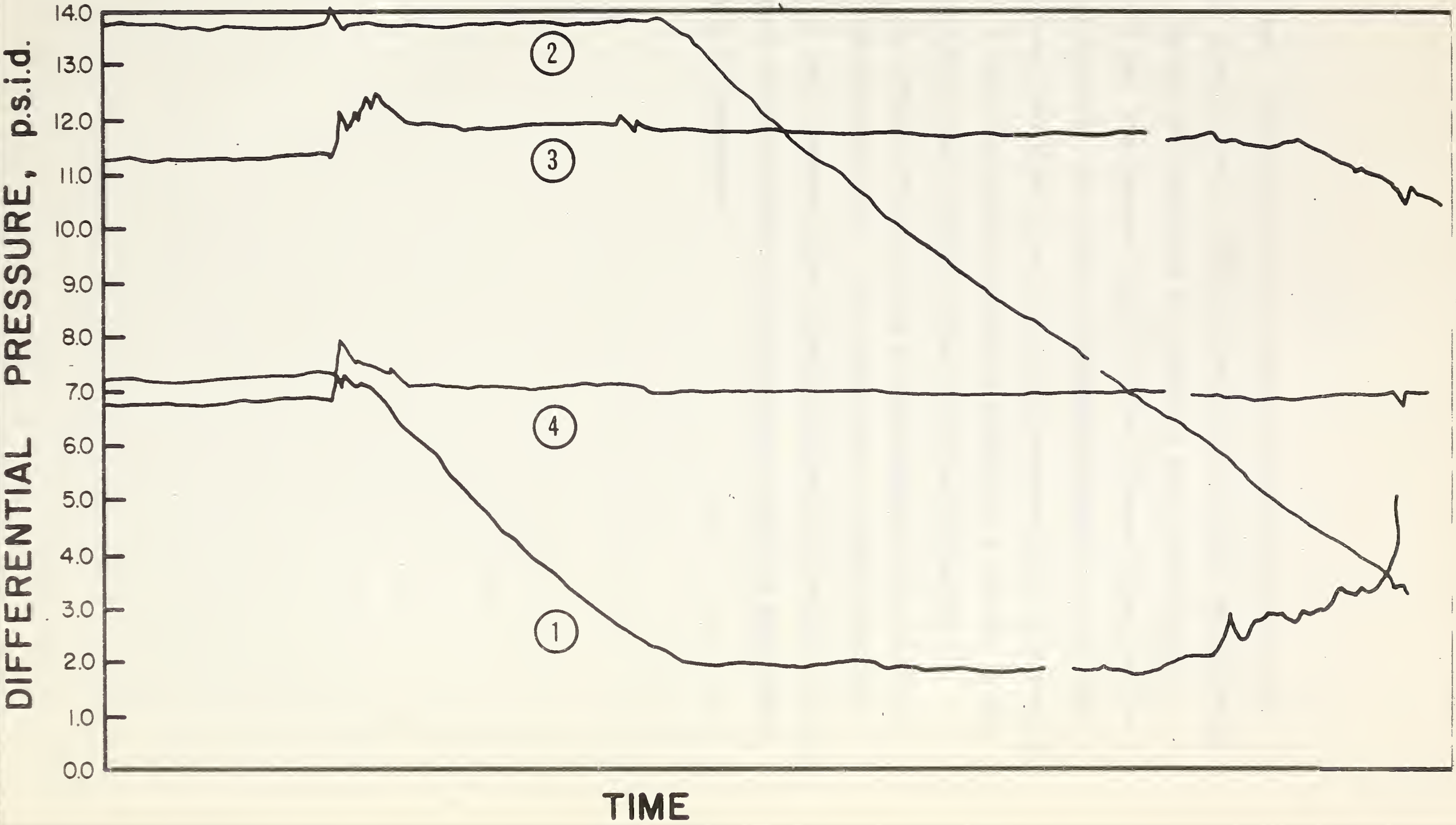

Displacement Pump. This pump was of the double-cylinder type and was geared for discharge rates of from 10 to 1200 cc per hour per cylinder and calibrated to 0.01 cc. The pump was manifolded to a series of high pressure sample containers such that simultaneous injection of two different fluids could be carried out if required. All absolute displacement pressures as well as the upstream and downstream pressure on the core were measured with a 3000 p.s.i.a. Heise gauge. A Grove back pressure regulator, supplied by a nitrogen bottle, was used to maintain a back pressure on the core during displacements.

The effluent produced during a displacement was run through a Ruska Model 7598 Flash Separator. This separator had a pressure range of 0 to 500 p.s.i.g. and a graduated glass separation column with a volume of 50 cc. Any gas produced from the separator was measured with a wet test meter before being vented to the atmosphere.

Experimental Procedure:

Prior to the introduction of any liquid into the core the entire apparatus was pressure tested to 2000 p.s.i.g. with nitrogen to check for leaks. A vacuum was also imposed upon the core for 24 hours as an additional check. Air was then flowed through the core at various rates in order to obtain the permeability of the core to air as well as to check the operation of the pressure sensing and recording devices. The data obtained during these air permeability tests are shown in Table 3-B of Appendix B.

The core was then evacuated for 24 hours and at the end of this time saturated with varsol. Knowing the amount of varsol injected, the porosity of the core was calculated. Varsol was then displaced through the core at 7 different rates and liquid permeabilities were calculated. The data for these liquid permeability tests are shown in Table 4-B of Appendix B. Subsequently during the project, after the number of pressure transducers had been reduced to 3 from 4, pure varsol was again displaced through the core at 5 additional rates. At the time of these latter displacements pure propane was also displaced through the core at 15 different rates.

Prior to the initiation of an actual miscible type displacement, the clean core was evacuated for 24 hours. The core was saturated with varsol and a check on the core porosity was obtained. Approximately 5 pore volumes of crude oil were then injected into the core displacing the varsol. If some reservoir fluid other than crude oil were to be used then the initial saturation with varsol was not carried out. When the core was saturated with reservoir fluid all lines leading to the transducers and the Heise gauge were purged of gas and filled with liquid. A back pressure was then imposed upon the system and the pressure in the core, transducers, and displacing fluid containers, was gradually built up to the desired displacement pressure. This back pressure

was generally in the region of 1600 p.s.i.g.

All flow through the core was then stopped and the system was allowed to come to equilibrium. When this condition was attained the transducers were zeroed and initial pump and production readings were taken. The displacement pump was once again started and additional reservoir fluid was injected through the core. This was continued until stable pressure differentials from the Visicorder were obtained along the entire core length. When this occurred the injection line was transferred from the reservoir fluid container to the displacing fluid container with out stopping the displacement pump. A stop watch was then started and all production and injection data were recorded from this time on. Displacements were carried on as long as were deemed necessary in order to obtain sufficient data.

At the end of the displacement the injection pump was stopped and the core was depressured by bleeding off the back pressure regulator. Any production of fluids which occurred during this interval was noted and recorded. After the core had been depressured it was flushed with pentane until the effluent appeared to be pure pentane. During this flushing operation all effluent was collected and measured. The liquid portion of the effluent was then allowed to weather for a few days and, after the pentane had evaporated, any reservoir oil which had been produced during the flushing operation was measured and recorded.

After the core had been flushed with pentane, pure propane was flowed through it for several hours. The propane was then followed by approximately 150 cubic feet of nitrogen. The core was then dried by alternately flowing air through it and then imposing a vacuum on it for four days. An attempt was made to duplicate the entire procedure, from initial saturation to cleaning, during each displacement.

RESULTS AND DISCUSSION

Theoretical Results and Discussion of Critical Calculations:

A comparison of the measured and predicted critical temperatures and pressures of twelve different hydrocarbon mixtures is made in Table 1. The methods used for calculating criticals were those of Organick's; Kurata and Katz partially modified and Eilerts. The calculated criticals of all mixtures with the exception of "CH-P-843" were available in the Literature(10, 25).

The standard deviations in predicted critical temperatures and pressures were calculated and appear in Table 2. The following equation was used for this calculation:

$$\text{Standard Deviation} = \sqrt{\sum_{i=1}^{N} \frac{(\text{observed value} - \text{predicted value})^2}{N - 2}}$$

where N = number of mixtures.

From Table 2 it would appear that the method of Organick is superior to the others in predicting critical pressures. For predicting critical temperatures, Organick's and Eilerts' correlations compare favorably and both give better results than the Kurata-Katz procedure. These conclusions, of course, are made from comparison of a limited number of samples.

The compositions of each of the mixtures, with the exception of mixture number 11, are tabulated in Appendix A along with sample calculations of each method of predicting criticals. All mixtures contained appreciable amounts of methane, ranging from 64% in mixture C-1 to 82% in mixtures B-1 and C-2. The amount of C_{7+} components in each mixture was relatively small; from 2% in mixture C-2 to 12% in several of the other mixtures. Two of the mixtures, CH-P-843 and E, contained nitrogen as well as carbon dioxide while the rest contained CO_2 only. From Table 1 it can be seen that the deviations

TABLE 1

COMPARISON OF CRITICAL CALCULATIONS

Mixture No	Author	Measured Criticals Tc(°R)	Measured Criticals Pc(psia)	By Organick Tc(°R)	By Organick Pc(psia)	By Eilerts et al using charts Tc(°R)	By Eilerts et al using charts Pc(psia)	By Modified Kurata Katz Tc(°R)	By Modified Kurata Katz Pc(psia)	Mol Fraction in Vapor Phase @ 14.7 psia & 75°F
1	Allen(1) A-1	744.7	5130	708	5320	689	5060	650	6640	0.865,26
2	A-2	710.7	5350	703	5330	683	5065	648	6290	0.868,81
3	B-1	559.7	6000	536	5760	616	6820	606	5980	0.893,61
4	B-2	619.7	5820	578	5780	625	6650	610	5950	0.887,82
5	B-3	671.7	5620	657	5600	660	5720	632	6800	0.868,40
6	C-1	654.7	2720	649	2930	651	2225	628	2740	0.888,09
7	C-2	459.7	2270	472	2220	470	1910	497	2070	0.983,95
8	D	698.7	5100	742	5100	705	4670	661	5640	0.858,30
9	E	604.7	5570	-	-	690	4040	-	-	0.883,36
10	F	702.7	5150	720	5200	695	5050	655	5810	0.863,25
11	Organick(25)	679.7	4000	730	4000	684	3440	657	4760	0.878,50
12	Eilerts(10) CH-P-843	396.5	1156	500	2500	495	1830	520	2130	0.978,63

STANDARD DEVIATIONS

No. of Mixtures	Organick's Method		Eilerts' Method		Modified Kurata-Katz	
	Tc (^oR)	Pc (psia)	Tc (^oR)	Pc (psia)	Tc (^oR)	Pc (psia)
12	-	-	49.3	716	-	-
11, excluding Mixture CH-P-843	-	-	40.4	721	-	-
11, excluding Mixture E	44.8	466	43.5	558	66.4	881
10, excluding Mixtures E and CH-P-843	30.6	134	30.5	541	55.4	869

$$\text{Standard Deviation} = \sqrt{\frac{\sum_{1}^{N} (\text{observed value} - \text{predicted value})^2}{N - 2}}$$

where: N = number of mixtures

were large for all methods when the mixture contained nitrogen. All the mixtures studied could be classified as gas condensates because of the small amount of liquid present at equilibrium conditions. The mole per cent of the mixture in the vapor phase at equilibrium conditions at 14.7 p.s.i.a. and 75°F varied from 85% for mixture D to 98% for mixture C-2.

Examining each method of predicting criticals individually, a few general conclusions can be drawn. Organick's correlation appears to be quite good for those mixtures with high methane concentrations and little or no acid gas components. However, if the concentration of the lighter components becomes too large, resulting in a low weight average equivalent molecular weight, Organick's correlation becomes inaccurate. This is due to the fact that the lines on the correlation grid change slope rapidly in this region at low weight average equivalent molecular weights. The accuracy of the Organick correlation can also be questioned when one is working in the central regions of the grid where all lines have been drawn in by interpolation.

The calculations involved in the Organick prediction are relatively simple providing an accurate A.S.T.M. distillation analysis of the C_{7+} portion of the liquid phase is available. Without this distillation analysis, the accuracy of the calculation suffers.

The prediction of criticals using Eilerts' correlations involve the most complex calculations of any of the three methods studied. Not only is an accurate U.S.B.M. distillation of the C_{7+} portion of the mixture required but also the vapor-liquid equilibrium ratios of the mixture must be calculated at a standard state. This of course entails a trial and error procedure. The prediction of critical temperatures by the Eilerts method compares quite favorably with results obtained using Organick's procedure. This is because both

procedures use the normal absolute boiling point of each component as a weighting factor when calculating critical temperature.

Prediction of critical pressure by the Eilerts method is not nearly as accurate as prediction of critical temperature especially if use is made of the original charts published in Monograph 10 of the U.S. Bureau of Mines. While Eilerts used all of the mixtures presented in Appendix A to develope his correlation, he balanced positive and negative deviations when drawing the final charts. Consequently, use of these charts can sometimes lead to a considerable error in the answer. This is particularly true when the mole fraction of the mixture in the vapor phase at 14.7 p.s.i.a. and 75°F approaches 1.0. In this region the slopes of the lines on the correlation chart approach infinity and it is difficult to obtain a satisfactory answer. This problem is also encountered when using the critical temperature correlation chart. In the region where the mole fraction in the vapor phase is less than 0.5, all lines have been extrapolated on both charts and the accuracy of the correlation in this region is questionable.

As was the case with Organick's method, the Eilerts correlation gives best results when the mole fraction of the mixture in the vapor phase is below 0.90 and when the mixture contains little or no nitrogen. The secondary disadvantage of the Eilerts procedure is the laborious calculations which have to be carried out in order to make use of the correlation. It is doubtful if the accuracy of the results obtained justify the work involved.

The third method of predicting criticals which was investigated was a partially modified version of the Kurata-Katz procedure. This, as far as can be determined, was the method used by Benham, Dowden and Kunzman when they developed their correlation for predicting miscibility. In this procedure use is made of the M* correction developed by Davis, Bertuzzi, Gore and Kurata

to account for the presence of nitrogen in the mixture when calculating critical pressure. However, critical temperatures predicted by Benham, Dowden and Kunzman were obtained using the original Kurata-Katz procedure. The predicted criticals shown in Table 1 under the heading Kurata-Katz were therefore calculated in the same manner.

The predicted criticals shown in Table 1 and the standard deviations shown in Table 2 indicate that the Kurata-Katz method was the least accurate procedure of the three investigated. Also there did not seem to be any trend to the Kurata-Katz method with regard to mole fraction of vapor present or mole fraction of nitrogen present. One drawback to predicting critical pressures with this method is the fact that the correlation graph plots critical pressure as a function of molal average critical pressure, molal average critical temperature, true calculated critical temperature and molal average molecular weight of the mixture. Thus if the true calculated critical temperature is in error then the predicted critical pressure obtained from the correlation chart will probably also be in error. In addition to this the molal average molecular weight can be inaccurate unless sufficient information about the C_{7+} portion of the mixture is available.

The advantage of the Kurata-Katz procedure is its relative simplicity and the comparatively easy calculations which are involved. When a distillation analysis of the C_{7+} portion of the mixture is unavailable then this method or its modified form is definitely the best procedure to use when calculating critical conditions. The limitations which are involved when using this method must be kept in mind however.

The accuracy of all the procedures available for calculating critical conditions is necessarily dependent upon the accuracy of the mixture

analysis. It is therefore imperative that as detailed an analysis as possible be obtained, if calculations of the critical temperature and pressure of a naturally occurring hydrocarbon mixture are to be attempted.

Discussion of Experimental Results:

Initial displacements were carried out on the Berea sandstone core to determine both its air and liquid permeabilities as well as the porosity of the core. These initial displacements also served to familiarize the investigators with the experimental equipment.

Air was flowed through the core at 10 different rates and the permeability of the core to air was calculated at each of these rates. The results of these calculations are shown in Table 3-B. From these observations the average permeability of the core to air was found to be 293.9 millidarcies. An attempt was made to plot air permeability against the inverse of the mean pressure in order to illustrate the Klinkenberg effect. However, the wedely scattered data which were obtained for the low flow rates used made this impractical.

The liquid permeability of the core was obtained by flowing varsol through it at various rates and absolute pressures. The data resulting from these displacements are shown in Table 4-B. In all, 37 displacements were carried out at different reservoir conditions. The resulting average liquid permeability of the core was calculated to be 266.4 millidarcies. While there was some variance in the experimental data obtained, all of the runs were used when the average permeability was calculated. The most pronounced deviations were observed to occur at low absolute reservoir pressures during low flow rates. As the reservoir pressure was increased during these low rates, the permeabilities obtained seemed to become more stable. The tendency for the permeability to vary with reservoir pressure was not as

marked at higher displacement rates. From these results it would appear that liquid permeabilities should be obtained during relatively high displacement rates (200 cc per hour or greater) for a porous media of the type under investigation.

Additional displacements of pure fluids through the core were carried out at various times during the investigation. To preserve continuity all of these "pure fluid displacements" will be discussed at this time. Tables 5-B to 8-B inclusive show the pressure data which were obtained during displacements of varsol, propane and pentane through the core. The data in Table 5-B were obtained while four differential pressure transducers were mounted on the core. The data in the other three tables were taken using only three transducers. The data from each of the Tables were plotted and appears as Figures 1-B to 4-B inclusive.

All results indicated that the pressure differentials across the entire core became increasingly non-uniform as the displacing rate increased. That is to say adjacent sections of the core were not subjected to the same pressure drops, especially at higher flow rates. This of course would be natural if the permeability of the core was not uniform throughout its entire length. When varsol and propane were used as the injection fluids, section 2, or the middle portion of the core, consistantly was subjected to the least pressure differential. This would indicate that section 2 was slightly more permeable than the end sections of the core.

The data shown for the displacement of pure pentane through the core were obtained at a later date than the data for either the varsol or propane displacements. The pentane displacements were carried out approximately midway through the investigation, prior to the start of Displacement No. F.

After completion of Displacement No. E and before the pentane displacements took place, the core was reversed in the flanges so that the original outlet end became the inlet face. The reasons for this reversal will be discussed later. The pressure differentials obtained while flowing pentane in this reversed direction are shown on Figure 4-B. On this plot the pressure differentials across sections 1 and 2 are quite similar while the pressure drop across section 3 is greater than for either of the first two sections. This is increasingly apparent as the flow rates increase. This phenomena could be due to damage to the original inlet end of the core during Displacements No. D and No. E.

Five miscible, liquid-liquid displacements were run on the core during the investigations. These displacements were numbered D, E, F, G, and H. The production data for each of them is contained in Tables 9-B to 13-B inclusive. Pressure profile data was obtained on four of the displacements, D, E, F and H and is recorded in Tables 14-B to 17-B inclusive. For each run, with the exception of number G, plots were drawn of:

1) Cumulative Oil Production (% OIP) versus Cumulative Fluid Injected (pore volumes),
2) Gas-Oil Ratio (cc/cc) and Oil Production Rate (cc/min) versus Cumulative Fluid Injected (pore volumes),

and 3) The Pressure Drop per Inch at any time versus the Original Pressure Drop per Inch (p.s.i.d./in.).

A plot of this last relationship is not included for Displacement No. G due to the low pressure differentials which were present during this run. The results of these miscible displacements will be discussed in the chronological order in which they were run.

The initial miscible flood performed was Displacement No. D where crude oil was displaced by liquid propane at a rate of 60 cc per hour. The ratio of the viscosity of the crude oil to the viscosity of the liquid propane was 70.5. During this flood, a recovery to initial solvent breakthrough of approximately 30 per cent of the original oil in place was obtained. The recovery of oil at secondary solvent breakthrough was 55 per cent of OIP and the final recovery was 75 per cent of OIP after injection of approximately 1.7 pore volumes of liquid propane. These recoveries, while seemingly low for a miscible type drive, are in general agreement with results obtained by other investigators(4, 24). The poor recoveries appear to be caused mainly by the adverse viscosity ratio encountered during the displacement of a relatively viscous crude oil by liquid propane.

A better idea of the displacement process can be obtained from the plot of GOR and oil production rate versus pore volumes of fluid injected. Up to injection of approximately 0.28 pore volumes, the effluent produced to the separator was a single liquid phase. At this point initial solvent breakthrough occurred and recovery of two separate phases began. After approximately 0.68 pore volumes of propane had been injected, a suggested second solvent breakthrough occurred as indicated by a rapid rise in GOR and a corresponding decline in production rate. The first premature arrival of propane may be attributed to the effects of viscous fingering. From this first solvent arrival until the secondary breakthrough, it is suggested that the propane and oil are intimately mixed and completely miscible such that the fluid flowing is an oil enriched with injected propane. There is some evidence from the results that the mechanism after the secondary breakthrough is similar to the subordinate stripping action of a non-equilibrium

two-phase gas drive displacement thus accounting for the high residual oil saturation at the termination of the test.

The pressure profile plot for this displacement also indicates the presence of viscous fingers. The profile along the core is initially stabilized and is a straight line at unit value. With the injection of displacing fluid, a zone of very low pressure drop advanced into the core. This zone of low pressure drop reached the downstream 6 inches of the core after only 0.139 pore volumes of fluid had been injected. The pressure drop, of course, was primarilly due to the highly viscous oil being displaced by a fluid of much lower viscosity.

The second miscible flood undertaken was Displacement No. E where commercial varsol was displaced by liquid propane at a rate of 200 cc per hour. The ratio of the viscosity of the varsol to the viscosity of the propane in this case was 8.6. The recovery of original varsol was 45 per cent of "initial oil in place" when solvent breakthrough occurred during this flood. At the end of the test approximately 1.8 pore volumes of propane had been injected into the core and 95 per cent of the "initial oil in place" had been recovered. (During subsequent discussions the term "initial oil in place" shall refer to whatever fluid the core was saturated with before a displacement was carried out). During blowdown and cleanup operations, after completion of the run, all remaining varsol in the core was recovered.

Neither the recovery data nor the GOR and oil production rate data indicated the occurance of a secondary solvent breakthrough during this displacement. Initial solvent breakthrough occurred after 0.4 pore volumes of propane had been injected into the core. From this point until

the end of the test the GOR steadily increased while the oil production rate decreased gradually. These results indicate that viscous fingering was not such a prominant factor during this displacement as it was during Displacement No. D. This is also borne out by the fact that the pressure profile data shows that the outlet 12 inches of the core did not exhibit a drop in pressure differential until 0.261 pore volumes of propane had been injected.

After completion of Displacement No. E, an attempt was made to rerun the previous test involving crude oil and propane. Difficulties were encountered however when the core was being saturated with crude oil. During this saturation it was observed that practically all of the pressure drop across the core, when crude oil was flowing at 60 cc per hour, was confined to the inlet 12 inches of the core. The core was backflushed with pentane and cleaned and dried before another attempt was made to saturate it with crude oil. Again the results were unfavorable with the definite indication of plugging taking place at the inlet end. The core was again backflushed and cleaned and was then dismantled from its flanges. Upon examining the core it was observed that the rubber end gaskets had swelled until they were partially covering the face of the core. It was also noted that the inlet end of the core was very heavily oil-stained particularly on its bottom side. This indicated the possibility that gravity segregation took place during the flow of the heavy crude oil. It was decided to thoroughly clean the core with pentane, replace the original rubber gaskets with new gaskets and remount the core in the flanges in a reversed position. This was done with the result that the original partially-damaged inlet end now became the outlet end. From this time on it was noticed that the pressure differential across section 3 i.e. the outlet section, was slightly higher than it was across either of the other two sections.

The next miscible flood undertaken was Displacement No. F which, along with Displacement No. G, represent the portion of the investigation carried out at low viscosity ratios. Displacements No. F and No. G both entailed the displacement of commercial pentane by liquid propane at rates of 400 and 200 cc per hour respectively. The ratio of the viscosity of pentane to the viscosity of propane in these cases was 2.13. The recoveries of original pentane obtained at solvent breakthrough were 70.0 per cent of OIP at the faster rate and 65.0 per cent of OIP at the slower rate. Final liquid pentane recoveries of 79 and 78 per cent of OIP were obtained after only 0.9 pore volumes of propane had been injected. From this point until completion of the test, no additional liquid pentane was recovered during either displacement. Material balance calculations were carried out on both displacements and they indicated that approximately 20% of the original pentane in the core was vaporized in the separator and was measured in the effluent as a gas along with the propane. On the basis of these material balance calculations and the fact that during the cleanup of the core no additional liquid pentane was recovered, it can be assumed that 100 per cent of the original pentane in place was recovered during both displacements. Up to the time of initial solvent breakthrough it is thought that very little pentane was flashed into the vapor phase. However, after arrival of the miscible liquid to the separator, it is believed that portions of the liquid pentane started to vaporize as the propane flashed from liquid to gas.

Again, as in the case of propane displacing varsol, neither the recovery data nor the GOR and oil production data indicated the occurrance of a secondary solvent breakthrough. Initial solvent breakthrough occurred at the high rate after 0.68 pore volumes of propane had been injected. At the

low rate, initial solvent breakthrough was observed after 0.64 pore volumes of propane had been injected. It is possible that at the lower rate, diffusional effects at the flood front between the propane and pentane could account for an earlier breakthrough and resultant smaller recovery of initial oil in place. There was no evidence of viscous fingering taking place during either Displacements No. F or No. G. This, of course, is to be expected when the viscosity ratio of the displaced and displacing fluids is relatively low. The pressure profile data for Displacement No. F confirmed this as the outlet 12 inches of the core did not show a drop in pressure differential until 0.556 pore volumes of propane had been injected into the core.

The final miscible flood performed was Displacement No. H where a heating oil, Esso P-40, was displaced by liquid propane at a rate of 200 cc per hour. The ratio of the viscosity of the heating oil to the viscosity of the liquid propane was 14.2. During this displacement, a recovery to initial solvent breakthrough of approximately 35 per cent of the original oil in place was obtained. As was the case with Displacement No. D where crude oil was displaced by propane, it is thought that a secondary solvent breakthrough was detected. The recovery of oil at this secondary breakthrough was approximately 57 per cent of OIP. The final recovery obtained during this flood was 76 per cent of OIP after injection of 1.5 pore volumes of liquid propane.

The similarity between this heating oil displacement and the crude oil displacement is very evident even though there is a five fold difference in viscosity ratios between the two floods. During Displacement No. H, the heating oil test, the effluent produced to the separator was a single liquid phase up to injection of 0.33 pore volumes of propane. From this point on recovery of two separate phases was observed. After injection

of 0.71 pore volumes of propane, a rapid rise in GOR occurred accompanied by a corresponding decrease in oil production rate. This suggested the occurrance of a secondary solvent breakthrough similar to the one experienced during Displacement No. D. Again it is suggested that the flood exhibited miscible-type characteristics up to the time of secondary solvent breakthrough, but after this time the displacement resembled the subordinate stripping action of a non-equilibrium, two-phase, gas drive. The pressure profile data for this displacement also suggested the presence of viscous fingers. A decrease in pressure differential across the outlet 12 inches of the core was observed after injection of only 0.216 pore volumes of liquid propane.

A summary of all recovery data obtained during the investigation appears in Table 3.

TABLE 3

RECOVERIES OF RESERVOIR LIQUID

Displacement Number	Displacement Rate	Viscosity Ratio $\mu_{oil}/\mu_{solvent}$	Rec. of Res. Liquid at B.T.	Rec. of Res. Liquid After 1.0 PV Displaced
	(cc/hr)		(% OIP)	
No. D	60	70.5	30	65
No. E	200	8.6	45	83
No. F	400	2.13	70	79.5 +
No. G	200	2.13	65	78 +
No. H	200	14.2	35	67

The Cumulative Oil Recovery to Initial Solvent Breakthrough was plotted versus the Viscosity Ratios of the oils and solvent and appears as Figure 6. Superimposed upon this plot are the results obtained by Offeringa and van der Poel(24). during their miscible and immiscible tests on scaled models. As can be seen there is relatively good agreement between their results and the data obtained

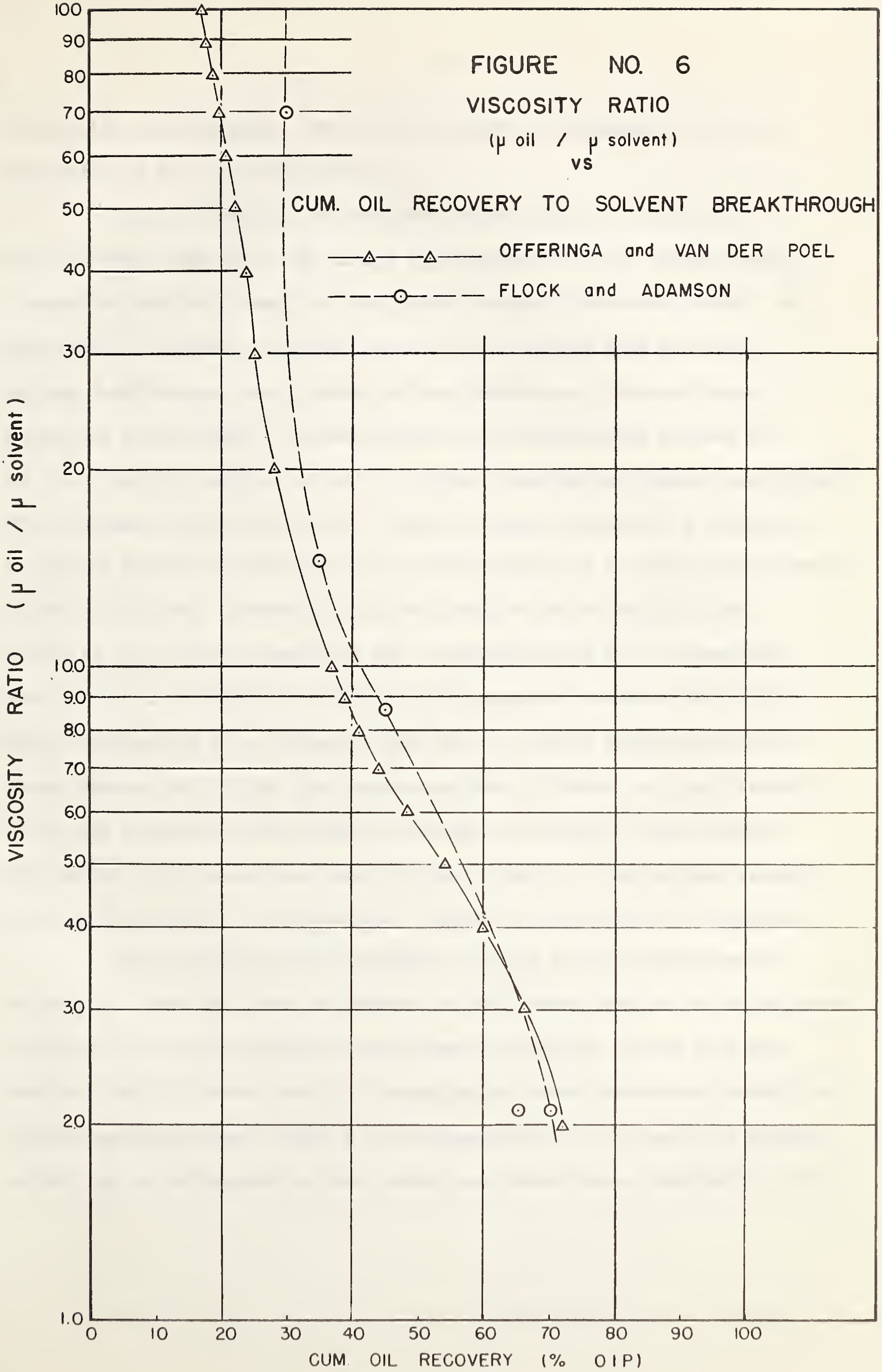
FIGURE NO. 6
VISCOSITY RATIO
(μ oil / μ solvent)
vs
CUM. OIL RECOVERY TO SOLVENT BREAKTHROUGH
OFFERINGA and VAN DER POEL
FLOCK and ADAMSON
VISCOSITY RATIO (μ oil / μ solvent)
CUM. OIL RECOVERY (% OIP)
100
90
80
70
60
50
40
30
20
10.0
9.0
8.0
7.0
6.0
5.0
4.0
3.0
2.0
1.0
0
10
20
30
40
50
60
70
80
90
100

during this investigation. The greatest degree of divergency occurs in the region of high viscosity ratios.

It is of interest to note that in the region of viscosity ratios greater than 10.0, the change in recovery of oil at solvent break through is relatively small for any marked change in viscosity ratio. In this region of adverse viscosity ratios, it is evident that the early solvent breakthroughs are a result of the formation of viscous fingers during the displacement. In the region of viscosity ratios between 1.0 and 10.0 however, recovery of oil to solvent breakthrough changes appreciably with a change in viscosity ratio. This, of course, indicates a constantly decreasing effect on recovery due to viscous fingering as the viscosity ratio decreases to unity. Therefore when the ratio of the viscosity of the reservoir oil to the viscosity of the displacing fluid is of a magnitude less than 10.0 it is believed that the displacement mechanism which takes place is primarily of a "plunger" type, where a graded transition zone is formed between the oil and the displacing fluid. However at high viscosity ratios the displacing fluid travels through the reservoir quite rapidly developing a wide transition zone with many fingers. Thus at high viscosity ratios, any attempt to correlate some "length of mixing zone" is meaningless.

These conclusions are somewhat verified by the data presented in Table 4. Here the "rate of advance of the leading edge of the mixing zone" is tabulated for the different displacements performed. These data were obtained from Visicorder charts. Comparing the tests which were carried out at the same displacement rate, i.e. Displacements No. E, G and H, a variance in the rate of advancement of the mixing zone can be seen, especially across

TABLE 4

GROWTH OF MIXING ZONES

Length of Core = 36 inches

Section 1 = 12 inches   Section 2 = 12 inches   Section 3 = 12 inches

(1) Displacement Number	(2) Displacement Rate	(3) Viscosity Ratio $\mu_{oil}/\mu_{solvent}$	(4) Rate of Advance of Leading Edge of Mixing Zone	(5)	(6)	(7)
			Sec. 1	Sec. 2	Sec. 3	Average
	(cc/hr)		(in./min.)			
No. D	60	70.5	-	-	-	-
No. E	200	8.6	1.33	1.00	0.60	0.98
No. F	400	2.13	1.00	1.00	0.90	0.97
No. G	200	2.13	0.55	0.55	0.55	0.55
No. H	200	14.2	1.72	1.09	0.85	1.22

the first two sections of the core. During Displacement No. G when the viscosity ratio was 2.13, the mixing zone stabilized quickly and travelled through sections one and two at exactly the same rate. However, as the viscosity ratio increased, the mixing zone spread initially quite quickly through section one and then progressively slowed down as it advanced toward the outlet face. This initial rapid advancement became more pronounced as the viscosity ratio increased from 8.6 to 14.2. These limited observations are in agreement with views expressed by other authors(20) when they investigated this phenomena of mixing zone growth. In order to rigorously examine the problem of mixing zone growth it is suggested that a longer porous system than the one used during this investigation is needed.

A visual examination of the interaction between liquid propane and Esso P-40 heating oil was made in a laboratory high pressure cell. These observations were carried out at 75°F and pressures ranging from 100 p.s.i.g. to 2000 p.s.i.g. Under static conditions, an interface between the propane and the heating oil was observed to be present throughout the entire range of pressures investigated. The transition zone between the propane and the heating oil was very narrow with little apparent mixing taking place between the two liquids. However, upon agitation, the two liquids became a single fluid even at the lowest pressure observed. No difficulty should be encountered therefore, in getting two fluids of this type to mix miscibly while travelling through a porous media.

The data which has been obtained during this investigation has resulted in the formulation of some general conclusions regarding the mechanisms which occur during a miscible type displacement. It is felt that the efficiency of any laboratory miscible displacement (compared to that predicted

theoretically) will be primarily influenced by the sweep efficiency within the core. This, in turn, is controlled by such factors as unfavorable mobility or viscosity ratio effects, reservoir inhomogeneities and gravitational segregation effects. Thus attempts to verify the predicted miscibility conditions of a system by laboratory tests will necessitate the suppressment or elimination of all causes of poor sweep efficiency. In this regard, gravity effects may be eliminated by using vertical systems while the development of fingering can perhaps be controlled by carrying out displacements at or below some critical velocity.

Discussion of Experimental Apparatus:

A brief discussion will be presented at this time outlining the advantages and disadvantages of the experimental apparatus which was designed for this investigation. The most delicate components of the apparatus were the differential pressure transducers. Originally four in number, they were mounted in series on a rack below the core. Stainless steel tubing, one eighth inch in diameter, was used to connect the pressure taps on the core to the high and low sides of each transducer. Each pressure transmitting line was valved once between the core and the transducer. After considerable difficulty had been encountered, it was realized that a line connected the ends of each transducer was necessary. The purpose of this equalizing connection was to maintain the same pressure on each side of a transducer during the time the entire system was being pressured up or depressured. This type of arrangement prevented any sudden, unsafe pressure drops being imposed across a transducer particularly during the period when the core was being depressured. When the number of transducers in use was reduced to three, the two end transducers were remounted in a manner just described with satisfactory results.

The extreme care which is required when calibrating and using this type of pressure sensing device cannot be overstressed. If additional transducers were added to the system, the entire bank of instruments will probably have to be mounted in a location remote from the core itself. This should present no difficulty or resulting loss in accuracy. The full scale deflection of the diaphram in the transducer requires the transmission of only about 0.1 cc of liquid with the result that pressure changes in the core are detected almost instantaneously providing the pressure lines are

filled with a non-compressible liquid.

The operation of the Visicorder presented little difficulty once the investigators became familiar with the instrument. The galvanometers were zeroed prior to the start of any test and then rechecked after the core and transducers were pressured up to the desired reservoir conditions. Care was taken during this operation that the voltage supply to the transducers was constant and stabilized. Occasionally the traces, corresponding to the two upstream galvanometers were noticed to vibrate rapidly during the preparation for a displacement. It was subsequently discovered that this vibration was caused by the transmission of harmonics which were present in the relatively long feed line from the injection pump to the core. These vibrations could be damped out immediately by attaching the inlet feed line securely to the frame of the pump. Adjustment must be made to the Visicorder every time a different paper speed is used to ensure that the trace intensification of the instrument remains uniform. This relatively easy adjustment will result in clearer and sharper traces being obtained. All records from the Visicorder may be permanized to prevent fading by a relatively simple fixing process. Although this was not done during the course of this investigation it is recommended as standard procedure for any subsequent work.

With regard to the remainder of the test apparatus, three main areas of difficulty were found. Firstly, the accuracy and efficiency of the gas measuring and venting system left room for improvement. It was discovered early in the investigation that the burette-type measuring devices were too small to handle the large quantity of propane which was produced during a test. Consequently a wet test meter was used to measure all gas flows.

The chief disadvantage of this procedure was the inherent inaccuracy of a wet test meter during low flow rates and its inability to instantaneously detect an initial gas breakthrough. Gas breakthrough therefore, had to be observed visually in the separator column and was recorded at that time when the first bubble of gas appeared at the outlet flowline into the separator. The system provided for venting the produced gas was also inadequate, mainly due to its remote location from the test apparatus. Because no suction can be applied to the discharge line from the wet test meter, a large diameter vent line is required in order that proper dissipation of the flammable gas can be achieved.

A second source of difficulty during the tests was the Grove Back-pressure Regulator. Designed to hold a constant down stream pressure on the system, it was found that after breakthrough of propane the regulator behaved very erratically. This was partly due of course, to the extreme cooling effect which took place across the regulator when the propane flashed into a vapor. When freezing did occur in the regulator, it was easily recognized by a decrease to zero in production and a corresponding increase in pressure in the core if the injection pump was still running.

During the running of a test, both the upstream and downstream pressure on the core had to be obtained from a single Heise gauge. This operation entailed the constant opening and closing of valves and probably resulted in some inaccuracies in the pressure readings. A response on the Visicorder chart would also occur whenever a valve close to the downstream end of the core was adjusted. For these reasons, the employment of two separate Heise gauges on the system could probably be justified. As was pointed out earlier in the discussion, plugging of the upstream end of the

core was detected after the repeated use of crude oil as a reservoir fluid. This condition could be avoided by mounting a filter apparatus between the upstream end of the core and the injection pump.

SUMMARY AND CONCLUSIONS

It can be concluded from the experimental results that the most important factor influencing the results of a laboratory miscible displacement test is the sweep efficiency within the core. The sweep efficiency, in turn, is primarily affected by adverse mobility or viscosity ratios, reservoir inhomogeneities and gravity segregation. Of these three, it would appear that the viscosity ratio was the dominant factor during the miscible displacement of reservoir fluids from the relatively homogeneous sandstone used during this investigation. Above viscosity ratios of 10.0 the presence of viscous fingers was indicated both by early solvent breakthrough and by rapidly decreasing pressure differentials. At viscosity ratios less that 10.0 the limited results obtained indicated that the mechanism of frontal advance more closely resembled the piston-like displacement visualized by many investigators. However, even at high viscosity ratios where the presence of viscous fingers was suspected, the recovery to breakthrough is similar in magnitude to that obtained by water floods for the same viscosity ratio. The subordinate production of a miscible flood is much greater however due to the more efficient stripping action which takes place. It is possible that at low viscosity ratios and low displacements rates, the effect of diffusional mixing at the flood front will influence the recovery of oil to solvent breakthrough.

The theoretical investigation reveals that while the method of predicting criticals used by Benham et al. during development of their correlation is not the most accurate available, it is probably reliable enough for use in an approximate correlation such as theirs. At any rate, it is believed that

the controlling factor in predicting the critical conditions for a certain fluid system in a porous media is not the method used to calculate criticals but is, in fact, the method used to determine the composition of fluid upon which the calculations are made. In this regard, it is suggested that the equipment designed and used during this investigation could be used to determine these compositions, particularly during miscible liquid-liquid displacements.

In the case of liquid-liquid displacements, the pressure differential present in any section of the core under steady state, laminar flow conditions, is directly related to the viscosity of the fluid which is flowing at that particular time and in that particular section. Therefore, knowing the pressure differential across any portion of the core, it would be possible to calculate the viscosity of the fluid which is flowing. Then by knowing the viscosities of various mixtures of the displaced and displacing fluid, the composition of the mixture in the core could be obtained. This composition profile could be correlated directly to the pressure differential which would occur in the core during the flow of one of these mixtures. Perhaps the simplest method of doing this would be to flow first, pure fluid through the core, observing the pressure drops, and then flow various known mixtures through the core and compare pressure differentials. The viscosities of these known mixtures could be calculated from the pressure differentials and checked in a laboratory viscometer. This procedure would also provide a comparison between what occurs in an idealized laboratory cell versus the actual behavior in a porous media. The pressure transducers and Visicorder equipment would be useful in many other phases of reservoir studies. Such things as water floods, alcohol displacements, gas displacements or any two-

phase operation could employ the use of equipment such as this.

While the original purpose of this investigation was to check the accuracy of theoretical methods for predicting critical conditions, it was soon discovered that the confirmation of predicted miscibility pressures and temperature by laboratory testing procedures necessitated the elimination or suppressment of all cause of poor pore displacement efficiency. The major portion of the work involved in this investigation was therefore directed toward this endeavour.

Restating the Conclusions:

1) The method of predicting criticals conditions developed by Benham, Dowden and Kunzman should be used as a first approximation only.

2) The method used by Benham, Dowden and Kunzman to predict the critical pressure and temperature of a naturally occurring hydrocarbon mixture is adequate.

3) If a more precise calculation of critical temperature and pressure is required, either Organick's or Eilerts' procedure should be used.

4) The most important single factor to be considered when calculating the critical conditions in a porous media is the composition of the fluid at any particular time.

5) The confirmation of miscibility conditions by laboratory core testing necessitates the elimination or suppressment of all causes of poor core sweep efficiency. The observation of low recoveries is not, by itself, conclusive evidence of lack of miscibility.

6) At viscosity ratios above 10.0, the mechanism of displacement in a sandstone system is primarily controlled by the presence of viscous fingers. Thus any attempt to correlate a "length of mixing zone" is meaningless.

7) At viscosity ratios less than 10.0 the mechanism of displacement more closely resembles the ideal piston like situation.

8) The oil recovery to breakthrough of the displacing phase at high viscosity ratios is similar in magnitude to that reported for water floods with the same viscosity ratio. However the subordinate production of a miscible flood is more efficient than that of a water flood.

9) From a practical point of view, any efforts placed on the elimination of gravitational effects and viscous fingering in field tests should result in more favorable recoveries by miscible displacement.

RECOMMENDATIONS

Because of the increasing importance of recovering more oil from known reservoirs, a continuing program investigating the limitations and advantages of a miscible type system is justified. Although the economics of a secondary recovery project involving miscible displacement are sometimes questionable, the efficiency of an ideal miscible flood is certainly attractive. With this in mind it is recommended that the research program concerned with miscible displacement be continued and broadened to include some of the following aspects:-

1) an intensified investigation of the mechanism of displacement in the region of viscosity ratios less than 10.0 using a vertical reservoir and additional pressure transducers.

2) an investigation of the results achieved using enriched gas mixtures as the displacing phase.

3) a formulation of a correlation relating pressure drop in the porous media to composition of fluid flowing in the system.

4) additional investigation of the growth of mixing zones at various displacement rates employing longer cores.

NOMENCLATURE

$\bar{B}$ = molal average boiling point, °R

n'_i = mole fraction of component "i"

B_i = normal boiling point for component "i", °R

W = weight average equivalent molecular weight

m_i = weight fraction of component "i"

M_{Ei} = equivalent molecular weight of component "i"

P_{cm} = measured critical pressure, psia

T_{cm} = measured critical temperature, °R

A_{ij} = characterization factor for binary mixture of components "i" and "j"

T_c = true critical temperature, °R

P_c = true critical pressure, psia

T_{c_n} = molal average critical temperature, °R

P_{c_n} = molal average critical pressure, psia

mT_c = weight average critical temperature, °R

mP_c = weight average critical pressure, psia

M = molecular weight

M^* = arbitrary variable

T_{ce} = estimated critical temperature, °R

P_{ce} = estimated critical pressure, psia

B_H = normal boiling point of heavy (liquid)portion of mixture, °R

B_L = normal boiling point of light (vapor) portion of mixture, °R

B_F = normal boiling point of entire mixture, °R

N_s = mole fraction of mixture in vapor phase at 14.7 psia and 75 °F

T_{cc} = calculated critical temperature, °R

P_{cc} = calculated critical pressure, psia

T_E = equivalent critical temperature, °R

λ = mole fraction of component in liquid phase

Q = injection rate, cc/hr

μ_o = viscosity of oil, cps

μ_s = viscosity of solvent, cps

k = permeability, md

P_{up} = upstream core pressure, psig

P_{down} = downstream core pressure, psig

L = length of core, cm.

A = cross-sectional area of core, cm^2

GOR = gas-oil ratio, cc/cc

scc = standard cubic centimeters at 14.7 psig and 60°F

stcc = stock tank cubic centimeters at atmospheric conditions

BIBLIOGRAPHY

1. Allen, J.C.: "Classification of Oil and Gas Wells", Oil and Gas Journ., (July 28, 1952), Vol. 51, No. 12, 355.

2. Aronofsky, J.S. and Heller, J.P.: "A Diffusion Model to Explain Mixing of Flowing Miscible Fluids in Porous Media", Trans. AIME (1957), 210, 345.

3. Benham, A.L., Dowden, W.E. and Kunzman, W.J.: "Miscible Fluid Displacement - Prediction of Miscibility", Trans. AIME (1960), 219, 229.

4. Blackwell, R.J., Rayne, J.R., and Terry, W.M.: "Factors Influencing the Efficiency of Miscible Displacement", Trans. AIME (1959), 216, 1.

5. Brown, G.G., Katz, D.L., Oberfell, G.G. and Alden, R.C.: "Natural Gasoline and the Volatile Hydrocarbons," NGAA (1948).

6. Clark, Norman J., Shearin, H.M., Schultz, W.P., Garms, Kenneth and Moore, J.L.: "Miscible Drive - Its Theory and Application", JPT (June 1958), 11.

7. Clark, N.J., Schultz, W.P. and Shearin, H.M.: "Condensing Gas Drive, Critical Displacement Process - New Injection Method Affords Total Oil Recovery", Pet. Engr. (Oct. 1956), 28, B-45.

8. Davis, P.C., Bertuzzi, A.F., Gore, T.L. and Kurata, F.: "Phase and Volumetric Behavior of Natural Gases at Low Temperatures and High Pressures", Trans. AIME (1954), 201, 245.

9. Deffrenne, P., Marle, C., Pacsirszki, J. and Jeantet, M.: "The Determination of Pressures of Miscibility", Preprint, AIME Annual Fall Meeting (1961)

10. Eilerts, C.K., et al.: "Phase Relations of Gas-Condensate Fluids", Monograph No. 10, U.S. Bureau of Mines (1957), Vol. 1, 101.

11. Flock, D.L.: "A Review of Analytical and Experimental Studies of Miscible Fluid Displacement", Unpublished.

12. Grieves, R.B. and Thodos, George: "The Critical Temperatures and Pressures of Binary Systems: Hydrocarbons of All Types and Hydrogen", AIChE Journal (1960), 6, No. 4, 561.

13. Habermann, B.: "The Efficiency of Miscible Displacement as a Function of Mobility Ratio", Trans. AIME (1960), 219, 264.

14. Handy, L.L.: "An Evaluation of Diffusion Effects in Miscible Liquid Displacement", Trans. AIME (1959), 216, 382.

15. Katz, D.L., Cornell, David, Kobayashi, Riki, Poettmann, Fred H., Vary, John A., Elenbaas, Jack R., and Weinaug, Charles F.: "Handbook of Natural Gas Engineering", McGraw-Hill Book Company Inc., (1959).

16. Kehn, D.M., Pyndus, G.T., and Gaskell, M.H.: "Laboratory Evaluation of Prospective Enriched Gas-Drive Projects", Trans. AIME (1958), 213, 382.

17. Koch, H.A. Jr. and Slobod, R.L.: "Miscible Slug Process", Trans. AIME (1957), 210, 40.

18. Koch, H.A. Jr. and Hutchinson, C.A. Jr.: "Miscible Displacements of Reservoir Oil Using Flue Gas", Trans. AIME (1958), 213, 7.

19. Kurata, Fred and Katz, D.L.: "Critical Properties of Volatile Hydrocarbon Mixtures", Trans. AIChE (1942), 38, 995.

20. Lacey, James W., Draper, Arthur L. and Binder, George B. Jr.: "Miscible Fluid Displacement in Porous Media", Trans. AIME (1958), 213, 76.

21. Lydersen, A.L., Greenkorn, R.A. and Hougen, O.A.: "Generalized Thermodynamic Properties of Pure Fluids", College of Engineering, University of Wisconsin, Engineering Experiment Station, Report No. 4, (October, 1955).

22. Mayfield, F.D.: "Critical States of Two-Component Paraffin Systems", Ind. Eng. Chem. (July 1942), Vol. 34, No. 7, 383.

23. Natural Gasoline Supply Men's Association: "Engineering Data Book", (1957).

24. Offeringa, J. and van der Poel, C.: "Displacement of Oil from Porous Media by Miscible Liquids", Trans. AIME (1954), 201, 310.

25. Organick, E.I.: "Prediction of Critical Temperatures and Critical Pressures of Complex Hydrocarbon Mixtures", Chem. Eng. Progr. Symposium Series, 49 (6), 81, (1953).

26. Round, G.F.: "A Review of Miscible Flooding Mechanisms", Research Council of Alberta Bulletin.

27. Sievert, John A., Dew, John N., and Conley, Francis R.: "The Deterioration of Miscible Zones in Porous Media", Trans. AIME (1958), 213, 228.

28. Slobod, R.L. and Koch, H.A. Jr.: "High Pressure Gas Injection - Mechanism of Recovery Increase", Drill. and Prod. Prac., API (1953), 82.

29. Smith, R.L. and Watson, K.M.: "Boiling Points and Critical Properties of Hydrocarbon Mixture", Ind. Eng. Chem. (Dec., 1947), Vol. 29, No. 12, 1408.

30. Stone, H.L. and Crump, J.S.: "Effect of Gas Composition Upon Oil Recovery by Gas Drive", Trans. AIME (1956), 207, 105.

31. van der Poel, C.: "Effect of Lateral Diffusivity on Miscible Displacement in Horizontal Reservoirs", Preprint, Annual Fall Meeting AIME, Dallas, Texas (October, 1961).

32. Warren, J.S., Price, H.S., Skiba, F.F. and Varga, R.S.: "Miscible Displacement: The Liquid-Liquid Case", Preprint, Annual Fall Meeting AIME, Dallas, Texas, (October, 1961).

33. Welge, H.J., Johnson, E.J., Ewing, S.P. Jr. and Brinkman, F.H.: "The Linear Displacement of Oil from Porous Media by Enriched Gas", J.P.T. (Aug. 1961), 787.

34. Wilson, J.F.: "Miscible Displacement - Flow Behavior and Phase Relationships for a Partially Depleted Reservoir", Trans. AIME (1960), 219, 223.

APPENDIX A

COMPOSITIONS OF SAMPLE HYDROCARBON MIXTURES(1,10)

Component	Mixture A-1	A-2	B-1	B-2	B-3	C-1	C-2	D	E	F	CH-P-843
	Mole Fractions and Properties										
C_1	0.7243	0.7292	0.8227	0.8165	0.7959	0.6433	0.8213	0.6865	0.6570	0.7164	0.76432
C_2	0.0557	0.0556	0.0284	0.0284	0.0281	0.0638	0.0637	0.0603	0.0869	0.0548	0.07923
C_3	0.0308	0.0306	0.0124	0.0124	0.0128	0.0605	0.0409	0.0232	0.0537	0.0310	0.04301
iC_4	0.0108	0.0106	0.0036	0.0037	0.0038	0.0107	0.0050	0.0089	0.0038	0.0102	0.01198
nC_4	0.0133	0.0120	0.0055	0.0055	0.0060	0.0458	0.0185	0.0220	0.0265	0.0156	0.01862
iC_5	0.0080	0.0078	0.0040	0.0042	0.0047	0.0189	0.0055	0.0130	0.0068	0.0133	0.00937
nC_5	0.0070	0.0069	0.0027	0.0028	0.0031	0.0215	0.0067	0.0113	0.0127	0.0083	0.00781
C_6	0.0179	0.0183	0.0125	0.0131	0.0150	0.0366	0.0103	0.0256	0.0173	0.0198	0.01405
C_7	0.1256	0.1223	0.1021	0.1073	0.1247	0.0954	0.0234	0.1245	0.1217	0.1231	0.02992
CO_2	0.0066	0.0067	0.0061	0.0061	0.0059	0.0035	0.0047	0.0156	0.0008	0.0075	0.00794
N_2	-	-	-	-	-	-	-	-	0.0128	-	0.01375
Critical Press. (p.s.i.a.)	5130	5350	6000	5820	5620	2720	2270	5100	5570	5150	1156
Critical Temp. (^{o}R)	745	711	560	620	672	655	-	699	605	703	396.5
GOR (CF/STB)	3800	3925	5450	5150	4325	4000	23,289	3285	3225	3790	-
^{o}API C_{7+}	42.6	-	45.4	-	-	53.4	-	45.0	39.5	42.8	-
MW C_{7+}	167	-	158	-	-	114	-	171	207	167	127.3

TABLE 2-A

CALCULATION OF CRITICALS BY ORGANICK'S METHOD FOR C-1

(1) Component	(2) Mol. Fract.	(3) Boiling Pt. (°R)	(4) Equiv.Mol. Wt.	(5) Actual Mol Wt.	(6) Mol.Fract. x Mol.Wt.	(7) Wt. Fract.	(8) W = (4) x (7)	(9) B = (2) x (3)
CO_2	0.0035	350.4	44	44	0.154	0.0042	0.1848	1.2264
C_1	0.6433	201.0	16.04	16.04	10.30	0.2836	4.5660	129.3033
C_2	0.0638	332.2	30.1	30.1	1.92	0.0528	1.5893	29.1944
C_3	0.0605	416.0	44.1	44.1	2.67	0.0735	3.2414	25.1680
iC_4	0.0107	470.6	54.5	58.1	0.621	0.0171	0.9320	5.0354
nC_4	0.0458	490.8	58.1	58.1	2.66	0.0732	4.2529	22.4786
iC_5	0.0189	541.8	69.0	72.2	1.36	0.0374	2.5806	10.2400
nC_5	0.0215	556.6	72.2	72.2	1.55	0.0427	3.0829	11.9669
C_6	0.0366	615.4	85.0	86.2	3.16	0.0870	7.3950	22.5236
C_{7+} gas	0.00823	717.9 (a)	114.2 (a)	114.2	0.938	0.0258	2.9464	5.9083
C_7 liquid	0.00131	668.9	100.2	100.2	0.131	0.0036	0.3607	0.8763
C_8 "	0.04980	717.9	114.2	114.2	5.700	0.1569	17.9180	35.7514
C_9 "	0.01718	763.1	128.2	128.2	2.200	0.0606	7.7689	13.1101
C_{10} "	0.00731	805.1	142.3	142.3	1.040	0.0286	4.0698	5.8853
C_{11} "	0.00338	844.3	156.3	156.3	0.529	0.0146	2.2820	2.8537
C_{12+} "	0.00819	881.0	170.3	170.3	1.391	0.0384	6.5395	7.2154
					36.324		69.7102	328.737

(a) Used properties of C_8 to describe x
From Fig. 4-88, NGHB (15)

Tcc = 212°F = 672°R
Pcc = 2750 p.s.i.a.

(1) Component	(2) Mol. Frac.	(3) Boiling Pt (°R)	(4) Equiv. Mol. Wt.	(5) Actual Mol Wt.	(6) Mol. Frac. x Mol. Wt.	(7) Wt. Frac.	(8) W = (4) x (7)	(9) $\bar{B}$ = (2) x (3)
CO_2	0.00794	350.4	44.01	44.01	0.3494	0.0138	0.6073	2.782
N_2	0.01375	139.3	28.02	28.02	0.3853	0.0149	0.4175	1.915
C_1	0.76432	201.0	16.04	16.04	12.2597	0.4849	7.7778	153.628
C_2	0.07923	332.2	30.1	30.10	2.3848	0.0944	2.8414	26.320
C_3	0.04301	416.0	44.1	44.1	1.8967	0.0750	3.3075	17.892
iC_4	0.01198	470.6	54.1	58.10	0.6960	0.0276	1.4932	5.638
nC_4	0.01862	490.8	58.1	58.10	1.0818	0.0429	2.4925	9.139
iC_5	0.00937	541.8	69.0	72.20	0.6765	0.0268	1.8492	5.077
nC_5	0.00781	556.6	72.2	72.20	0.5639	0.0223	1.6101	4.347
C_6	0.01405	615.4	85.0	86.20	1.2111	0.0479	4.0715	8.646
C_{7+} gas	0.010774	717.9 (a)	114.2 (a)	114.20	1.2304	0.0488	5.5730	7.735
C_7 liquid	0.001205	668.9	100.2	100.20	0.1207	0.0048	0.4810	0.806025
C_8 "	0.005761	717.9	114.2	114.20	0.6579	0.0260	2.9692	4.135822
C_9 "	0.004922	763.1	128.3	128.30	0.6315	0.0250	3.2075	3.755978
C_{10} "	0.003147	805.1	142.3	142.30	0.4478	0.0177	2.5187	2.533650
C_{11} "	0.001723	844.3	156.3	156.30	0.2693	0.0107	1.6724	1.454729
C_{12} "	0.001520	881.0	170.3	170.30	0.2589	0.0102	1.7371	1.339120
C_{13+} "	0.000868	915.5	184.4	184.40	0.1601	0.0063	1.1617	0.794654
					25.2818		45.7886	257.939

(a) Used properties of C_8 x (15)
From Figure 4-88 NGHB , Tcc = 40°F = 500°R
Pcc = 2500 p.s.i.a.

TABLE 4-A

CALCULATION OF CRITICALS BY MODIFIED KURATA-KATZ METHOD FOR C-1

(1) Component	(2) Mol. Fr.	(3) Mol. Wt.	(4) Tc (°R)	(5) Pc (psia)	(6) Mol. Av. Mol. Wt. = (2) x (3)	(7) Tcn = (2) x (4) °R	(8) Pcn = (2) x 5 psia
CO_2	0.0035	44.01	547.5	1070.2	0.154	1.91	3.74
C_1	0.6433	16.04	343.2	673.1	10.300	220.00	425.00
C_2	0.0638	30.1	549.9	708.3	1.920	35.00	45.20
C_3	0.0605	44.1	666.0	617.4	2.670	40.40	37.40
iC_4	0.0107	58.1	734.6	529.1	0.621	7.85	5.65
nC_4	0.0458	58.1	765.7	550.1	2.660	35.10	25.20
iC_5	0.0189	72.2	829.6	483.5	1.360	15.65	9.14
nC_5	0.0215	72.2	846.2	489.8	1.550	18.21	10.50
C_6	0.0366	86.2	914.2	440.1	3.160	33.40	16.10
C_{7+}	0.0954	114.0(a)	1010(b)	380.0(c)	10.860	96.20	36.20
					35.255	503.72	614.13

(a) Obtained from Table 1-A
(b) and (c) from Figure 30, NGAA(5) using S.G. = 0.71

(1) T_E from Fig. 57A, NGAA = 595 °R

(2) $\frac{T_E}{T_{cn}} = \frac{595}{503.72} = 1.182$

(3) $\frac{T_E}{T_{cn}}$ corrected from Fig. 62, NGAA(5)

(4) True Critical Temp. from Fig. 61 NGAA(5) = 616 °R

(5) From Fig. 4, Reference(8)

$$\frac{T_c \times P_{cn}}{P_c} = 140$$

(6) $P_{cc} = \frac{616 \times 614.13}{140}$

$= \underline{2700 \text{ p.s.i.a.}}$

TABLE 5-A

CALCULATION OF CRITICALS BY MODIFIED KURATA-KATZ METHOD FOR CH-P-843

(1)	(2)	(3)	(4)	(5)	(6)	(7)	(8)
Component	Mol. Fr.	Mol. Wt.	T_c (°R)	P_c (psia)	Mol. Av. Mol. Wt.	T_{cn} = (2) x (4)	P_{cn} = (2) x (5)
CO_2	0.00794	44.01	547.5	1070.2	0.350	4.347	8.497
N_2	0.01375	28.02	227.0	492.2	0.387	3.121	6.768
C_1	0.76432	16.04	343.2	673.1	12.250	262.315	514.464
C_2	0.07923	30.1	549.9	708.3	2.385	43.569	56.119
C_3	0.04301	44.1	666.0	617.4	1.900	26.645	26.554
iC_4	0.01198	58.1	734.6	529.1	0.706	8.801	6.339
nC_4	0.01862	58.1	765.7	550.1	1.100	14.257	10.243
iC_5	0.00937	72.2	829.6	483.5	0.676	7.773	4.530
nC_5	0.00781	72.2	846.2	489.8	0.564	6.609	3.825
C_6	0.01405	86.2	914.2	440.1	1.210	12.845	6.183
C_{7+}	0.02992	127.3(a)	1060(b)	360(c)	3.820	31.715	10.771
	1.00000				25.348	421.997	654.293

(a) Obtained from Table 1-A

(b) and (c) from Figure 30, NGAA(5) using S.G. - 0.74

---

(1) T_E from Figure 57A, NGAA(5) = 492°R

(2) $\frac{T_E}{T_{cn}} = 1.167$

(3) $\frac{T_E}{T_{cn}}$ corrected from Figure 62, NGAA(5) = 1.068

(4) True Critical Temperature Figure 61, NGAA(5) = 520°R

(5) From Figure 4, Reference(8)

$$\frac{T_c \times P_{cn}}{P_c} = 160$$

(6) $$P_{cc} = \frac{520 \times 654}{160}$$

$$= 2130 \text{ p.s.i.a.}$$

(after Eilerts et. al.)

Comp.	Mol.Frac. n'	Mol. Frac. Liquid Phase λ	Mol Frac. Gas Phase $(n'-\lambda)$	Boiling Point $B = (^{\circ}R)$	λB	$(n'-\lambda)B$	$n'B$	T_c $(^{\circ}R)$	$n'BT_c$	P_c (psia)	$n'P_c$
CO_2	0.0035	0.00001	0.00349	350.4	0.0035	1.223	1.226	547.5	671.2	1070.2	3.75
C_1	0.6433	0.00036	0.64294	201.0	0.0724	129.231	129.303	343.2	44376.8	673.1	433.00
C_2	0.0638	0.00024	0.06356	332.2	0.0797	21.115	21.194	549.9	11654.6	708.3	45.19
C_3	0.0605	0.00087	0.05963	416.0	0.3619	24.806	25.168	666.0	16761.9	617.4	37.35
iC_4	0.0107	0.00039	0.01031	470.6	0.1835	4.852	5.035	734.6	3698.7	529.1	5.66
nC_4	0.0458	0.00237	0.04343	490.8	1.1632	21.315	22.479	765.7	17212.2	550.1	25.19
iC_5	0.0189	0.00240	0.01650	541.8	1.3003	8.940	10.240	829.6	8495.1	483.5	9.14
nC_5	0.0215	0.00350	0.01800	556.6	1.9481	10.019	11.967	846.2	10126.5	489.8	10.53
C_6	0.0366	0.01460	0.02200	615.4	8.9848	13.539	22.524	914.2	20591.4	440.1	16.11
C_7	0.0019	0.00131	0.00059	668.9	0.8763	0.395	1.271	972.4	1235.9	395.9	0.75
C_8	0.0566	0.04980	0.00680	717.9	35.7514	4.882	40.633	1024.9	41644.8	362.2	20.50
C_9	0.0179	0.01718	0.00072	763.1	13.1101	0.549	13.659	1073	14656.1	334	5.98
C_{10}	0.0074	0.00731	0.00009	805.1	5.8853	0.072	5.958	1115	6643.2	312	2.31
C_{11}	0.0034	0.00338	0.00002	844.3	2.8537	0.017	2.871	1151	3304.5	290	0.99
C_{12}	0.0082	0.00819	0.00001	881.0	7.2154	0.009	7.224	1185	8560.4	272	2.23
	1.0000	0.11191	0.88809		79.7896	240.964	320.752		209633.3		618.68

$$B_H = \frac{\Sigma \lambda B}{\Sigma \lambda} = \frac{79.7896}{0.11191} = 713.0^{\circ}R$$

$$B_L = \frac{\sum (n' - \lambda)B}{\sum (n' - \lambda)} = \frac{240.964}{0.88809} = 271.3^{\circ}R$$

$$B_F = \frac{\sum n'B}{\sum n'} = \frac{320.752}{1} = 320.8^{\circ}R$$

$$\left(\frac{T_{cm}}{\sum n'BT_c / \sum n'B}\right) = 0.996 \text{ from charts} \quad (10)$$

$$\therefore T_{cc} = 653.6 \times 0.996 = \underline{651.0^{\circ}R}$$

$$B_H/B_L = 2.628$$

$$\frac{B_H - B_L}{B_F} = 1.377$$

$$N_s = \sum (n' - \lambda) = 0.88809$$

$$T_{ce} = \frac{\sum n'BT_c}{\sum n'B} = \frac{209633.3}{320.752} = 653.6^{\circ}R$$

$$P_{cn} = \frac{\sum n'P_c}{\sum n'} = \frac{618.68}{1} = 618.7 \text{ psia.}$$

$$\left(\frac{P_{cm}}{\sum n'P_c / \sum n'}\right) = 3.73 \text{ from charts} \quad (10)$$

$$\therefore P_{cc} = 618.7 \times 3.73 = \underline{2308 \text{ psia}}$$

Comp.	Mol.Frac. n'	Mol. Frac. Liquid Phase λ	Mol Frac. Gas Phase $(n'-\lambda)$	Boiling Point $B = (^{o}R)$	λB	$(n'-\lambda)B$	$n'B$	T_c (^{o}R)	$n'BT_c$	P_c (psia)	$n'P_c$
CO_2	0.00794	0.000002	0.007938	350.4	0.000701	2.781	2.782	547.5	1523.1	1070.2	8.5
N_2	0.01375	0.000000	0.013750	139.3	0.000000	1.915	1.915	227.0	434.7	492.2	6.8
C_1	0.76432	0.000073	0.764247	201.0	0.014673	153.614	153.628	343.2	52725.1	673.1	514.5
C_2	0.07923	0.000052	0.079178	332.2	0.017274	26.303	26.320	549.9	14464.0	708.3	56.1
C_3	0.04301	0.000106	0.042904	416.0	0.044096	17.848	17.892	666.0	11916.1	617.4	26.6
iC_4	0.01198	0.000076	0.011904	470.6	0.035766	5.602	5.638	734.6	4141.7	529.1	6.3
nC_4	0.01862	0.000171	0.018449	490.8	0.083927	9.055	9.139	765.7	6997.7	550.1	10.2
iC_5	0.00937	0.000226	0.009144	541.8	0.122447	4.954	5.077	829.6	4211.9	483.5	4.5
nC_5	0.00781	0.000250	0.007560	556.6	0.139150	4.208	4.347	846.2	3678.4	489.8	3.8
C_6	0.01405	0.001118	0.012932	615.4	0.688017	7.958	8.646	914.2	7904.2	440.1	6.2
C_7	0.00585	0.001205	0.004645	668.9	0.806025	3.107	3.913	979.4	3832.4	395.9	2.3
C_8	0.01040	0.005761	0.004639	717.9	4.135822	3.330	7.466	1024.9	7651.9	362.2	3.8
C_9	0.00613	0.004922	0.001208	763.1	3.755978	0.922	4.678	1073.0	5019.5	334	2.0
C_{10}	0.00338	0.003147	0.000233	805.1	2.533650	0.188	2.721	1115.0	3033.9	312	1.1
C_{11}	0.00176	0.001723	0.000037	844.3	1.454729	0.031	1.486	1151.0	1710.4	290	0.5
C_{12}	0.00153	0.001520	0.000010	881.0	1.339120	0.009	1.348	1185.0	1597.4	272	0.4
C_{13}	0.00087	0.000868	0.000002	915.5	0.794654	0.002	0.796	1217.0	968.7	257	0.2
	1.00000	0.021220	0.978780		15.9660	241.827	257.792		131811.1		653.8

$$B_H = \frac{\sum \lambda B}{\sum \lambda} = \frac{15.9660}{0.021220} = 752.403^{o}R$$

$$B_H/B_L = 3.045$$

$$T_{ce} = \frac{\sum n'BT_c}{\sum n'B} = \frac{131,811.1}{257.792} = 511.3^{o}R$$

$$B_L = \frac{\sum (n' - \lambda)B}{\sum (n' - \lambda)} = \frac{241.827}{0.978780} = 247.069^{o}R$$

$$\frac{E_H - B_L}{B_F} = 1.960$$

$$Pc_n = \frac{\sum n'P_c}{\sum n'} = 653.8 \text{ p.s.i.a.}$$

$$B_F = \frac{\sum n' B}{1} = 257.792^{o}R$$

$$N_s = \sum (n' - \lambda) = 0.97870$$

$$Tcc = Tce \times \left(\frac{Tcm}{\sum n'Btc/\sum n'B} \right) = 511.3 \times 0.97 = \underline{495.96^{o}R}$$

$$Pcc = \frac{\sum n'Pc}{\sum n'} \times \left(\frac{Pcm}{\sum n'Pc/\sum n'} \right) = 653.8 \times 2.8$$

$$= \underline{1830.6 \text{ p.s.i.a.}}$$

APPENDIX B

TABLE 1-B

DESCRIPTION OF BEREA SANDSTONE CORE

Core Length = 36 in. = 91.4 cm.

Core Diameter = 2 in. = 5.18 cm.

Core Cross-sectional Area = 21.05 cm.^{2}

Core Bulk Volume = 113 cu. in. = 1925.0 cc.

Core Porosity (Average) = 16.3%

Core Permeability to Air = 293.9 millidarcies

Core Permeability to Liquid (varsol) = 266 millidarcies

TABLE 2-B

FLUID PROPERTIES

(1)	(2)	(3)	(4)	(5)	(6)
Property	Crude Oil Sample	Varsol	Pentane	Propane	Esso P-40
M.W.	197.78 (calc)	-	72.146	44.094	-
Density at 60/60 (gm/cc)	0.848 (calc)	-	0.63116	0.5077	0.8165
Density at 76°F (gm/cc)	0.8536	0.7809	-	-	0.8090
Kinematic μ (centistokes)	1.2200	9.097	-	-	1.969
Absolute μ (centipoise)	0.9528	7.765	0.23	0.110 at 1500 psia 0.108 at 1000 psia	1.534
Mol. % N_2	0.0	-	-	-	-
Mol. % CO_2	0.0	-	-	-	-
Mol. % H_2S	0.0	-	-	-	-
Mol. % C_1	0.0	-	-	-	-
Mol. % C_2	0.0	-	-	-	-
Mol. % C_3	0.0	-	-	-	-
Mol. % iC_4	0.0	-	-	-	-
Mol. % nC_4	6.60	-	-	-	-
Mol. % iC_5	3.48	-	-	-	-
Mol. % nC_5	6.01	-	-	-	-
Mol. % C_6	7.80	-	-	-	-
Mol. % C_{7+}	76.11	-	-	-	-
S.G. C_{7+}	0.877	-	-	-	-
M.W. C_{7+}	237.0	-	-	-	-

TABLE 3-B

AIR PERMEABILITY DATA

Length of Core = 91.4 cm. Area of Core = 21.05 cm.^{2} μ_{air} = 0.018325 cps.

μ/A = 8.7×10^{-4} cps/cm.^{2}

(1)	(2)	(3)	(4)	(5)	(6)	(7)	(8)	(9)
Pressure Upstream	Pressure Downstream	Q at Atmos. Press.	Q at Atmos. Press.	Q at Downstream	$P_m = \frac{(1)+(2)}{2}$	(1)-(2)	$k = \frac{91.4 \times 8.7 \times 10^{-4} \times (2) \times (4) \times 10^3}{(6) \times (7)}$	$1/P_m$
(abs.atm)	(abs.atm)	(ft^3/ sec.)	(cc/ sec.)	(cc/ sec.)	(abs.atm)	(abs.atm)	(millidarcies)	(atm^{-1})
1.836	0.952	1.72×10^{-4}	4.89	4.72	1.394	0.884	290.0	0.717
2.313	0.986	3.05 "	8.65	8.05	1.645	1.327	289.0	0.608
2.618	1.020	4.18 "	11.89	10.70	1.819	1.598	298.5	0.551
2.998	1.054	5.59 "	15.90	13.85	2.026	1.944	296.0	0.494
3.338	1.122	6.90 "	19.60	16.08	2.230	2.216	297.5	0.449
3.638	1.190	8.40 "	23.85	18.40	2.414	2.448	291.0	0.415
3.978	1.292	9.90 "	28.10	19.94	2.635	2.686	289.5	0.380
4.558	1.463	13.09 "	35.8	22.40	3.011	3.095	280.0	0.332
5.168	1.701	16.65 "	47.3	26.50	3.435	3.467	303.0	0.291
5.538	1.870	20.00 "	56.7	27.85	3.704	3.668	304.5	0.270

Average Permeability to Air = 293.9 md.

TABLE 4-B

LIQUID (VARSOL) PERMEABILITY DATA

Length of Core = 91.4 cm. Area of Core = 21.05 cm.^{2} μ_{varsol} = 0.9528 cp.

$\mu L/A$ = 4.13 cp./cm.

(1)	(2)	(3)	(4)	(5)	(1)	(2)	(3)	(4)	(5)
Q	Pressure Upstream	Pressure Downstream	ΔP (Transducers)	k	Q	Pressure Upstream	Pressure Downstream	ΔP (Transducers)	k
(cc/sec)	(psig)	(psig)	(atm.)	(md.)	(cc/sec)	(psig)	(psig)	(atm.)	(md.)
0.0333	8	atmos.	0.566	243	0.0694	20	atmos.	1.13	254
0.0333	236	227	0.498	276	0.0694	584	567	1.10	260
0.0333	421	413	0.498	276	0.0694	1046	1031	1.065	269
0.0333	645	639	0.481	286	0.0694	1668	1654	1.12	256
0.0333	825	815	0.461	298	0.0694	1775	1763	1.12	256
0.0333	1006	998	0.457	301	0.0833	21	atmos.	1.26	273
0.0333	1225	1216	0.491	280	0.0833	620	601	1.29	267
0.0333	1399	1392	0.501	274	0.0833	1136	1118	1.32	261
0.0333	1605	1591	0.512	269	0.0833	1824	1802	1.30	265
0.0417	1605	atmos.	0.720	240	0.111	28	atmos.	1.775	258
0.0417	258	250	0.655	263	0.111	580	560	1.750	262
0.0417	510	500	0.648	266	0.111	1037	1013	1.725	266
0.0417	765	757	0.630	274	0.111	1810	1782	1.79	256
0.0417	1025	1015	0.630	274	0.139	35	atmos.	2.10	273
0.0417	1295	1284	0.659	262	0.139	624	594	2.16	266
0.0417	1619	1607	0.661	261	0.139	1142	1107	2.22	259
0.0555	14	atmos.	0.852	269	0.139	1810	1775	2.18	264
0.0555	579	567	0.866	264					
0.0555	1018	1002	0.890	258					
0.0555	1784	1772	0.884	260					

Average Permeability to Liquid (Varsol) = 266.4 md.

TABLE 5-B

PRESSURE PROFILE DATA FLOWING VARSOL

Length of Core = 36 inches

Section 1 = 6 in. Section 2 = 12 in. Section 3 = 12 in. Section 4 = 6 in.

μ_{varsol} = 0.9528 cps.

(1)	(2)	(3)	(4)	(5)	(6)	(7)	(8)	(9)	(10)	(11)
Q	Pressure Differential (ΔP) by Transducers					Pressure Differential per inch ($\Delta P/\Delta L$)				
	Sec. 1	Sec. 2	Sec. 3	Sec. 4	Total	Sec. 1	Sec. 2	Sec. 3	Sec. 4	Total
(cc/hr.)	(p.s.i.d.)					(p.s.i.d./in.)				
120	1.2	2.6	2.1	1.3	7.2	0.18	0.22	0.17	0.22	0.20
150	1.4	3.5	2.9	1.7	9.5	0.23	0.29	0.24	0.29	0.265
200	2.1	4.4	3.8	2.3	12.8	0.35	0.375	0.32	0.38	0.355
250	2.7	5.5	5.5	2.8	16.5	0.45	0.46	0.46	0.47	0.46
300	3.4	6.8	5.9	3.4	19.5	0.56	0.57	0.49	0.56	0.54
400	4.6	9.5	8.4	4.7	27.2	0.76	0.79	0.70	0.78	0.76
500	4.9	11.6	9.7	5.8	32.0	0.82	0.97	0.81	0.96	0.89

TABLE 6-B

PRESSURE PROFILE DATA FLOWING VARSOL

Length of Core = 36 inches

Section 1 = 12 in. Section 2 = 12 in. Section 3 = 12 in.

μ_{varsol} = 0.9528 cps

(1)	(2)	(3)	(4)	(5)	(6)	(7)
			Pressure Differential (ΔP) by Transducers			
Q	Pressure Upstream	Pressure Downstream	Sec. 1	Sec. 2	Sec. 3	Total
(cc/hr.)	(p.s.i.g.)	(p.s.i.g.)		(p.s.i.d.)		
40	1630	1626	1.0	0.95	1.0	2.95
50	1630	1625	1.2	1.15	1.2	3.55
60	1633	1628	1.4	1.4	1.4	4.20
80	1635	1630	1.9	1.9	1.9	4.80
100	1636	1630	2.4	2.4	2.4	7.20
120	1638	1630	2.8	2.8	2.8	8.40
400	1653	1628	9.1	8.7	9.1	26.90

TABLE 7-B

PRESSURE PROFILE DATA FLOWING PROPANE

Length of Core = 36 inches

Section 1 = 12 in. Section 2 = 12 in. Section 3 = 12 in.

(1) Q (cc/hr.)	(2) Pressure Upstream (p.s.i.g.)	(3) Pressure Downstream (p.s.i.g.)	(4) Pressure Differential (ΔP) by Transducers Sec. 1	(5) Sec. 2 (p.s.i.d.)	(6) Sec. 3	(7) Total
40	1585	1585	0.1	0.1	0.1	0.30
50	1585	1585	0.1	0.1	0.1	0.30
60	1585	1585	0.15	0.15	0.15	0.45
80	1575	1574	0.2	0.2	0.2	0.60
100	1577	1576	0.2	0.2	0.2	0.60
120	1577	1576	0.3	0.3	0.3	0.90
200	1575	1573	0.5	0.5	0.5	1.5
250	1567	1565	0.6	0.6	0.6	1.8
300	1559	1557	0.7	0.7	0.7	2.1
400	1589	1585	1.0	0.95	1.0	2.95
500	1590	1585	1.2	1.15	1.2	3.55
600	1590	1594	1.5	1.4	1.5	4.4
800	1587	1581	2.0	1.9	2.0	5.9
1000	1594	1587	2.5	2.4	2.5	7.4
1200	1591	1581	3.0	2.8	3.0	8.8

TABLE 8-B

PRESSURE PROFILE DATA FLOWING PENTANE

Length of Core = 36 inches

Section 1 = 12 in. Section 2 = 12 in. Section 3 = 12 in.

(1) Q	(2) Pressure Upstream	(3) Pressure Downstream	(4) Pressure Differentials (ΔP) by Transducers	(5)	(6)	(7)
			Sec. 1	Sec. 2	Sec. 3	Total
(cc/hr.)	(p.s.i.g.)	(p.s.i.g.)		(p.s.i.d.)		
40	1.0	0.0	0.2	0.2	0.2	0.8
50	1.0	0.0	0.3	0.3	0.3	0.9
60	1.0	0.0	0.3	0.3	0.4	1.0
80	2.0	0.0	0.4	0.4	0.4	1.2
200	1017	1014	1.1	1.0	1.1	3.2
400	1024	1019	2.1	2.0	2.2	6.3
400	6.0	0.0	2.2	2.1	2.3	6.6
500	8.0	0.0	2.5	2.5	2.9	7.9
800	12.0	0.0	4.0	4.0	4.5	12.5

TABLE 9-B

PRODUCTION DATA

Displacement No. D

Propane Displacing Crude Oil

$Q = 60$ cc/hr

$\mu_{oil}/\mu_{solvent} = 70.5$

Initial Oil in Place = 311.0 cc

$T = 76^{\circ}F$

(1) Time (min: sec)	(2) Pressure Upstream (psig)	(3) Pressure Downstream (psig)	(4) Cum.Oil Produced (stcc)	(5) Cum.Gas Produced (cc at 14.7/60)	(6) Oil Prod. Rate (cc/min)	(7) GOR (scc/stcc)	(8) Cum.Fluid Injected (cc)	(9) Cum.Fluid Injected (PV)	(10) Cum.Gas Produced (res.cc)	(11) Total Cum. Fluid Prod. (res.cc)
0:00	1642	1598	0	0	0	0	0	0.000	0	0.0
4:30	1641	-	7.0	0	1.5	0	-	-	0	7.0
7:00	1639	-	-	-	-	0	-	-	0	-
10:00	1637	1601	13.0	0	0.9	0	10.14	0.033	0	13.0
13:45	1635	-	16.9	0	1.0	0	13.82	0.045	0	16.9
15:45	1634	1601	19.1	0	1.1	0	15.94	0.051	0	19.1
17:45	1633	-	21.2	0	1.05	0	17.82	0.057	0	21.2
19:45	1632	-	23.4	0	1.1	0	20.00	0.064	0	23.4
22:00	1632	-	25.7	0	1.0	0	22.32	0.072	0	25.7
25:20	1631	-	29.2	0	1.05	0	25.68	0.085	0	29.2
29:45	1630	1602	33.9	0	1.05	0	30.16	0.097	0	33.9
32:25	1629	1602	36.7	0	1.0	0	32.90	0.106	0	36.7
37:00	1628	-	41.5	0	1.05	0	37.58	0.121	0	41.5
42:30	1627	-	47.4	0	1.1	0	43.28	0.139	0	47.4
49:45	1625	1605	55.3	0	1.1	0	50.66	0.163	0	55.3
56:15	1623	-	62.2	0	1.05	0	57.35	0.184	0	62.2
60:00	1622	1605	66.2	0	1.05	0	61.24	0.197	0	66.2
64:40	1621	-	71.2	0	1.05	0	65.98	0.212	0	71.2
68:35	1620	-	75.2	0	1.0	0	70.03	0.226	0	75.2
71:20	1619	1606	78.2	0	1.0	0	72.82	0.234	0	78.2
75:10	1618	-	82.2	0	1.0	0	76.72	0.246	0	82.2
79:15	1617	-	86.2	0	1.0	0	80.84	0.260	0	86.2
81.50	1616	-	89.2	0	1.2	0	83.58	0.269	0	89.2
84:30	1615	-	92.2	0	1.15	0	86.12	0.278	0	92.2
85:30	1615	-	95.5	0	3.3	0	87.22	0.280	0	95.5
			SOLVENT BREAKTHROUGH							
91:15	1612	-	101.2	200.0	1.0	35.2	93.22	0.300	0.62	101.82
96:15	1610	-	105.4	559.6	0.85	85.5	98.18	0.316	1.71	107.11

TABLE 9-B (Continued)

(1) Time	(2) Pressure Upstream	(3) Pressure Downstream	(4) Cum.Oil Produced	(5) Cum.Gas Produced	(6) Oil Prod. Rate	(7) GOR	(8) Cum.Fluid Injected	(9) Cum.Fluid Injected	(10) Cum.Gas Produced	(11) Total Cum. Fluid Prod.
(min: sec)	(psig)	(psig)	(stcc)	(cc at 14.7/60)	(cc/min)	(scc/stcc)	(cc)	(PV)	(res.cc)	(res.cc)
99:35	1609	1602	107.0	755.0	0.50	122.0	100.63	0.323	2.32	109.32
100:15	1608	-	108.0	905.1	1.50	150.1	102.22	0.329	2.79	110.79
102:30	1607	-	110.0	1185.4	0.90	140.1	105.04	0.338	3.66	113.66
105:30	1605	-	112.0	1477.1	0.65	145.9	107.88	0.347	4.56	116.56
108:30	1605	-	114.0	1785.7	0.65	154.3	110.82	0.356	5.52	119.52
113:20	1602	1597	117.0	2352.0	0.60	188.8	115.76	0.372	7.29	124.29
116:10	1601	-	119.0	2722.9	0.65	185.5	117.62	0.379	8.45	127.45
119:25	1600	-	121.0	3144.9	0.60	211.0	120.88	0.388	9.76	130.76
122:40	1600	-	123.0	3595.1	0.60	225.1	124.24	0.400	11.16	134.16
125:45	1600	1594	125.0	4059.5	0.65	232.2	127.43	0.410	12.61	137.61
130:30	1598	-	128.0	4707.9	0.65	216.1	132.22	0.425	14.63	142.63
134:30	1597	-	130.0	5211.9	0.50	252.0	135.68	0.436	16.20	146.20
137:02	1595	-	132.0	5721.6	0.85	254.9	138.92	0.446	17.79	149.79
140:19	1594	1590	134.0	6231.3	0.60	254.9	142.16	0.458	19.37	153.37
145:29	1593	-	137.0	7080.8	0.60	283.2	147.48	0.475	22.01	159.01
149:07	1592	1587	139.0	7618.8	0.55	269.0	151.18	0.486	23.69	162.69
153:09	1590	-	141.0	8270.1	0.50	330.7	155.26	0.500	25.75	166.75
156:45	1589	1585	143.0	8949.6	0.55	339.8	159.02	0.513	27.86	170.86
160:18	1588	-	145.0	9544.3	0.55	297.4	162.62	0.523	29.71	174.71
163:43	1588	1584	147.0	10,110.6	0.60	283.2	166.12	0.535	31.48	178.48
169.07	1587	-	152.0	11,016.7	0.55	302.0	171.68	0.551	34.30	186.30
173:03	1587	1583	154.0	11,667.9	0.50	325.6	175.72	0.565	36.33	190.33
180:30	1585	1582	158.0	12,942.2	0.55	318.6	183.46	0.590	40.31	198.31
184:45	1585	-	160.0	13,848.3	0.45	453.1	187.60	0.603	43.13	203.13
189:00	1584	-	162.0	14,471.3	0.45	311.5	191.98	0.616	45.07	207.07
197:50	1582	1577	168.0	16,226.9	0.45	438.9	201.05	0.647	50.54	218.54
208:10	1578	-	172.0	18,265.6	0.50	407.8	211.77	0.679	56.91	228.91
222:20	1577	1574	178.0	21,025.5	0.45	459.8	226.19	0.726	65.55	243.55
236:00	1575	-	183.0	23,985.4	0.35	591.4	240.10	0.772	74.80	257.80
251:00	1574	-	188.0	27,383.4	0.35	679.5	255.27	0.820	85.40	273.40
267:30	1573	1571	193.0	31,077.7	0.30	738.9	272.42	0.875	96.95	289.95
287:00	1583	1582	198.0	33,003.2	0.25	385.1	292.22	0.940	102.98	300.98
295:30	1585	-	200.0	35,098.6	0.25	1047.7	301.07	0.969	108.21	308.21

TABLE 9-B (Continued)

(1)	(2)	(3)	(4)	(5)	(6)	(7)	(8)	(9)	(10)	(11)
Time	Pressure Upstream	Pressure Downstream	Cum. Oil Produced	Cum. Gas Produced	Oil Prod. Rate	GOR	Cum. Fluid Injected	Cum. Fluid Injected	Cum. Gas Produced	Total Cum. Fluid Prod.
(min: sec)	(psig)	(psig)	(stcc)	(cc at 14.7/60)	(cc/min)	(scc/stcc)	(cc)	(PV)	(res.cc)	(res.cc)
305:30	1593	1590	202.0	40,408.7	0.20	2655.2	311.24	1.000	121.51	323.51
316.00	1593	-	204.0	43,212.0	0.20	1401.7	321.70	1.032	128.52	332.52
338:00	1586	1584	207.0	49,469.8	0.18	1564.5	344.82	1.120	144.12	351.12
361:00	1585	-	211.0	55,840.9	0.17	1592.8	368.27	1.185	160.02	371.02
386:00	1580	-	215.0	62,891.6	0.16	1762.7	392.02	1.261	177.62	392.62
413:00	1575	1573	219.0	70,990.0	0.15	2024.6	421.52	1.355	197.82	416.82
441:00	1574	-	223.0	78,493.7	0.14	1875.9	449.77	1.445	216.62	439.62
472.00	1571	1568	225.0	87,300.0	0.13	2201.6	481.47	1.550	238.62	463.62
502:00	1568	-	229.0	96,332.8	0.13	2258.2	513.52	1.650	261.22	490.22
532:00	1568	1565	233.0	105,393.9	0.13	-	543.52	1.750	293.52	526.52
After Blowdown			265.7							
After Cleanup			315.7							

End of Displacement.

Recovery of Oil to Breakthrough = 30.7% OIP

Recovery of Oil after Displacement of 1.750 Pore Volumes = 75% OIP

TABLE 10-B

PRODUCTION DATA

Displacement No. E

Propane Displacing Varsol

$Q = 200$ cc/hr

$\mu_{oil}/\mu_{solvent} = 8.6$

Initial Oil in Place = 319.16 cc

$T = 76^{\circ}F$

(1) Time (min:sec)	(2) Pressure Upstream (p.s.i.g)	(3) Pressure Downstream (p.s.i.g.)	(4) Cum. Oil Produced (s.t. cc)	(5) Cum. Gas Produced (cc at 14.7/60)	(6) Oil Prod. Rate (cc/min)	(7) GOR (scc/stcc)	(8) Cum. Fluid Injected (cc)	(9) Cum. Fluid Injected (PV)
0:00	1583	1569	0	0	0	0	0.00	0.000
1:45	1583	-	8.0	0	4.55	0	5.80	0.018
4:35	1583	-	15.0	0	2.33	0	10.40	0.033
6:30	1583	1570	25.0	0	5.00	0	22.10	0.069
9:25	1581	-	35.0	0	3.33	0	32.18	0.101
12:20	1581	-	45.0	0	3.33	0	42.08	0.132
15:40	1580	-	57.2	0	3.62	0	53.45	0.167
18:40	1580	1570	67.2	0	3.33	0	63.80	0.200
21:30	1579	-	77.2	0	3.33	0	73.40	0.230
24:25	1579	-	87.2	0	3.33	0	83.40	0.261
27:30	1579	-	98.0	0	3.60	0	94.00	0.294
30:55	1578	1572	110.0	0	3.16	0	105.60	0.331
34:30	1578	-	122.0	0	3.16	0	117.83	0.369
37:20	1577	-	132.0	0	3.33	0	127.40	0.398
39:20	1577	-	143.0	0	5.50	0	136.00	0.426
SOLVENT BREAKTHROUGH								
42:50	1576	1572	153.0	170.0	3.00	17.0	146.24	0.469
46:00	1576	-	163.0	481.6	3.30	31.2	157.00	0.492
48:15	1575	-	173.0	849.9	4.30	36.8	168.00	0.526
54.55	1574	-	187.8	1473.1	2.19	40.5	184.12	0.576
57:30	1570	1567	197.8	2294.6	3.20	82.2	196.24	0.614
61:20	1566	1564	207.8	3484.3	2.50	119.0	209.34	0.655
65:25	1565	-	217.8	4957.3	2.50	147.3	223.36	0.700

TABLE 10-B (Continued)

(1) Time (min:sec)	(2) Pressure Upstream (p.s.i.g)	(3) Pressure Downstream (p.s.i.g.)	(4) Cum. Oil Produced (s.t. cc)	(5) Cum. Gas Produced (cc at 14.7/60)	(6) Oil Prod. Rate (cc/min)	(7) GOR (scc/stcc)	(8) Cum. Fluid Injected (cc)	(9) Cum. Fluid Injected (PV)
70:00	1558	1556	227.8	6883.5	2.22	192.6	238.88	0.750
74:50	1553	-	237.3	9546.2	1.98	280.0	255.36	0.800
81:00	1543	1542	247.3	13455.3	1.66	390.9	277.10	0.869
88:35	1530	-	257.3	18667.5	1.33	521.2	302.36	0.946
97:00	1519	1516	267.3	25069.4	1.17	640.2	331.34	1.04
106:35	1507	-	277.3	32717.7	1.05	764.8	364.12	1.11
122:30	1505	-	286.3	47164.5	0.56	1600	418.35	1.31
132:00	1503	-	290.7	55945.9	0.47	1980	451.01	1.41
136:00	-	-	292.7	60478.2	0.50	2270	-	-
147:40	1500	-	296.7	73791.9	0.35	3335	503.75	1.57
160:00	1500	-	300.7	82998.2	0.33	2300	545.95	1.71
170:00	1500	-	304.1	92771	0.34	2880	580.55	1.82
After Blowdown			314.1					
After Cleaning			320.6					
End of Displacement								

Recovery of oil to breakthrough = 45% OIP

Recovery of oil after displacement of 1.82 pore volumes = 95% OIP

TABLE 11-B PRODUCTION DATA

Displacement No. F Propane Displacing Pentane $Q = 400$ cc/hr

$\mu_{oil}/\mu_{solvent} = 2.13$ Initial Oil in Place = 312.65 cc $T = 76^{\circ}F$

(1) Time	(2) Pressure Upstream	(3) Pressure Downstream	(4) Cum.Oil Produced	(5) Cum. Gas Produced	(6) Oil Prod. Rate	(7) GOR	(8) Cum.Fluid Injected	(9) Cum.Fluid Injected	(10) Cum.Gas Produced	(11) Total Cum. Fluid Prod.
(min: sec)	(psig)	(psig)	(stcc)	(cc at 14.7/60)	(cc/min)	(scc/stcc)	(cc)	(PV)	(res.cc)	(res.cc)
0:00	1030	1025	0	0	0	0	0	0.000	0	0
3:01	1030	1025	22	0	7.3	0	20.6	0.066	0	22
4:50	1030	-	35	0	6.5	0	33.3	0.107	0	35
6:20	1030	-	45	0	6.7	0	43.2	0.138	0	45
8:35	1030	-	61	0	7.6	0	58.7	0.188	0	61
10:20	1032	1027	73	0	6.0	0	70.7	0.226	0	73
11:45	1033	1028	83	0	6.7	0	80.6	0.258	0	83
13:15	1031	1028	93	0	6.7	0	90.6	0.290	0	93
15:15	1031	-	107	0	7.0	0	104.0	0.334	0	107
16:45	1031	-	117	0	6.7	0	114.2	0.366	0	117
18:10	1031	-	127	0	6.7	0	124.0	0.398	0	127
19:30	1031	-	137	0	7.5	0	133.6	0.428	0	137
21:00	1031	-	147	0	6.7	0	143.0	0.459	0	147
22:30	1030	-	158	0	7.3	0	153.5	0.492	0	158
24:00	1030	1028	168	0	6.7	0	163.8	0.525	0	168
25:30	1030	-	178	0	6.7	0	173.9	0.556	0	178
26:50	1030	-	188	0	7.0	0	183.3	0.588	0	188
28:15	1030	-	198	0	6.7	0	192.9	0.619	0	198
29.45	1030	-	209	0	7.3	0	203.1	0.650	0	209
SOLVENT BREAKTHROUGH										
31:00	1030	-	219	Tr.	8.8	0	212.0	0.680	Tr.	219
33:00	1029	1026	229	1070	5.0	107	225.4	0.721	3.4	232.4
36:00	1027	-	239	3360	3.0	336	246.0	0.790	14.0	253.0

TABLE 11-B (Continued)

(1) Time	(2) Pressure Upstream	(3) Pressure Downstream	(4) Cum.Oil Produced	(5) Cum.Gas Produced	(6) Oil Prod. Rate	(7) GOR	(8) Cum.Fluid Injected	(9) Cum.Fluid Injected	(10) Cum.Gas Produced	(11) Total Cum. Fluid Prod.
(min: sec)	(psig)	(psig)	(stcc)	(cc at 14.7/60)	(cc/min)	(scc/stcc)	(cc)	(PV)	(res.cc)	(res.cc)
39:30	1018	1015	247	7,830	2.9	425	269.3	0.864	24.8	271.8
46:00	1012	-	247	19,720	0.0	∞	312.5	1.000	62.4	309.4
49:00	-	-	-	-	-	-	-	-	-	-
52:15	996	993	247	33,260	0.0	∞	356.8	1.140	105.8	352.8
57:20	985	-	247	44,560	0.0	∞	391.9	1.255	141.7	388.7
59:20	965	962	247	48,810	0.0	∞	402.0	1.290	155.2	402.2

End of Displacement

Recovery of oil to breakthrough = 70% OIP

Total recovery of oil = 100% OIP (79.5% in liquid phase and
21.5% in vapor phase)

TABLE 12-B

PRODUCTION DATA

Displacement No. G

Propane Displacing Pentane

$Q = 200$ cc/hr

$\mu_{oil}/\mu_{solvent}$

Initial Oil in Place = 314.00 cc

$T = 76^{o}F$

(1) Time	(2) Pressure Upstream	(3) Pressure Downstream	(4) Cum.Oil Produced	(5) Cum.Gas Produced	(6) Oil Prod. Rate	(7) GOR	(8) Cum.Fluid Injected	(9) Cum.Fluid Injected	(10) Cum.Gas Produced	(11) Total Cum. Fluid Prod.
(min: sec)	(psig)	(psig)	(stcc)	(cc at 14.7/60)	(cc/min)	(scc/stcc)	(cc)	(PV)	(res.cc)	(res.cc)
0:00	1022	1019	0	0	0	0	0.00	0.000	0	0
2:35	1022	-	10.0	0	4.0	0	8.90	0.028	0	10.0
5:25	1022	-	20.0	0	3.5	0	18.64	0.059	0	20.0
8:20	1023	1020	30.0	0	3.4	0	28.39	0.090	0	30.0
12:30	1023	-	45.0	0	3.7	0	42.98	0.136	0	45.0
15:55	1023	-	56.5	0	2.9	0	54.49	0.173	0	56.5
18:50	1024	1021	66.5	0	3.4	0	64.42	0.205	0	66.5
21:40	1024	-	76.5	0	3.5	0	74.18	0.236	0	76.5
24:30	1023	-	86.5	0	3.5	0	83.85	0.265	0	86.5
27:20	1023	-	96.5	0	3.5	0	93.42	0.297	0	96.5
30:45	1023	-	106.0	0	2.7	0	105.12	0.335	0	106.0
33:35	1024	1022	116.0	0	3.5	0	115.00	0.366	0	116.0
36:30	1024	-	126.0	0	3.4	0	124.56	0.396	0	126.0
39:15	1024	-	136.0	0	3.6	0	134.20	0.428	0	136.0
42:05	1024	-	146.0	0	3.5	0	143.88	0.457	0	146.0
45:00	1023	1022	156.0	0	3.4	0	153.72	0.489	0	156.0
47:50	1025	1023	166.0	0	3.5	0	163.48	0.520	0	166.0
50:40	1025	1024	176.0	0	3.5	0	172.98	0.550	0	176.0
53:25	1025	1024	186.0	0	3.6	0	182.55	0.580	0	186.0
56:25	1025	-	196.0	0	3.3	0	192.65	0.613	0	196.0
58:50	1025	-	206.0	0	4.0	0	201.18	0.640	0	206.0
				SOLVENT BREAKTHROUGH						
61:20	1025	-	216.0	141.5	4.0	14.2	210.16	0.669	0.45	216.45
64:00	1022	-	226.0	567	3.8	42.5	222.18	0.706	1.86	227.86
67.30	1022	-	231.0	1,417	1.4	170.0	230.50	0.731	4.46	235.46
70:30	1018	-	236.0	2,832	1.6	283.0	240.94	0.765	8.95	244.95
74:45	1015	-	241.0	5,437	1.2	521.0	255.36	0.812	16.94	257.94

TABLE 12-B (Continued)

(1) Time (min:sec)	(2) Pressure Upstream (psig)	(3) Pressure Downstream (psig)	(4) Cum.Oil Produced (stcc)	(5) Cum.Gas Produced (cc at 14.7/60)	(6) Oil Prod. Rate (cc/min)	(7) GOR (scc/stcc)	(8) Cum.Fluid Injected (cc)	(9) Cum.Fluid Injected (PV)	(10) Cum.Gas Produced (res.cc)	(11) Total Cum. Fluid Prod. (res.cc)
81:10	1009	-	245.0	10,757	0.6	1330	277.56	0.881	33.85	278.85
85:10	1005	-	245.0	14,437	0	∞	289.62	0.920	45.60	290.60
89:00	1003	-	245.0	18,397	0	∞	303.66	0.964	58.20	303.20
94:30	1000	-	245.0	24,347	0	∞	323.12	1.030	77.10	322.10
99:50	997	-	245.0	29,727	0	∞	341.18	1.085	94.25	339.25
105:30	996	-	245.0	35,817	0	∞	360.00	1.145	113.65	358.65
111:00	989	-	245.0	-	0	∞	378.00	1.205	-	-

End of Displacement

Recovery of Oil to Breakthrough = 65% OIP

Total Recovery of Oil = 100% OIP (78% in Liquid Phase and
22% in Vapor Phase)

TABLE 13-B

PRODUCTION DATA

Displacement No. H   Propane Displacing Esso P-40 $Q = 200$ cc/hr

$\mu_{oil}/\mu_{solvent} = 14.2$ Initial Oil in Place = 315.0 cc $T = 76^{\circ}F$

(1) Time (min:sec)	(2) Pressure Upstream (p.s.i.g.)	(3) Pressure Downstream (p.s.i.g.)	(4) Cum. Oil Produced (s.t. cc)	(5) Cum. Gas Produced (cc at 14.7/60)	(6) Oil Prod. Rate (cc/min)	(7) GOR (scc/stcc)	(8) Cum. Fluid Injected (cc)	(9) Cum. Fluid Injected (PV)
0:00	1025	1003	0	0	0	0	0	0.000
2:30	1025	-	10	0	4.0	0	8.36	0.027
5:15	1024	1003	20	0	3.6	0	17.92	0.057
8:10	1021	1003	30	0	3.5	0	27.84	0.088
11:05	1020	-	40	0	3.5	0	37.97	0.120
14:00	1019	-	50	0	3.5	0	47.70	0.151
17:00	1018	1003	61	0	3.7	0	58.18	0.185
19:55	1016	-	71	0	3.5	0	68.06	0.216
22:50	1014	-	81	0	3.5	0	77.78	0.246
25:40	1013	1003	91	0	3.6	0	87.72	0.278
28:35	1011	-	101	0	3.5	0	97.69	0.310
30:55	1010	-	111	0	4.3	0	105.48	0.335
SOLVENT BREAKTHROUGH								
34:00	1008	-	121	Tr.	3.2	0	116.26	0.368
38:10	1005	1000	131	1130	2.4	113	130.44	0.414
40:45	1004	-	136	2260	2.0	226	139.04	0.441
43:05	1003	-	141	3250	2.1	198	147.26	0.468
45:35	1002	-	146	4380	2.0	226	155.88	0.494
48:20	1002	-	151	5655	1.8	255	165.18	0.525
51:20	1001	998	156	7070	1.7	283	175.24	0.556
54:10	1001	-	161	8485	1.8	283	185.12	0.588
57:00	1001	-	166	9760	1.8	255	194.60	0.616
59:50	1000	-	171	11,035	1.8	225	204.28	0.646

TABLE 13-B (Continued)

(1) Time (min:sec)	(2) Pressure Upstream (p.s.i.g.)	(3) Pressure Downstream (p.s.i.g.)	(4) Cum. Oil Produced (s.t. cc)	(5) Cum. Gas Produced (cc at 14.7/60)	(6) Oil Prod. Rate (cc/min)	(7) GOR (scc/stcc)	(8) Cum. Fluid Injected (cc)	(9) Cum. Fluid Injected (PV)
62:45	1000	-	176	16,535	1.7	300	214.42	0.680
65:55	1000	996	181	18,035	1.5	300	225.00	0.715
69:15	998	-	186	20,015	1.5	396	236.47	0.750
73:05	998	-	191	22,275	1.3	452	249.60	0.791
77:25	997	-	196	25,105	1.15	566	264.35	0.838
82:00	997	-	200	27,935	1.1	708	279.86	0.885
86:45	997	-	205	31,335	1.05	680	296.14	0.940
91:55	997	-	210	35,015	0.96	736	313.85	0.995
94:55	997	995	213	37,280	1.0	755	324.04	1.030
103:15	997	-	220	43,520	0.85	891	352.76	1.118
108:35	997	-	225	47,340	0.95	765	371.00	1.179
114:35	997	-	230	51,730	0.83	878	391.52	1.240
122:30	997	-	235	57,960	0.63	1242	418.52	1.330
137:20	997	-	241	70,710	0.40	2120	469.23	1.490

After Blowdown:- 268.4
After Cleaning:- 316.4 cc
End of Displacement

Recovery of oil to breakthrough = 35% OIP

Recovery of oil after displacement of 1.5 pore volumes = 76% OIP

TABLE 14-B PRESSURE PROFILE DATA

Displacement No. D Propane Displacing Crude Oil Q = 60 cc/hr

Length of Core = 36 in.

Sec. 1 = 6 in. Sec. 2 = 12 in. Sec. 3 = 12 in. Sec. 4 = 6 in.

(1)	(2)	(3)	(4)	(5)	(6)
Time	Pressure Differential per inch ($\Delta P/\Delta L$)				
	Sec. 1	Sec. 2	Sec. 3	Sec. 4	Total
(min:sec)	(p.s.i.d./in.)				
0:00	1.13	1.53	0.96	1.23	1.22
4:30	0.83	1.52	1.00	1.20	1.20
7:00	0.60	1.52	1.00	1.20	1.14
10:00	0.40	1.19	0.99	1.18	0.98
13:45	0.30	1.05	0.99	1.18	0.93
15:45	0.30	0.99	0.99	1.18	0.91
17:45	0.30	0.92	0.98	1.18	0.88
19:45	0.30	0.83	0.98	1.17	0.85
22:00	0.28	0.77	0.98	1.17	0.83
25:20	0.30	0.68	0.98	1.17	0.80
29:45	0.33	0.53	0.98	1.17	0.75
32:25	0.38	0.45	0.98	1.17	0.74
37:00	0.52	0.30	0.93	1.17	0.69
42:30	0.60	0.22	0.82	1.17	0.64
49.45	0.57	0.17	0.67	1.17	0.57
56:15	0.57	0.14	0.52	1.15	0.51
60:00	0.53	0.13	0.43	1.13	0.47
64:40	0.50	0.12	0.37	1.08	0.43
68:35	0.48	0.12	0.32	0.98	0.39
71:20	0.47	0.11	0.28	0.90	0.36
75:10	0.47	0.10	0.26	0.77	0.33
79:15	0.45	0.09	0.23	0.58	0.28
81:50	0.45	0.09	0.22	0.52	0.26
84:30	0.45	0.09	0.21	0.47	0.25
85:30	0.45	0.08	0.20	0.45	0.24
91:15	0.42	0.08	0.17	0.38	0.21
96:15	0.42	0.08	0.16	0.35	0.20
99:35	0.40	0.08	0.16	0.32	0.20
100:15	0.40	0.08	0.16	0.32	0.20
102:30	0.40	0.07	0.15	0.30	0.19
105:30	0.40	0.07	0.14	0.28	0.18
108:30	0.40	0.07	0.14	0.28	0.18
113:20	0.40	0.07	0.13	0.25	0.17
116:10	0.40	0.07	0.13	0.25	0.17
119:25	0.38	0.06	0.12	0.23	0.16
122:40	0.38	0.06	0.11	0.22	0.16
125:45	0.38	0.06	0.11	0.22	0.16

TABLE 14-B (Continued)

(1)	(2)	(3)	(4)	(5)	(6)
	Pressure Differential per in (ΔP/ΔL)				
Time	Sec. 1	Sec. 2	Sec. 3	Sec. 4	Total
(min:sec)	(p.s.i.d./in.)				
130:30	0.37	0.05	0.10	0.20	0.14
134:40	0.37	0.05	0.10	0.20	0.14
137:02	0.37	0.05	0.10	0.20	0.14
140:19	0.37	0.05	0.09	0.18	0.14
145:29	0.37	0.05	0.08	0.18	0.14
149:07	0.35	0.05	0.08	0.18	0.13
153:09	0.35	0.05	0.08	0.18	0.13
156:45	0.35	0.05	0.08	0.18	0.13
160:18	0.33	0.05	0.07	0.18	0.13
163:43	0.33	0.05	0.07	0.17	0.12
169:07	0.33	0.05	0.07	0.17	0.12
173:03	0.33	0.05	0.07	0.17	0.12
180:30	0.33	0.04	0.06	0.15	0.11
184:45	0.33	0.04	0.06	0.15	0.11
189:00	0.32	0.04	0.06	0.12	0.11
197:50	0.32	0.04	0.06	0.12	0.11
208:10	0.30	0.04	0.05	0.10	0.10
222:20	0.28	0.04	0.04	0.08	0.09
236:00	0.28	0.04	0.04	0.08	0.09
251:00	0.28	0.04	0.04	0.08	0.09

Pressures Became Erratic

TABLE 15-B

PRESSURE PROFILE DATA

Displacement No. E Propane Displacing Varsol Q = 200 cc/hr

Length of Core = 36 inches

Section 1 = 12 in. Section 2 = 12 in. Section 3 = 12 in.

(1) Time	(2) Pressure Differential per inch ($\Delta F/\Delta L$) Sec. 1	(3) Sec. 2	(4) Sec. 3	(5) Total
(min:sec)	(p.s.i.d./in.)			
0:00	0.39	0.37	0.39	0.38
1:45	0.35	0.37	0.38	0.36
4:35	0.28	0.37	0.38	0.34
6:30	0.24	0.37	0.38	0.33
9:25	0.18	0.37	0.38	0.31
12:20	0.14	0.34	0.38	0.29
15:40	0.10	0.31	0.38	0.26
18:40	0.10	0.26	0.38	0.25
21:30	0.08	0.23	0.38	0.23
24:25	0.075	0.20	0.35	0.21
27:30	0.07	0.18	0.34	0.20
30:55	0.06	0.17	0.33	0.18
34:30	0.06	0.14	0.29	0.16
37:20	0.05	0.13	0.27	0.15
39:30	0.05	0.12	0.26	0.14
42:50	0.05	0.10	0.24	0.13
46:00	0.05	0.09	0.22	0.12
48:15	0.05	0.08	0.20	0.11
54:55	0.05	0.075	0.16	0.095
57:30	0.05	0.07	0.14	0.085
61:20	0.05	0.07	0.13	0.08
65:25	0.04	0.07	0.12	0.075
70:00	0.04	0.06	0.10	0.05
74:50	0.04	0.06	0.09	0.06
81:00	0.04	0.06	0.08	0.06
88:35	0.04	0.05	0.075	0.055
97:00	0.04	0.05	0.07	0.05
106:35	0.04	0.05	0.06	0.05
122:30	0.04	0.04	0.06	0.05
132:00	0.04	0.04	0.05	0.045
136:00	0.04	0.04	0.05	0.045
147:00	0.03	0.04	0.05	0.040
160:00	0.04	0.04	0.05	0.045
170:00	-	-	-	-

TABLE 16-B PRESSURE PROFILE DATA

Displacement No. F Propane Displacing Pentane Q = 400 cc/hr.

Length of Core = 36 inches

Section 1 = 12 in. Section 2 = 12 in. Section 3 = 12 in.

(1)	(2)	(3)	(4)	(5)
	Pressure Differential per inch ($\Delta P/\Delta L$)			
Time	Sec. 1	Sec. 2	Sec. 3	Total
(min:sec)	(p.s.i.d./in.)			
0:00	0.165	0.175	0.180	0.175
3:01	0.165	0.175	0.180	0.175
4:50	0.140	0.165	0.180	0.165
6:20	0.125	0.165	0.180	0.160
8:35	0.115	0.165	0.180	0.155
10:20	0.100	0.165	0.180	0.155
11:45	0.090	0.165	0.180	0.145
13:15	0.090	0.160	0.180	0.145
15:15	0.083	0.150	0.180	0.140
16:45	0.083	0.140	0.180	0.135
18:10	0.083	0.135	0.180	0.135
19:30	0.083	0.125	0.180	0.130
21:00	0.083	0.115	0.180	0.128
22:30	0.083	0.110	0.180	0.125
24:00	0.083	0.110	0.180	0.125
25:30	0.083	0.100	0.175	0.120
26:50	0.083	0.100	0.165	0.117
28:15	0.083	0.090	0.160	0.111
29:45	0.083	0.090	0.150	0.108
31:00	0.083	0.090	0.140	0.105
33:00	0.083	0.090	0.135	0.103
36:00	0.083	0.083	0.125	0.097
39:30	0.083	0.083	0.117	0.095
46:00	0.083	0.083	0.100	0.089
52:15	0.083	0.083	0.090	0.086
57:20	0.083	0.083	0.083	0.083
59:20	0.083	0.083	0.083	0.083

TABLE 17-B

PRESSURE PROFILE DATA

Displacement No. H — Propane Displacing Esso P-40 — Q = 200 cc/hr

Length of Core = 36 inches

Section 1 = 12 in. — Section 2 = 12 in. — Section 3 = 12 in.

(1)	(2)	(3)	(4)	(5)
Time	Pressure Differential per inch ($\Delta P/\Delta L$)			
	Sec. 1	Sec. 2	Sec. 3	Total
(min:sec)	(p.s.i.d./in.)			
0:00	0.659	0.666	0.717	0.681
2:30	0.550	0.650	0.709	0.636
5:15	0.384	0.650	0.709	0.580
8:10	0.250	0.634	0.709	0.530
11:05	0.183	0.567	0.709	0.486
14:00	0.150	0.492	0.709	0.450
17:00	0.125	0.375	0.709	0.403
19:55	0.117	0.275	0.666	0.353
22:50	0.100	0.234	0.567	0.300
25:40	0.092	0.217	0.467	0.258
28:35	0.083	0.200	0.384	0.222
30:55	0.075	0.183	0.325	0.195
34:00	0.075	0.175	0.284	0.178
38:10	0.067	0.150	0.267	0.161
40:45	0.067	0.142	0.250	0.153
43:05	0.067	0.133	0.242	0.147
45:35	0.058	0.125	0.233	0.139
48:20	0.058	0.117	0.216	0.131
51:20	0.050	0.108	0.200	0.119
54:10	0.050	0.100	0.183	0.111
57:00	0.050	0.100	0.175	0.108
59:50	0.050	0.100	0.167	0.105
62:45	0.050	0.092	0.158	0.100
65:55	0.050	0.092	0.150	0.097
69:15	0.050	0.083	0.142	0.092
73:05	0.050	0.083	0.133	0.089
77:25	0.050	0.075	0.125	0.083
82:00	0.050	0.067	0.125	0.081
86:45	0.042	0.067	0.117	0.075
91:55	0.042	0.067	0.117	0.075
94:55	0.042	0.059	0.108	0.070
103:15	0.042	0.059	0.100	0.067
108:35	0.042	0.059	0.092	0.064
114:35	0.042	0.059	0.083	0.061
122:30	0.042	0.050	0.075	0.056
137:20	-	-	-	-

TABLE 18-B VOLTAGE CALIBRATION OF TRANSDUCERS

Transducers Model PM80TC ± 15 - 350

(1) Transducer Serial No.	(2) Transducer Resistance (ohms)	(3) Calibration Factor (microvolt/volt/psi)	(4) Galvanometer Resistance (ohms)	(5) $1/S_V$ of Galvanometer (millivolts/in)	(6) Applied Voltage to Transducer for Full (14 psid) Deflection (volts)
No. 2639	356.9	173.9	65.4	0.414	5.949
No. 3691	355.8	148.7	65.4	0.414	6.889
No. 3713	350.5	123.4	65.4	0.414	8.459
No. 3692	354.5	155.8	65.4	0.414	6.539
No. 3830	347.0	125.9	65.4	0.414	8.169

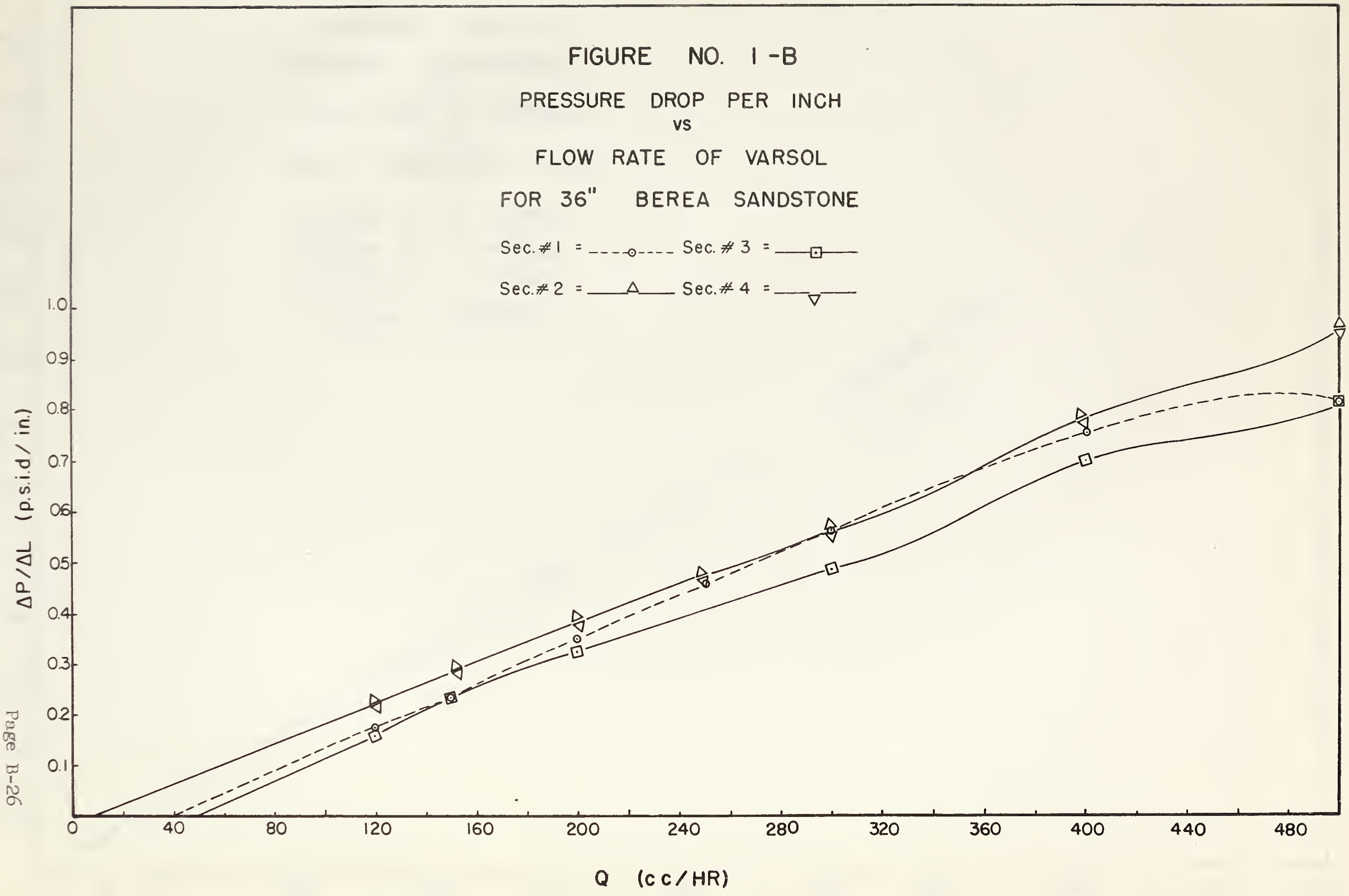

FIGURE NO. 1-B

PRESSURE DROP PER INCH
vs
FLOW RATE OF VARSOL
FOR 36" BEREA SANDSTONE

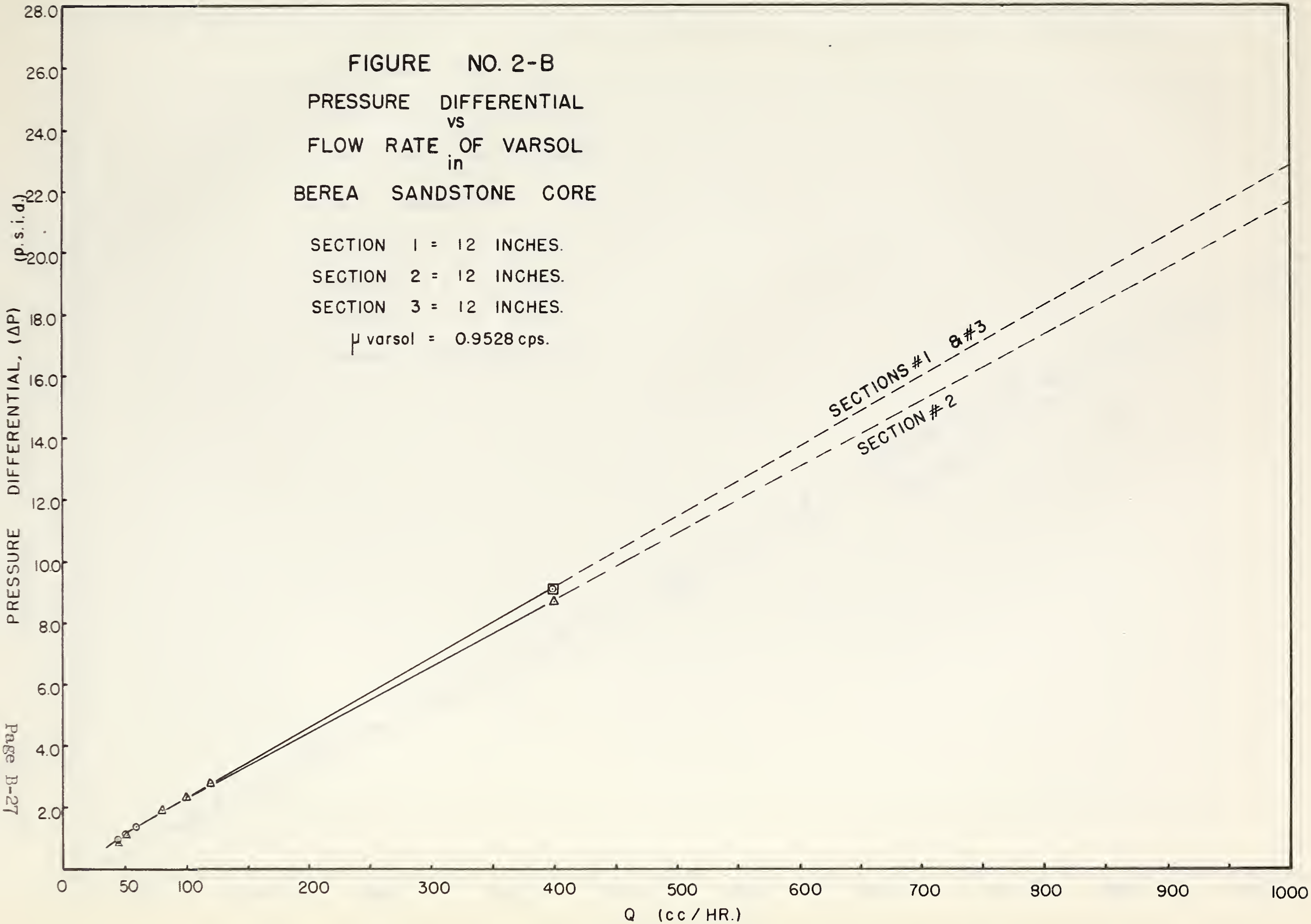

FIGURE NO. 2-B

PRESSURE DIFFERENTIAL
vs
FLOW RATE OF VARSOL
in
BEREA SANDSTONE CORE

SECTION 1 = 12 INCHES.
SECTION 2 = 12 INCHES.
SECTION 3 = 12 INCHES.
μ varsol = 0.9528 cps.

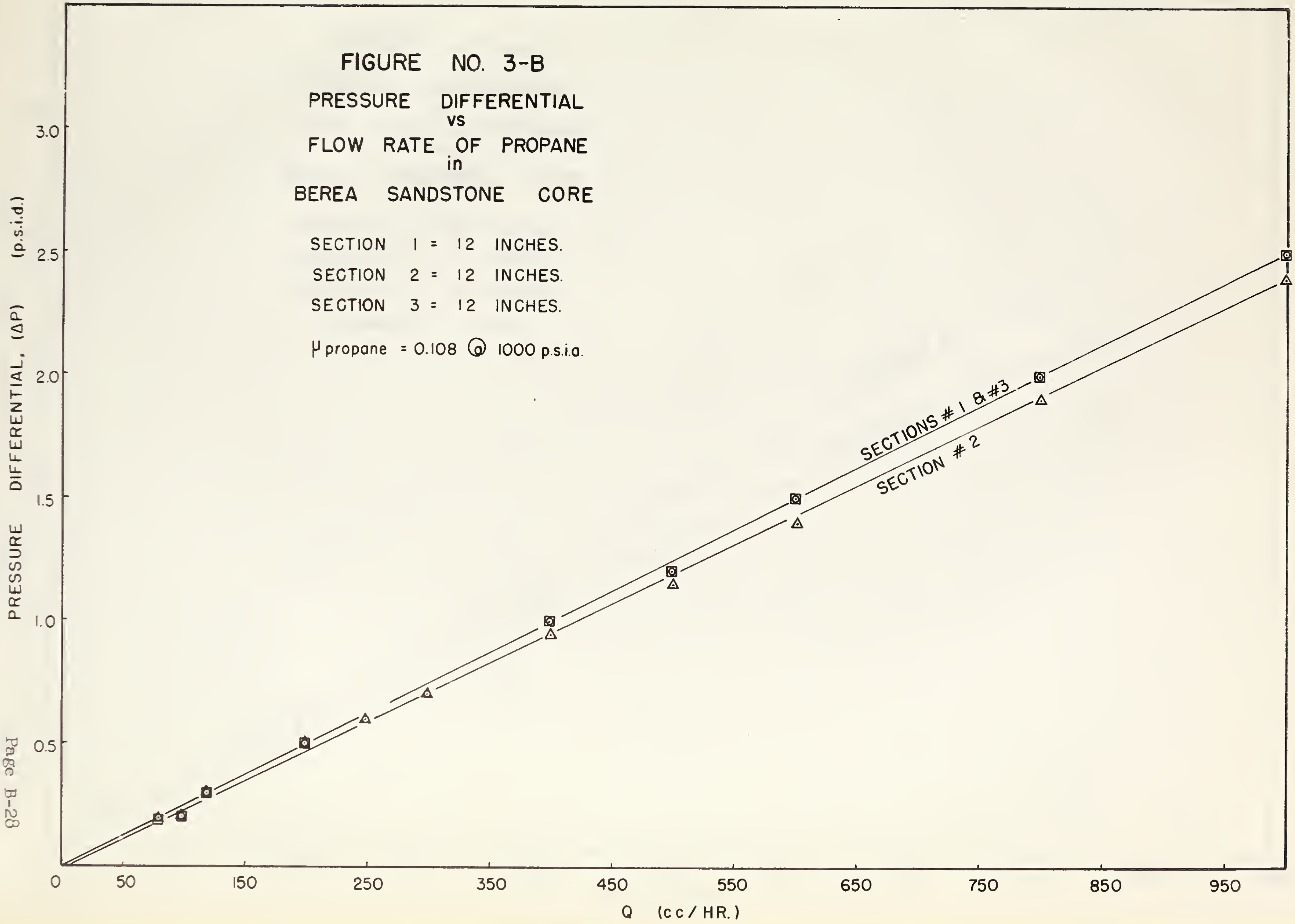

FIGURE NO. 3-B

PRESSURE DIFFERENTIAL vs FLOW RATE OF PROPANE in BEREA SANDSTONE CORE

SECTION 1 = 12 INCHES.
SECTION 2 = 12 INCHES.
SECTION 3 = 12 INCHES.

$\mu_{propane}$ = 0.108 @ 1000 p.s.i.a.

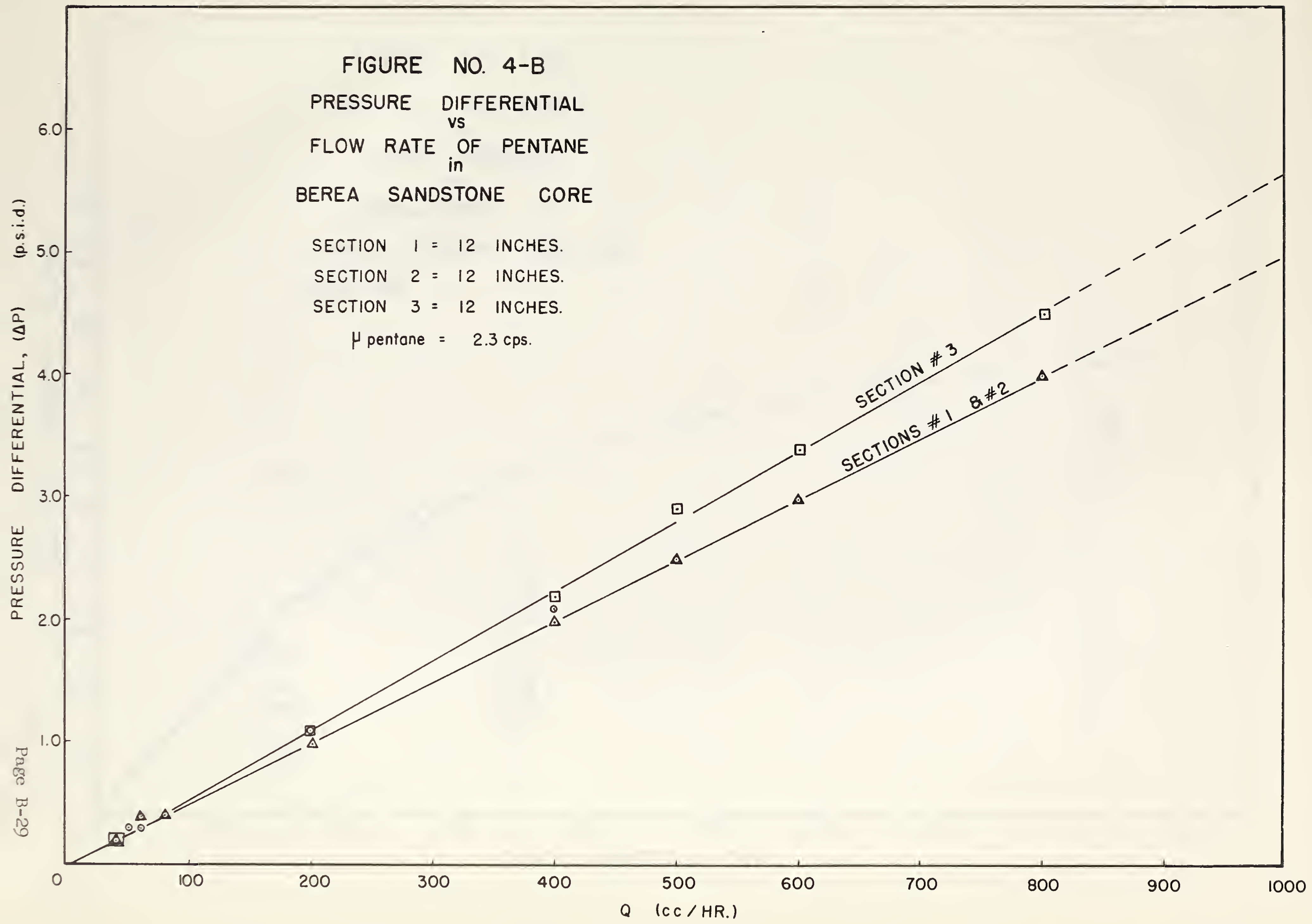

FIGURE NO. 4-B

PRESSURE DIFFERENTIAL vs FLOW RATE OF PENTANE in BEREA SANDSTONE CORE

SECTION 1 = 12 INCHES.
SECTION 2 = 12 INCHES.
SECTION 3 = 12 INCHES.
μ pentane = 2.3 cps.

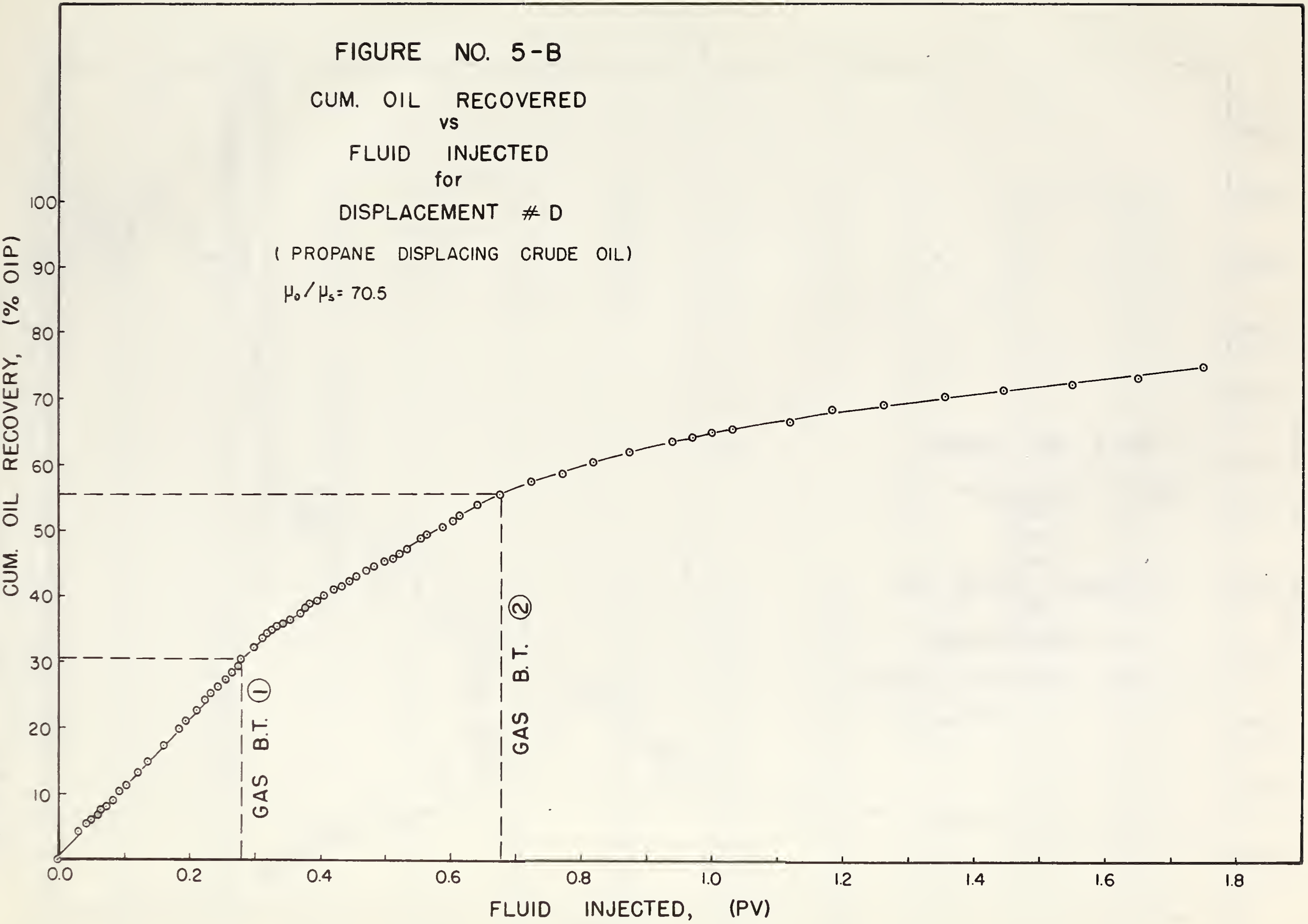

FIGURE NO. 5-B

CUM. OIL RECOVERED
vs
FLUID INJECTED
for
DISPLACEMENT # D

(PROPANE DISPLACING CRUDE OIL)

$\mu_o / \mu_s = 70.5$

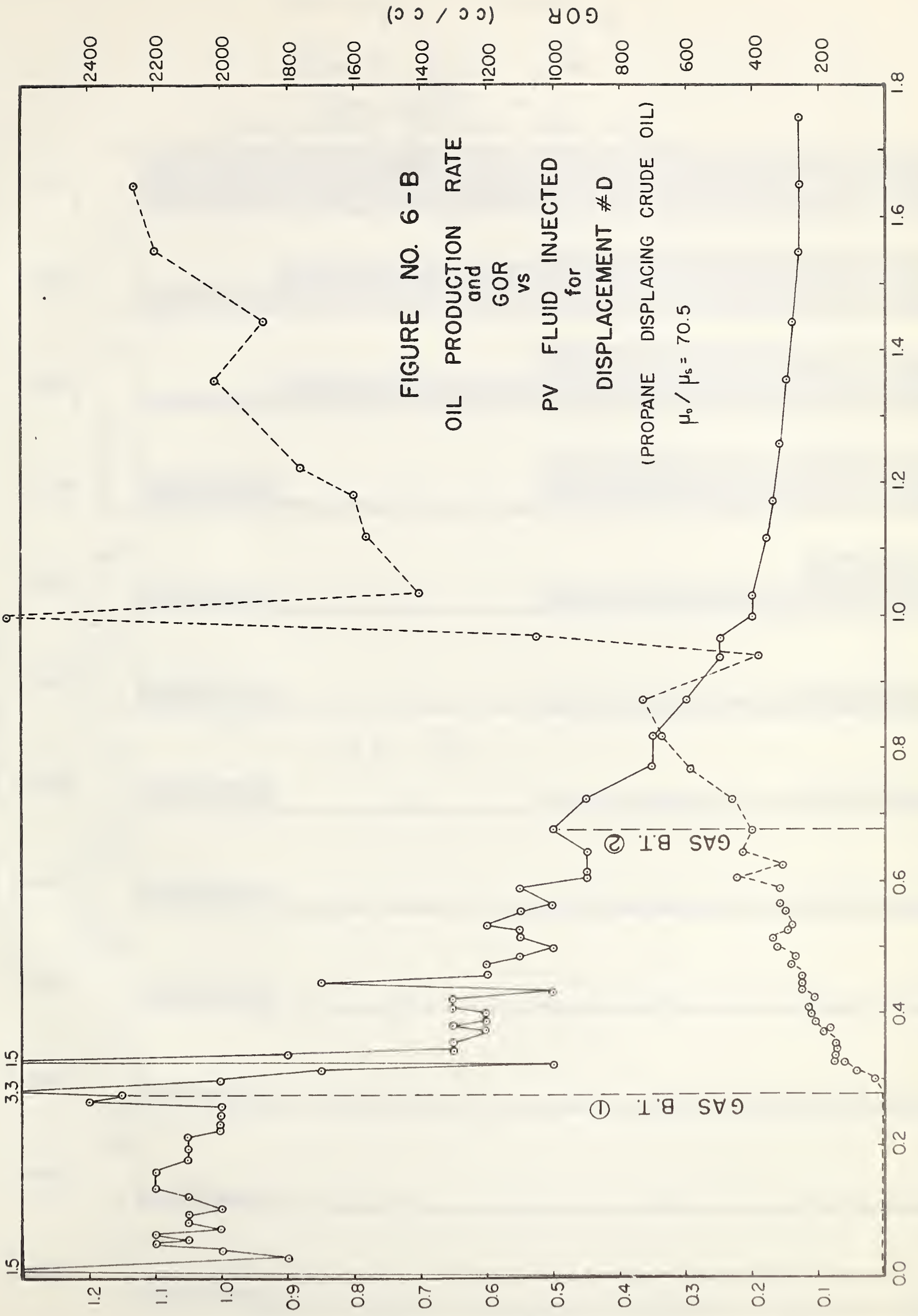

FIGURE NO. 6-B

OIL PRODUCTION RATE and GOR vs PV FLUID INJECTED for DISPLACEMENT #D

(PROPANE DISPLACING CRUDE OIL)

$\mu_o / \mu_s = 70.5$

FIGURE NO. 7-B

$(\Delta P/\Delta L)_{t=t} \,/\, (\Delta P/\Delta L)_{t=0}$

vs

DISTANCE ALONG CORE

for

DISPLACEMENT # D

(PURE PROPANE DISPLACING CRUDE OIL)

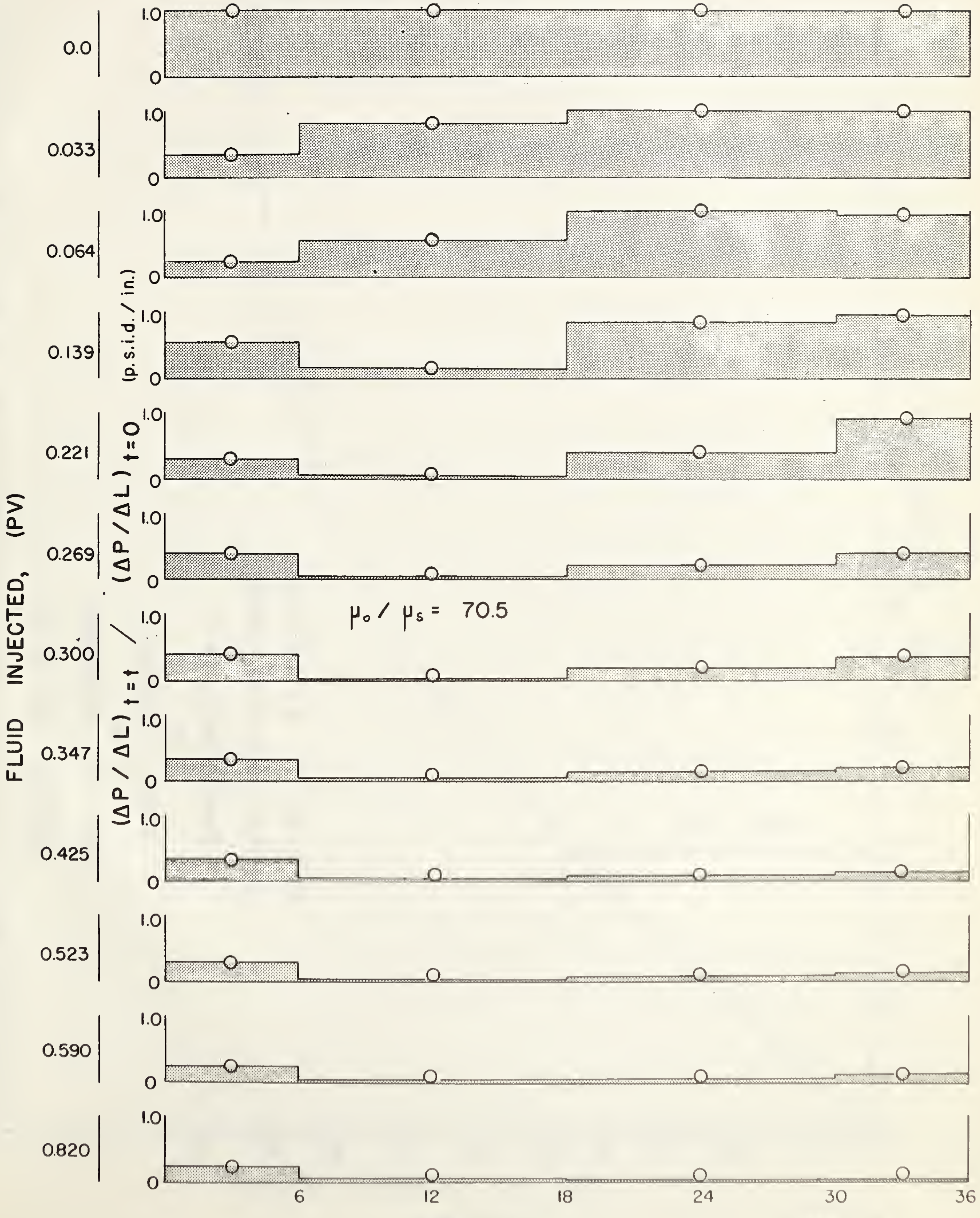

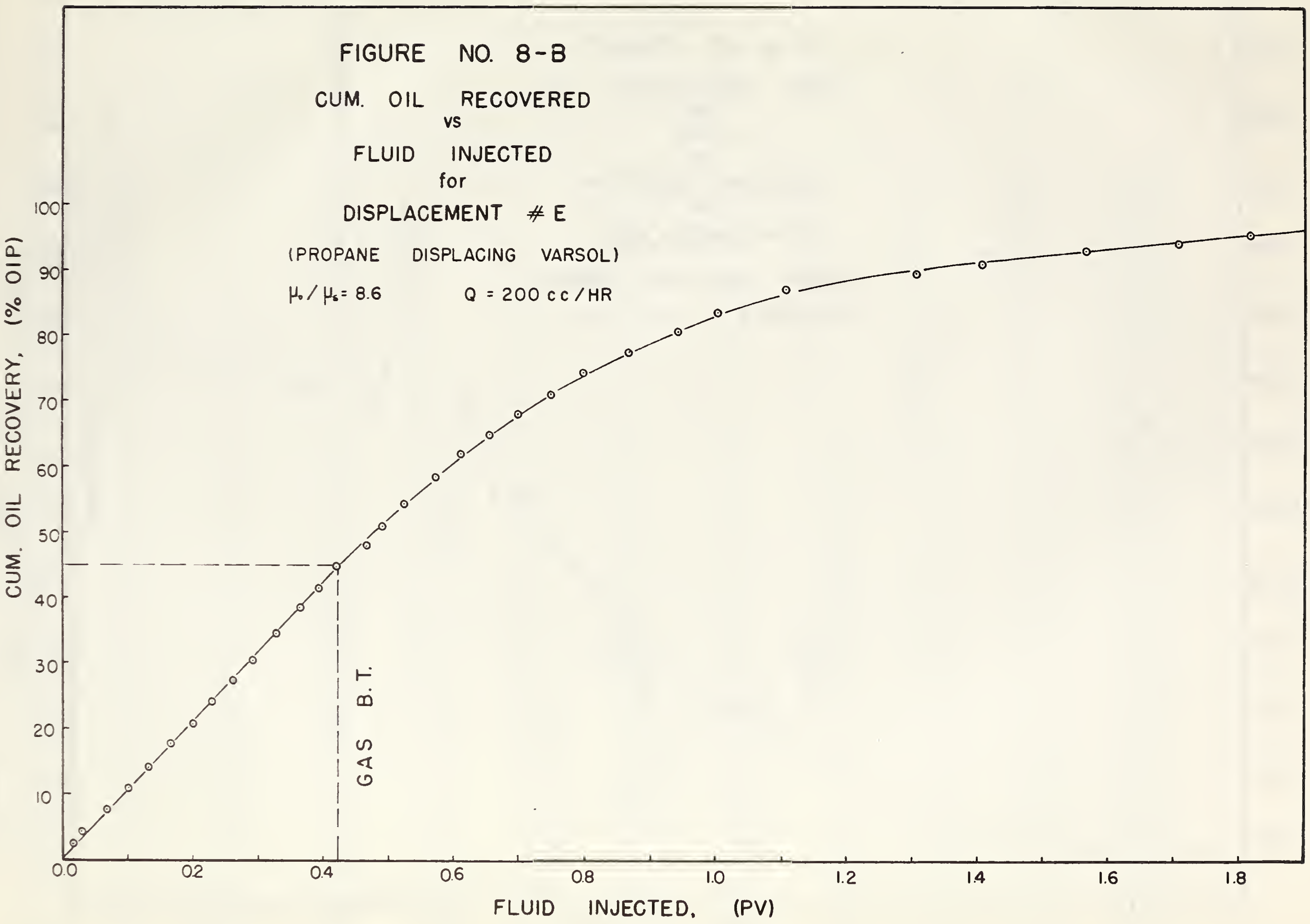

FIGURE NO. 8-B
CUM. OIL RECOVERED
vs
FLUID INJECTED
for
DISPLACEMENT # E
(PROPANE DISPLACING VARSOL)
$\mu_o / \mu_s = 8.6$ Q = 200 cc/HR

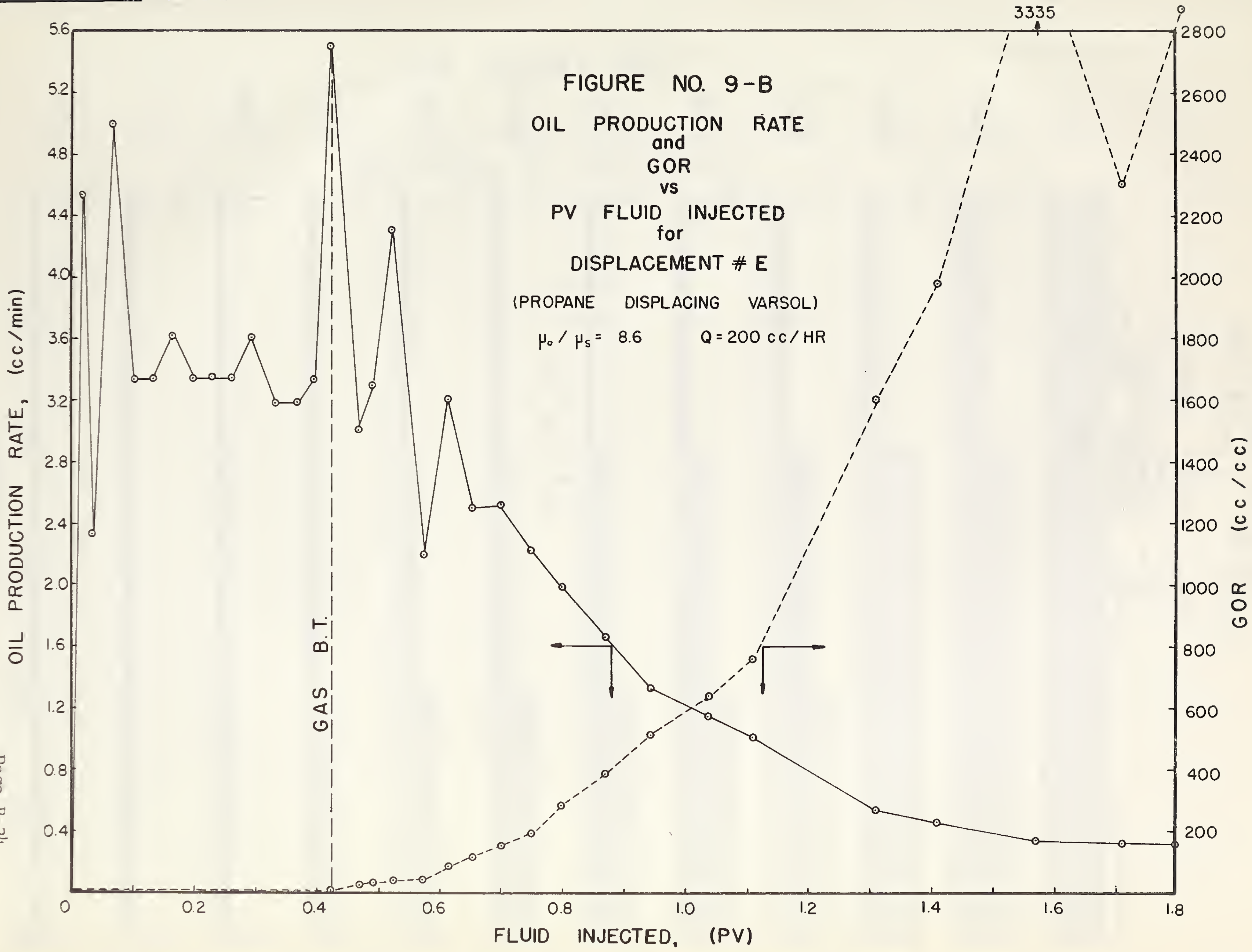

FIGURE NO. 9-B

OIL PRODUCTION RATE
and
GOR
vs
PV FLUID INJECTED
for
DISPLACEMENT # E

(PROPANE DISPLACING VARSOL)

$\mu_o / \mu_s = 8.6$ $Q = 200$ cc/HR

FIGURE NO. 10-B

$(\Delta P / \Delta L)_{t=t} \;/\; (\Delta P / \Delta L)_{t=0}$

vs

DISTANCE ALONG CORE

for

DISPLACEMENT # E

(PROPANE DISPLACING VARSOL)

Q = 200 cc/HR.

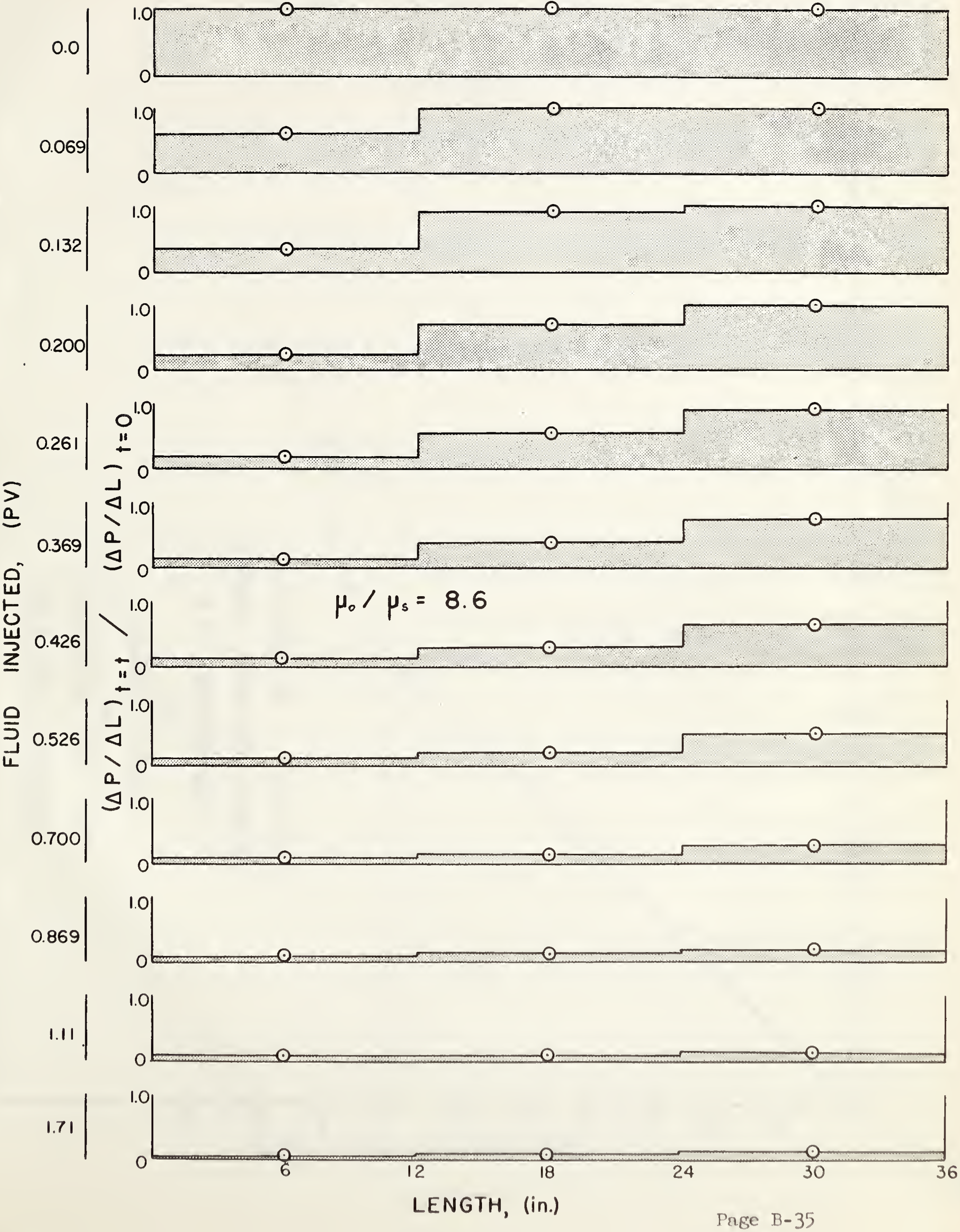

$\mu_o / \mu_s = 8.6$

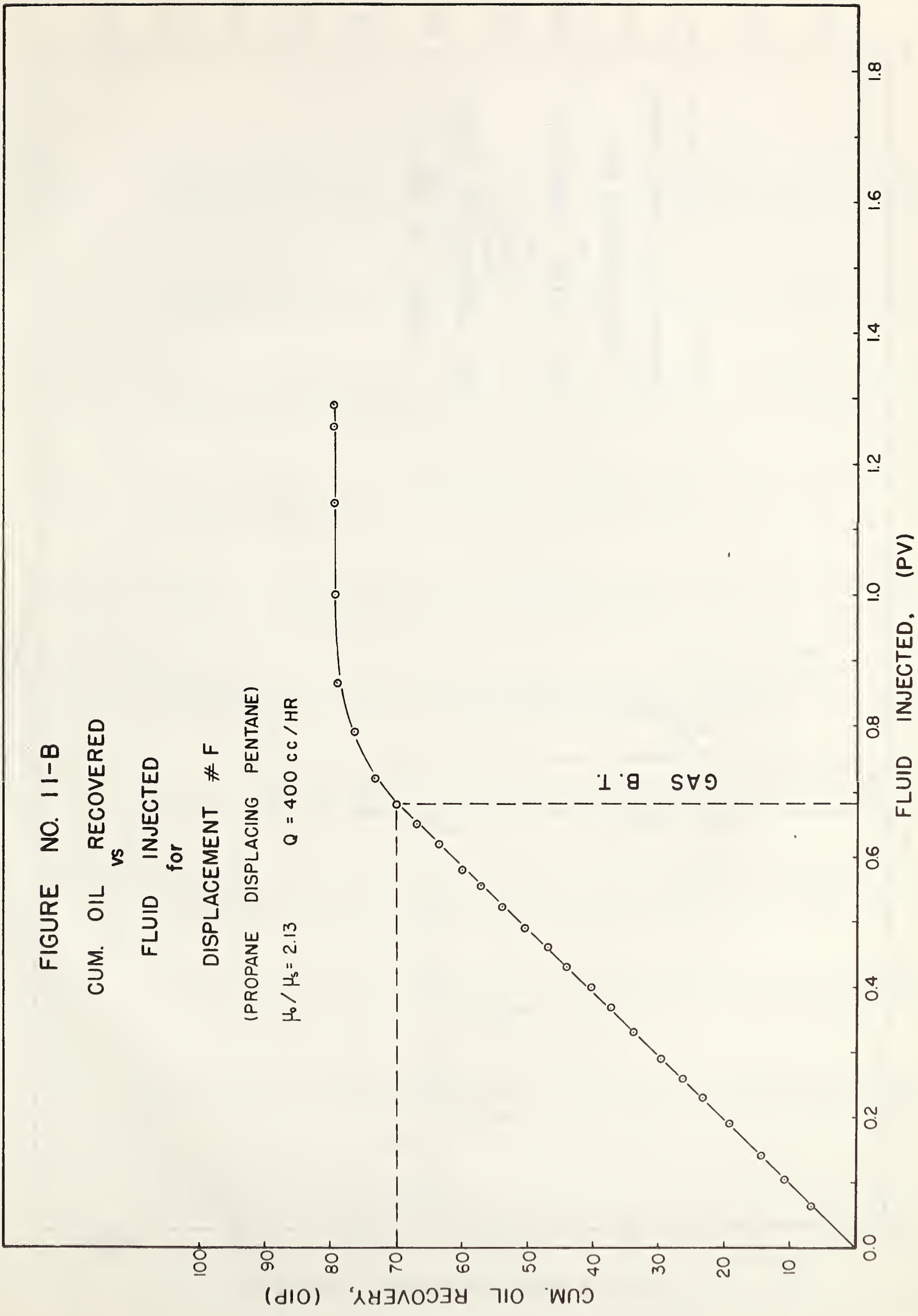

FIGURE NO. 11-B

CUM. OIL RECOVERED vs FLUID INJECTED for DISPLACEMENT # F

(PROPANE DISPLACING PENTANE)

$\mu_o / \mu_s = 2.13$ Q = 400 cc/HR

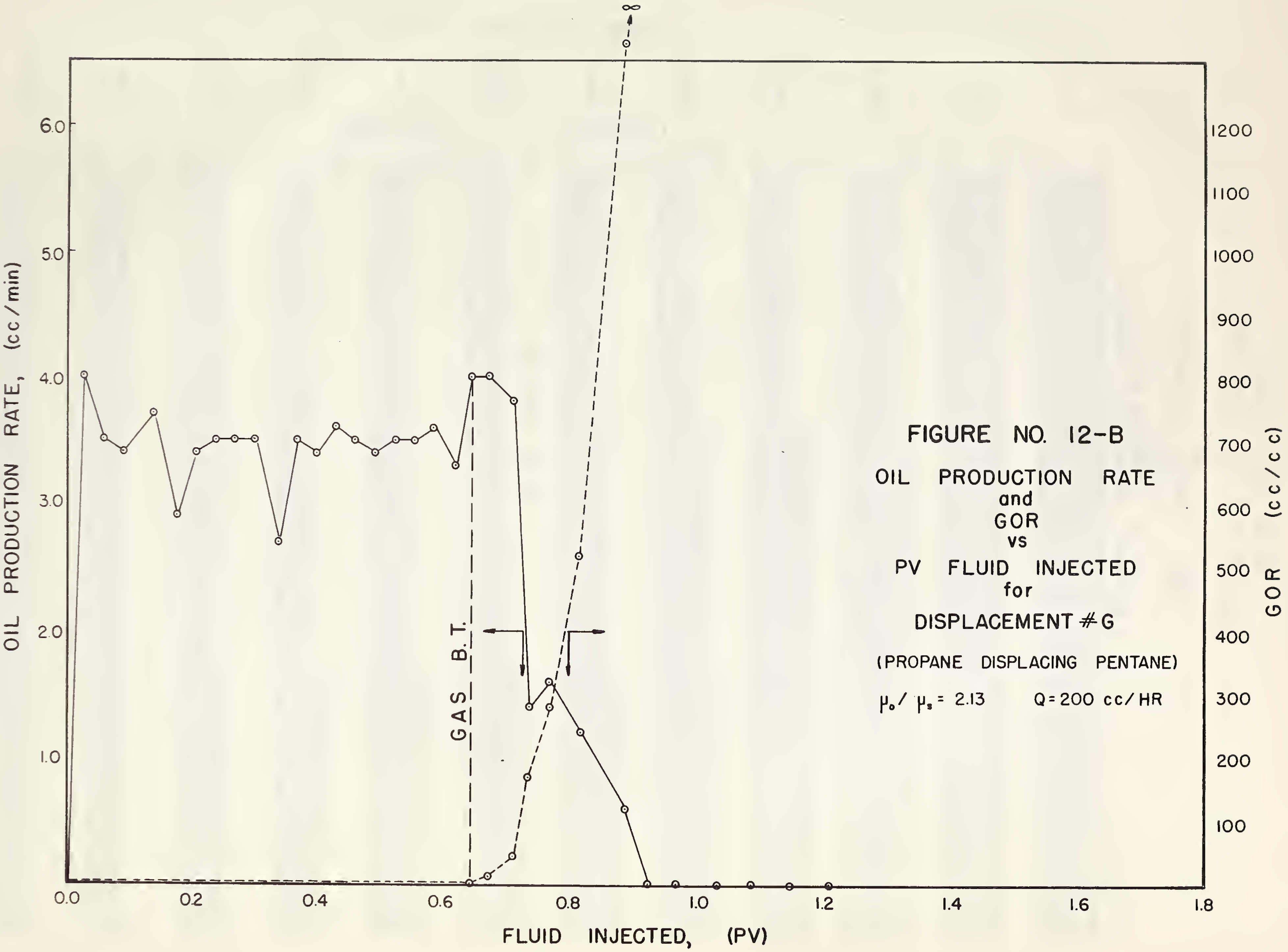

FIGURE NO. 12-B

OIL PRODUCTION RATE
and
GOR
vs
PV FLUID INJECTED
for
DISPLACEMENT #G

(PROPANE DISPLACING PENTANE)

$\mu_o / \mu_s = 2.13$ Q = 200 cc/HR

FIGURE NO. 13-B

$(\Delta P/\Delta L)_{t=t} \,/\, (\Delta P/\Delta L)_{t=0}$

vs

DISTANCE ALONG CORE

for

DISPLACEMENT # F

(PROPANE DISPLACING PENTANE)

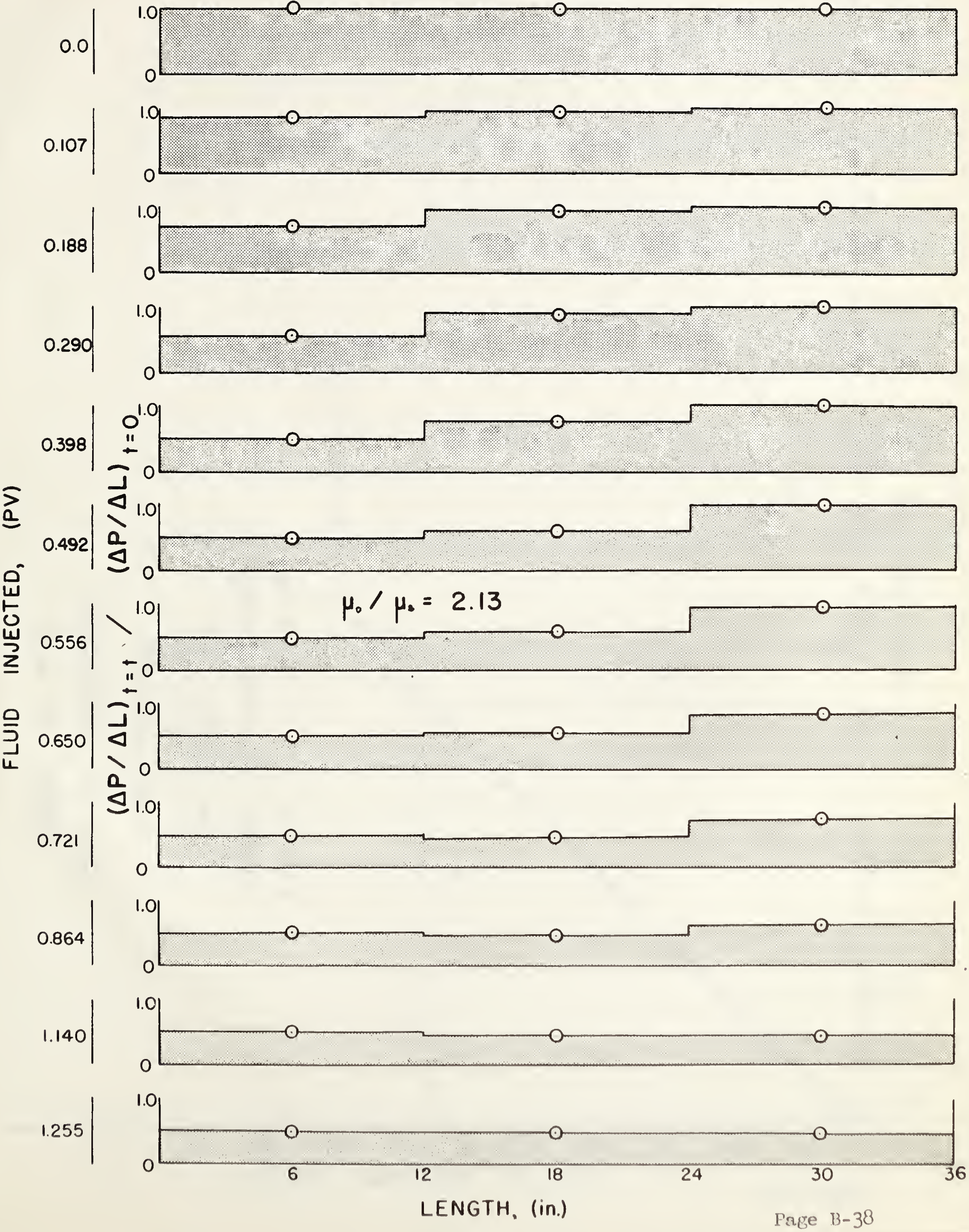

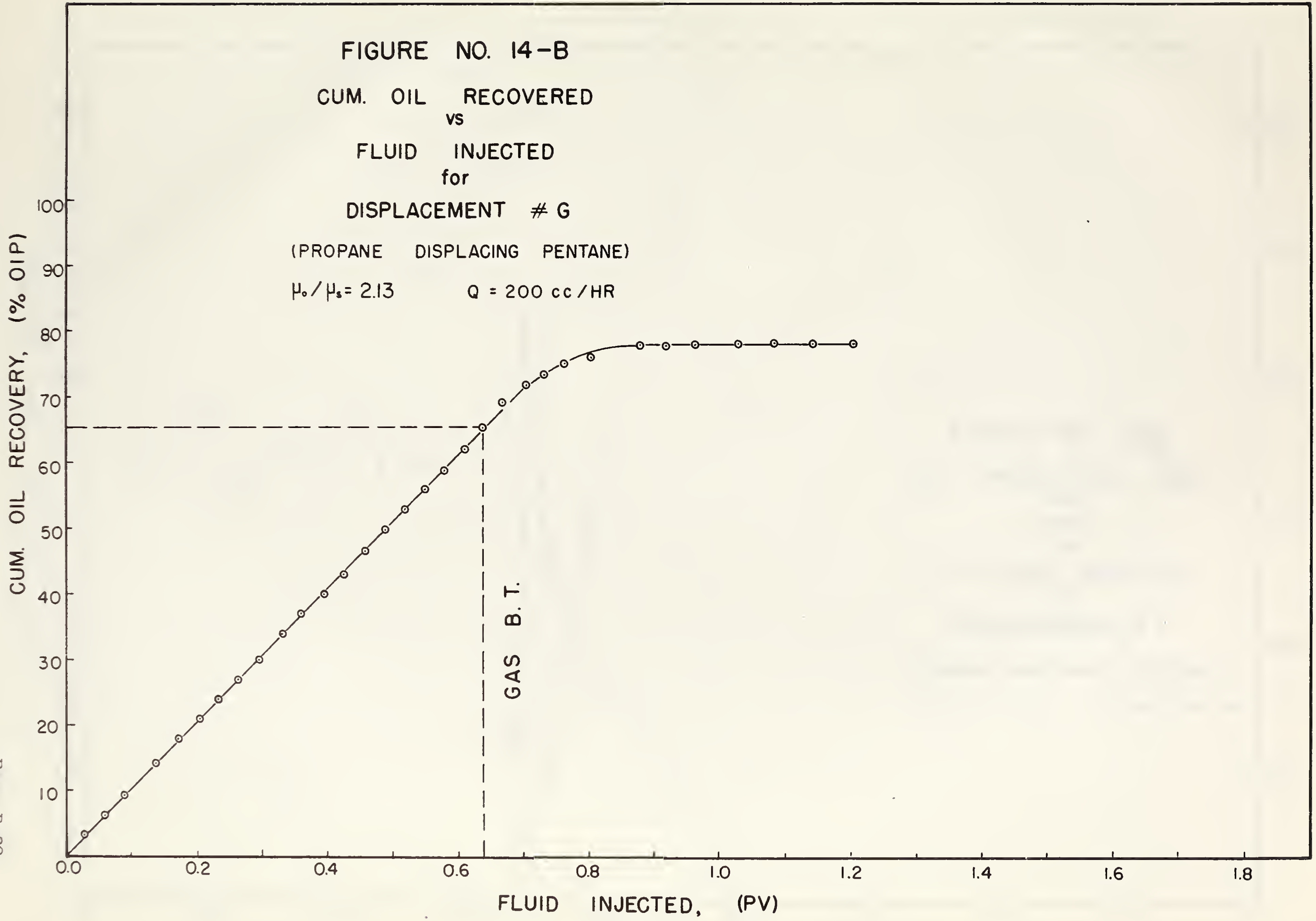
FIGURE NO. 14-B

CUM. OIL RECOVERED
vs
FLUID INJECTED
for
DISPLACEMENT # G

(PROPANE DISPLACING PENTANE)

$\mu_o/\mu_s = 2.13$ Q = 200 cc/HR

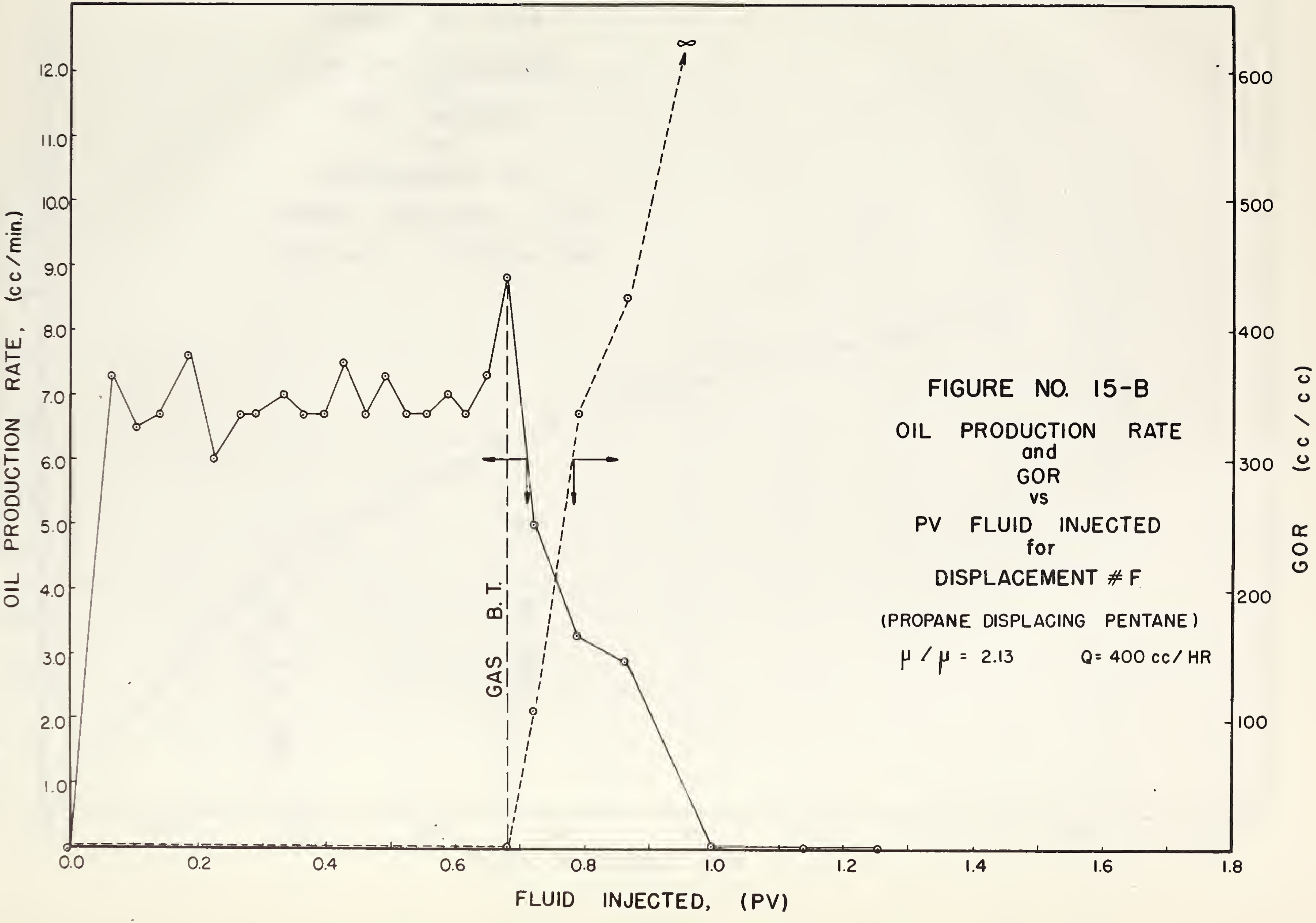

FIGURE NO. 15-B

OIL PRODUCTION RATE
and
GOR
vs
PV FLUID INJECTED
for
DISPLACEMENT # F

(PROPANE DISPLACING PENTANE)

$\mu / \mu = 2.13$ Q= 400 cc/HR

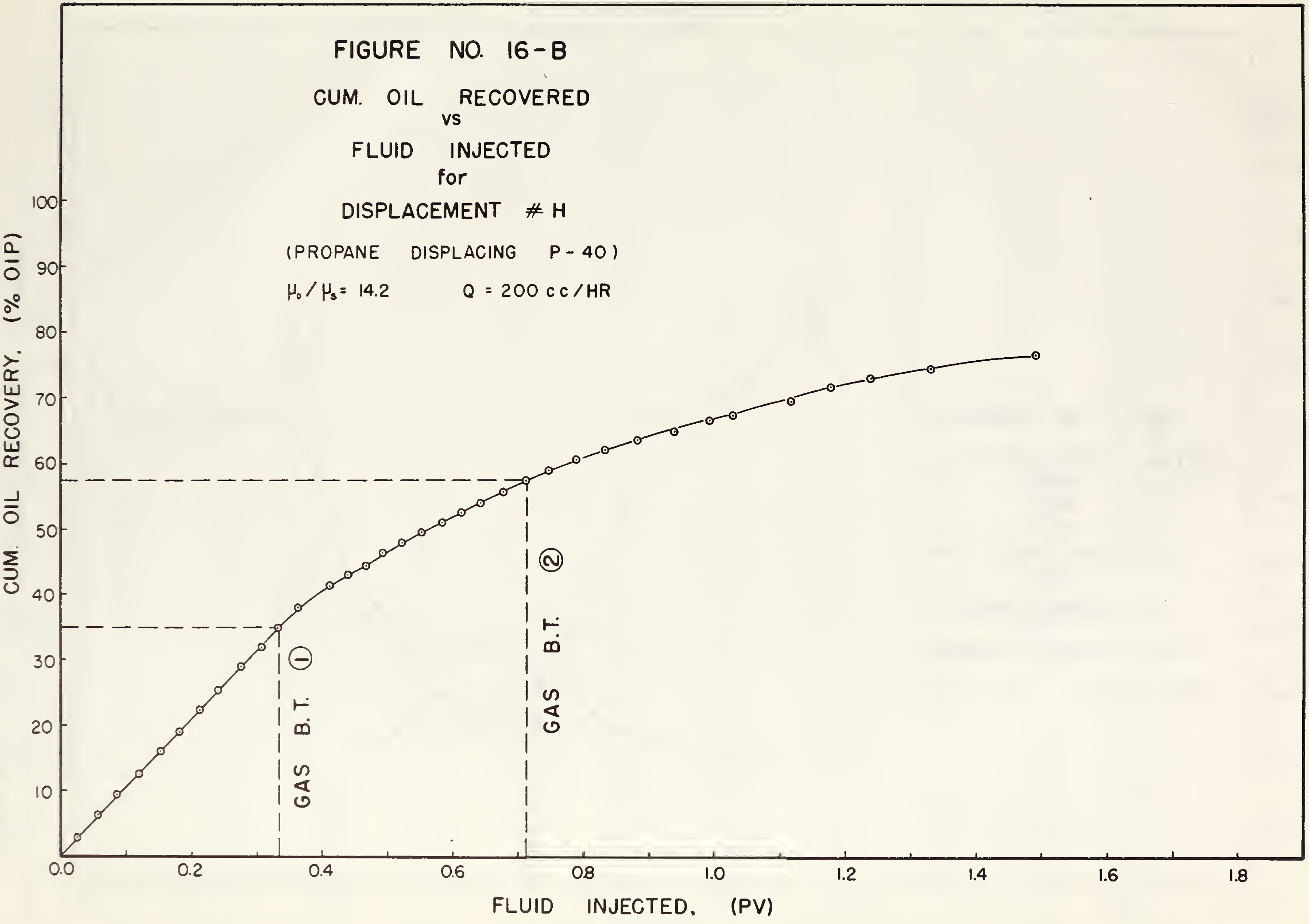

FIGURE NO. 16-B

CUM. OIL RECOVERED
vs
FLUID INJECTED
for
DISPLACEMENT # H

(PROPANE DISPLACING P-40)

$\mu_o / \mu_s = 14.2$ Q = 200 cc/HR

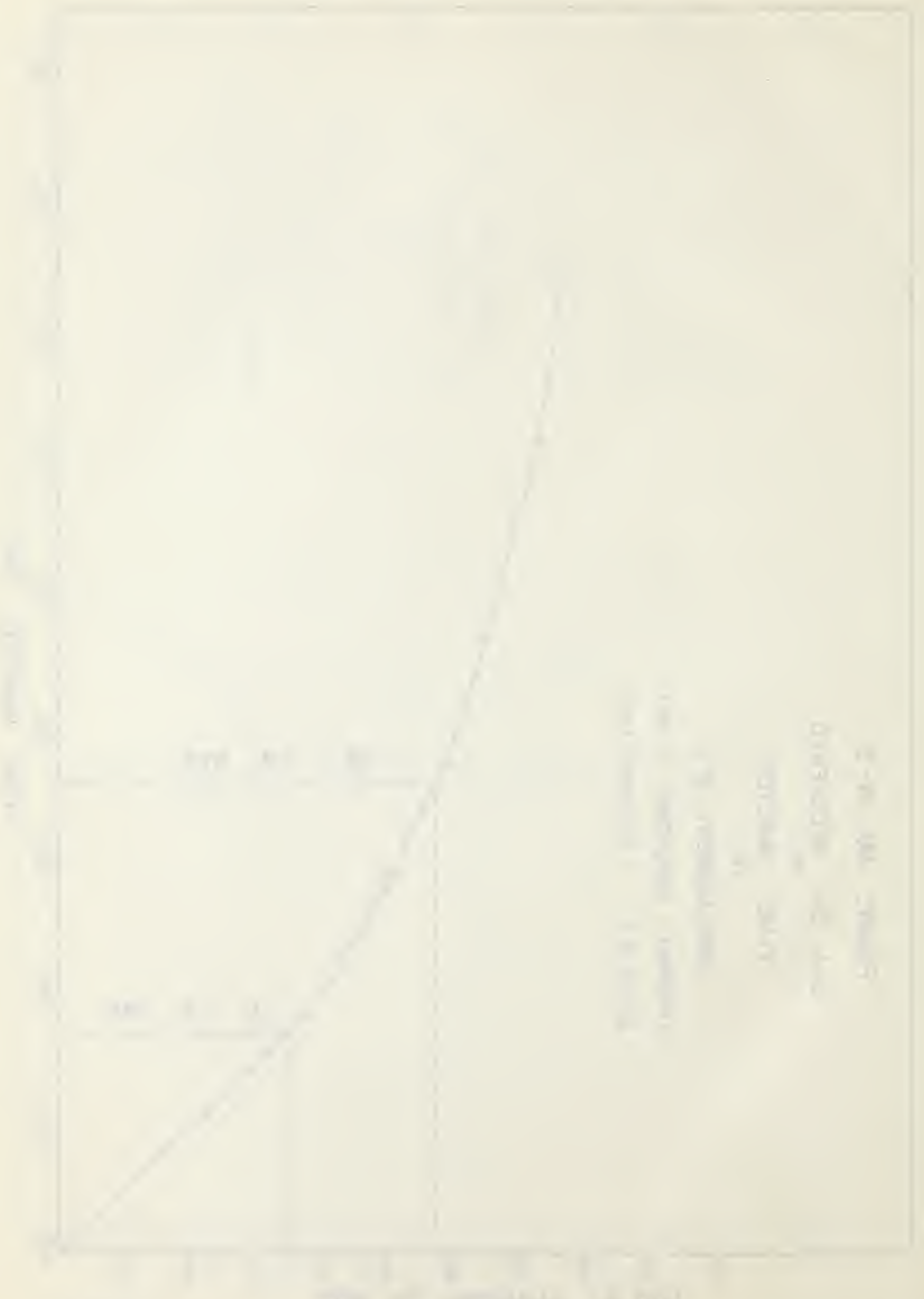

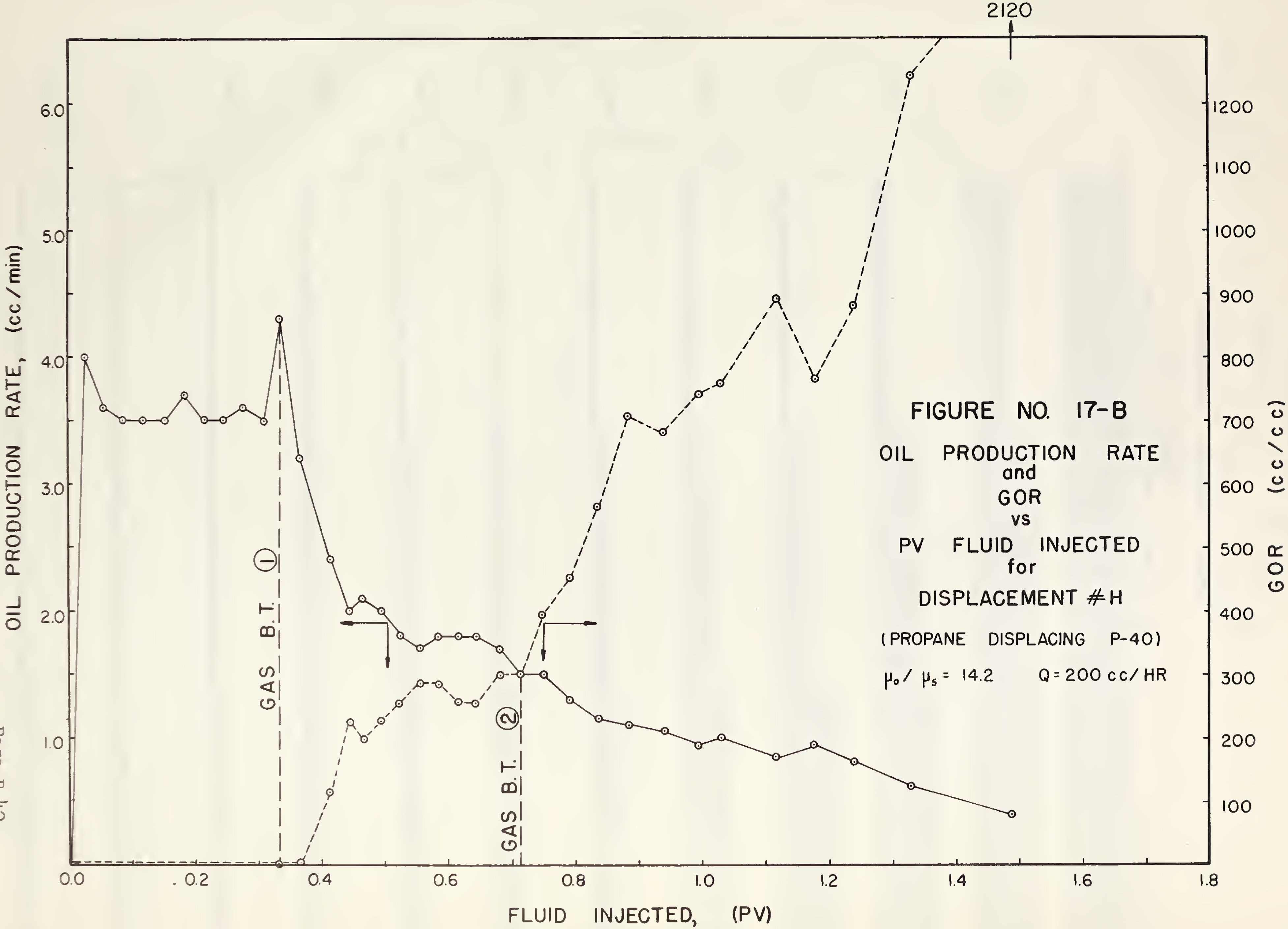

FIGURE NO. 17-B

OIL PRODUCTION RATE
and
GOR
vs
PV FLUID INJECTED
for
DISPLACEMENT #H

(PROPANE DISPLACING P-40)

$\mu_o / \mu_s = 14.2$ Q = 200 cc/HR

FIGURE NO. 18-B

$(\Delta P/\Delta L_{t=t} / \Delta P/\Delta L)_{t=0}$

VS

DISTANCE ALONG CORE

for

DISPLACEMENT # H

(PROPANE DISPLACING ESSO P-40)

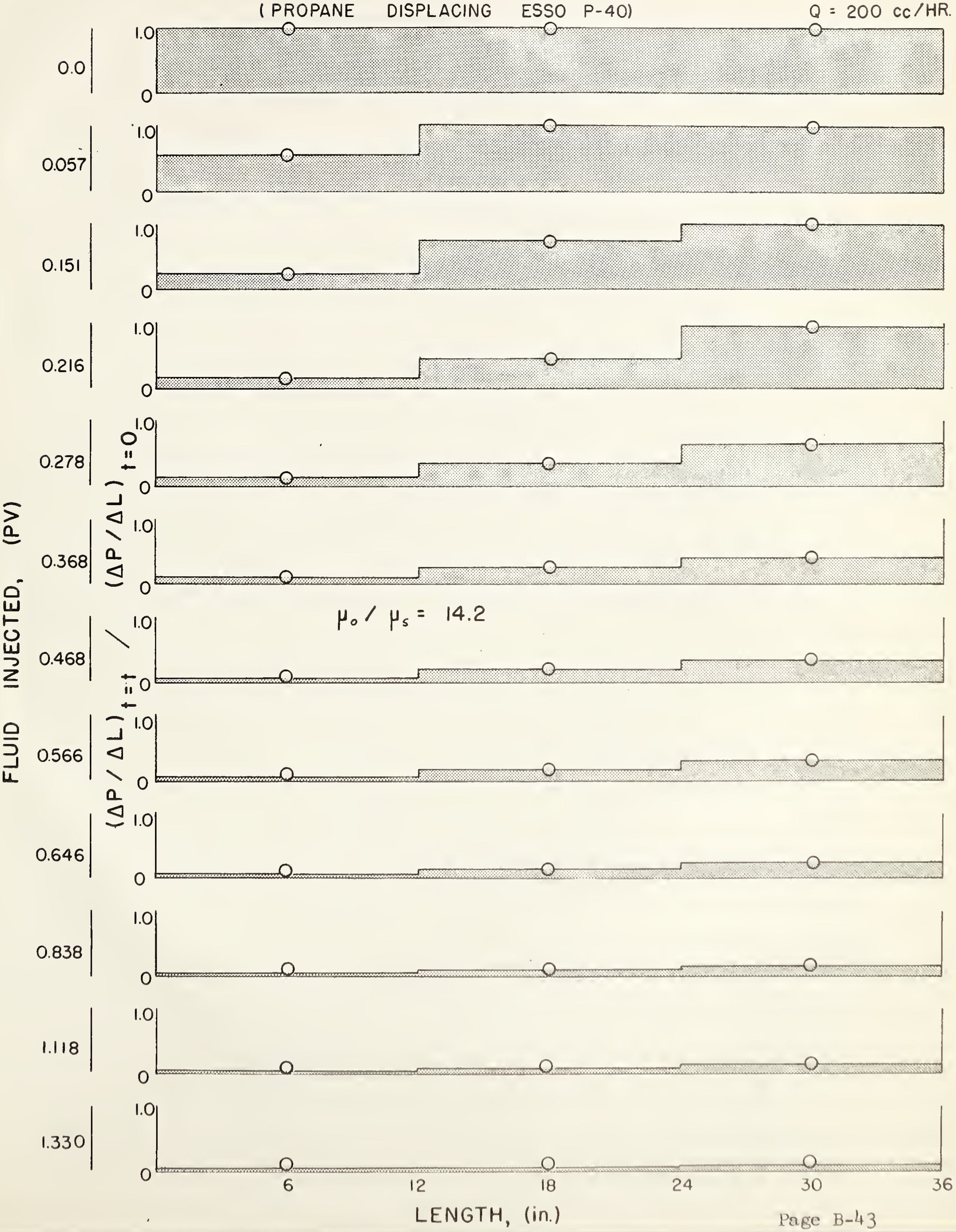

B29800